R&D of an Innovative Composite Scaffold Incorporated with Phytoestrogenic Icaritin for Treatment of Steroid-associated Osteonecrosis Lesion in Rabbits

XIE, Xinhui

A Thesis Submitted in Partial Fulfillment of the Requirements for the Degree of Doctor of Philosophy in Orthopaedics and Traumatology

The Chinese University of Hong Kong

June, 2010

ProQuest LLC
789 East Eisenhower Parkway
P.O. Box 1346
Ann Arbor, MI 48106-1346

Thesis/Assessment Committee

Professor Hung Leung Kim (Chair)
Professor Qin Ling (Thesis Supervisor)
Professor Leng Yang (Thesis Co-supervisor)
Professor Zhang Ge (Thesis Co-supervisor)
Professor Zhang Yuanting (Committee Member)
Professor Wang Jiansheng (External Examiner)
Professor Lu William Weijia (External Examiner)

ACKNOWLEDGEMENTS

I would like to express my sincere gratitude to my supervisor Professor Ling Qin, for his academic guidance, patience, encouragement and support in the past three years. I would like to give heartful gratitude to my co-supervisor Professor Ge Zhang (The Chinese University of Hong Kong) and Yang Leng (The Hong Kong University of Science and Technology), for their supervision, never-ending patience and generous support. Special thanks to Professor Ge Zhang, for his consistent taking care of me in academics and life since 2007 when I came to this department. Thank my supervisor Professor Tingting Tang in Shanghai Jiaotong University, for his great support and encouragement in the past years. I wish to thank Professor Louis Cheung, Professor Benson Yeung, Mr. Bruma Fu and Dr. Francis Chen for their invaluable advice and helpful comments in my study.

Thank Dr. Xinluan Wang, Dr. Hui Shen, Dr. Berry He, Mr. Zhong Liu, Mr. Gene Man, Mr. Dong Yao, Miss Lizheng Zheng, Miss Shihui Chen, Miss Heng Wu, Mr. Boris Guo, Dr. Peng Zhang and Dr. Tao Tang in our team for their patient and cautious help in my study; Thank Miss Vivian Hung, Miss Tsz-Ning Fong, Miss Fiona Yu and Miss Winnie Lee in our Department for their kind assistances and encouragement during my Ph.D study. My sincere thanks also go to my close friends, Dr. Yunfeng Rui, Dr. Ming Ni and Dr. Minghui Sun, for their kindly supports in my laboratory work. Thank Prof. Xiaohua Pan and Dr. Yugang Wang in Shenzhen People's Hospital for their generous support in animal provision and surgery support.

Last but not the least, I would like to thank my family for their encouragement

and support in these years.

This thesis work was supported by NSFC-RGC Joint Grant (N_CUHK405/08), Hong Kong Innovation and Technology Support Programme (GHP/001/08) and SG200810200102A/Shenkexin 2009-37.

TABLE OF CONTENTS

ABSTRACT

Bone defect is a common orthopaedic problem caused by many pathologic disorders such as tumor, trauma or metabolic diseases, including osteonecrosis (ON). ON is a disabling clinical condition characterized by the death of osteocytes, aggregation of marrow fat cells, a decrease in activity of bone marrow stem cells (BMSCs) pool, and degeneration of trabecular bone matrix, which affect more frequently young adults that usually leads to bone and articular cartilage destruction in joints, especially in hip and knee. High dose of steroid is one of the risk factors associated with ON, which sometimes is used for treatment of some medical conditions such as systemic lupus erythematosus (SLE), organ transplantation, asthma, rheumatologic arthritis (RA), and severe acute respiratory syndrome (SARS). Core decompression has been efficacious for treatment of early ON stages when the necrotic lesion is still small in size. However, ON lesion, weakens the cancellous bone within and adjacent to the necrotic region. Thus orthopaedic challenges in repair for steroid-associated ON lesion after core decompression may include the impaired osteogenic potential of stem-cell-pool under the influence of pulsed steroid and lack of platform for bone or/and neovascularization ingrowth after removal of large size necrotic bone.

The proposed strategies for treatment of steroid-associated ON lesion are to provide biocompatible scaffold with required structure to fill the defect area after core decompression and osteogenic stimulator facilitating the repair of ON lesion. Previous works show that the PLGA (poly-lactic glycolic acid) and TCP (tricalcium

phosphate) have good biocompatibility, osteoconduction and biodegradation to be used in bone defect repair, however no significant osteopromotive effects. Many endogenous factors are osteopromotive and also eventually osteoinductive, such as bone morphogenic proteins (BMPs). As an extraneous molecular, Icaritin, a small molecule derived from *Epimedium*-derived flavonoids (EF), is found to be able to facilitate matrix calcification, stimulate osteogenesis and inhibit adipogenesis of BMSCs. The present thesis work hypothesizes that the PLGA/TCP incorporating Icaritin to form a porous composite scaffold is osteopromotive and is able to enhance the repair of necrotic bone defect with steroid-associated ON after core decompression.

The content of this thesis is divided into the following four major parts:

For the first part, porous osteopromotive composite scaffolds PLGA/TCP/Icaritin were designed and produced by using rapid-prototyped technology. The porosity, pores size, pores connection and the mechanical property of scaffolds were evaluated. The results showed that the structure and the mechanical property were not changed by incorporated Icaritin. After that, the degradation characteristics of this porous scaffold as well as the released property of Icaritin from composite scaffolds were examined by dipping into saline, The volume and dry weight of PLGA/TCP/Icaritin scaffold were found to decrease during 12-week degradation and its macro- and micro- porous structure was maintained, while porous structure of pure PLGA/TCP scaffold was lost over time. The Icaritin was released slowly from the porous scaffold into the degradation medium combined with the

release of Ca and lactic acid. These findings implied that the PLGA/TCP/Icaritin scaffold had good degradation properties and therefore PTGA/TCP provided a good system for slow release of osteopromotive Icaritin.

For the second part of the thesis work, the study aimed to investigate the in vitro toxicity of PLGA/TCP/Icaritin scaffolds using L929 mouse fibroblasts in vivo biocompatibility using implantation of scaffold in muscles, as well as the proliferation and osteogenic differentiation of BMSCs from rabbits and osteoblast-like UMR 106 cells on these scaffolds. The results showed the extracts of PLGA/TCP/Icaritin scaffold did not inhibit the growth of L929 cells. An acceptable healing pattern was found for composite materials with fibrous connective tissues were observed between the muscles and the scaffolds as a capsule and obvious neovascularization ingrowth. The PLGA/TCP/Icaritin scaffold was beneficial for both attachment and proliferation of BMSCs. The increased ALP activity and extracellular calcium deposition implied its ability to promote osteogenesis of BMSCs. The expression of several genes (osteocalcin and bone sialoprotein) related to osteogenesis of osteoblast-like UMR 106 cells was increased when cells were cultured on the composite scaffold. These findings indicated that the PLGA/TCP/Icaritin composite porous scaffolds were non-toxic, biocompatible and osteopromotive for orthopaedic applications.

The third part of the study aimed to establish the ON model in rabbits by injecting a combined lipopolysaccharide (LPS) and methylprednisolone (MPS) using an established protocol. Core decompression was introduced to mimic a bone defect

model in necrotic area. No LPS/MPS treated rabbits were served as control. The results at week 12 after operation showed that the new formed bone in bone defect area in rabbits with ON was less than that in rabbits without ON by following up with a high-resolution peripheral quantitative computed tomography (HR-pQCT) known as xtremeCT and histology evaluation ($p<0.05$). Insensitive fibrous connective tissues within bone defect, accompanied by inferior mechanical properties in terms of compression load, elastic modules and energy at failure were found in osteonecrosis groups as compared with normal group. These findings indicated the delayed bone healing in necrotic lesion in steroid-associated ON.

The forth part or the last part of the thesis work was in vivo efficacy study using rabbit model. The PLGA/TCP/Icaritin scaffold was implanted into the bone tunnel after core-decompression in initial necrotic bone defect in rabbits with steroid-associated ON to observe the effect of bone defect repair. The results showed that the new bone formed in both PLGA/TCP/Icaritin scaffold group and PLGA/TCP scaffold group was more than that in the group without scaffold implantation ($p<0.05$) and that in PLGA/TCP/Icaritin scaffold group was more than that in PLGA/TCP scaffold group ($p<0.05$). At the same time, the neovascularization was also studied and was found in PLGA/TCP/Icaritin porous scaffold, suggesting that the PLGA/TCP/Icaritin scaffold facilitated the vessel ingrowth due to its proper porous structure.

In summary, with fine biodegradation, biocompatibility, osteopromotion in vitro, the PLGA/TCP/Icaritin composite porous scaffold materials enhanced the bone

repair at necrotic defect lesion in rabbits with steroid-associated ON. The findings implied that the porous composite PLGA/TCP/Icaritin scaffold would be an appropriate osteopromotive scaffold implant or bone graft substitute biomaterial for potential application in skeletal tissue engineering. It was the first study to incorporate or homogenize the Chinese herbal molecule into the porous composite biomaterials for medical testing. Though the osteopromotive effect in ON model was observed in vivo, the molecular mechanism of osteogenesis remains for future investigations.

摘 要

骨缺損是骨科臨床實踐中非常常見的並發症，腫瘤、創傷、骨代謝性疾病和骨壞死等都能夠導致骨缺損的發生。骨壞死的特徵包括骨細胞的壞死、脂肪細胞侵潤、骨髓基質乾細胞的活性（包括數量和成骨能力）下降以及骨基質降解。骨壞死通常好發於年輕人，引起骨和關節軟骨下骨的破壞，尤其是大關節如髖關節和膝關節。高劑量激素經常用於治療系統性紅斑狼瘡、器官移植、風濕病、類風濕性關節炎和嚴重的呼吸系統窘迫綜合症，同時它也是導致骨壞死發生的一個重要危險因素。在骨壞死的早期，當壞死程度相對比較輕微的時候，髓內減壓是一種有效的治療手段，它可以防止骨壞死進一步發展，從而防止關節進一步破壞塌陷。但是髓內減壓後取出部分壞死骨會導致壞死區及其周圍骨的力學強度下降，這種小的骨缺損也會導致關節破壞塌陷。因此在對激素性骨壞死行髓內減壓治療後面臨的困難包括：1）激素引起局部幹細胞數量和成骨活性的下降；2）壞死骨去除後遺留的缺損不利於新生骨和血管長入。

因此，針對髓內減壓後骨缺損的治療有兩個目的：第一就是提供一個生物相容性好的支架，這個支架能夠填充骨缺損部位，具有適當的三維結構有利於引導骨組織和血管長入；第二就是要具有成骨因子，提高局部幹細胞成骨能力，從而促進壞死區域新骨形成。既往已有研究顯示 PLGA(聚乳酸聚乙醇酸共聚物)和 TCP(磷酸三鈣)具有良好的生物相容性、骨傳導性和降解性，能夠用於骨缺損的治療，但是缺乏骨誘導性。很多內源性生長因子具有骨形成促進作用和骨誘導作用如 BMPs（骨形態形成蛋白），但是這些因子價格昂貴，並且理化性質不穩定和局部存留時間短。在我們既往的工作中，我們發現了一種來源於淫羊藿黃酮類化合物的外源性小分子淫羊藿素，這種小分子有利於促進基質鈣化、促

進骨髓基質乾細胞的成骨作用和抑制其成脂作用。我們的目的就是將 PLGA/TCP 作為載體與淫羊藿素形成 PLGA/TCP/淫羊藿素混合材料，利用 PLGA/TCP 的骨傳導作用和淫羊藿素的骨形成促進作用可以治療激素性骨壞死髓內減壓術後導致的骨缺損，提高骨修復效果。

本論文研究內容總共分 4 部分內容：

第一，利用快速成型技術製備 PLGA/TCP/淫羊藿素多孔混合支架材料。研究了淫羊藿素對 PLGA/TCP 混支架材料的孔隙率、孔徑、孔的連通率和力學性質等特徵，同時用電鏡觀察了材料表面結構。結果顯示添加淫羊藿素不影響混合材料的結構和力學特徵。材料具有多孔性，分大孔和微孔兩種水平的孔徑。然後將 PLGA/TCP/淫羊藿素混合支架材料置於生理鹽水中，觀察多孔材料的降解特性，同時觀察淫羊藿素從材料中的釋放動力學。結果顯示材料在生理鹽水中浸泡 12 週後體積和乾重都有下降，PLGA/TCP/淫羊藿素材料的大孔和微孔孔徑都不同程度下降但是多孔結構仍然保持完整，但是純 PLGA/ TCP 材料的表面微孔結構消失。材料的力學強度在 12 週降解後低於降解之前。在材料的降解過程中，降解液中鈣離子和乳酸的濃度不斷增加伴隨著淫羊藿素的緩慢釋放。這些結果都顯示 PLGA/TCP/淫羊藿素混合多孔支架材料具有良好的降解性能，並且是一個很好的淫羊藿素緩釋系統。

第二，用小鼠成纖維細胞系 L929 以及肌肉植入研究了材料的體外和體內細胞毒性，用兔的骨髓基質乾細胞和成骨樣細胞觀察了材料促進成骨的作用。結果顯示混合材料的浸提液沒有明顯抑制 L929 細胞的生長。體內肌肉植入試驗顯示機體對材料有正常的生物學反應，在材料和肌肉之間形成纖維結締組織囊，並有新生血管長入。 PLGA/TCP/淫羊藿素混合支架材料有利於骨髓基質乾細胞

的貼附，遷移和生長，能夠促進骨髓基質乾細胞的鹼性磷酸酶表達和細胞外基質鈣沉積。在材料表面生長的成骨樣細胞的成骨基因(骨鈣素和骨唾液蛋白)表達增加。這些結果顯示 PLGA/TCP/淫羊藿素混合支架材料無細胞毒性，同時具有良好的生物相容性和骨形成促進作用，具有骨科應用潛能。

第三，用內毒素(LPS，脂多醣)和激素（MPS，甲基潑尼松龍）在兔體內建立骨壞死不癒合模型。骨壞死模型建立以後，在骨壞死區行髓內減壓術去除部分壞死骨。在正常兔體內行同樣外科手術做為對照組。手術後 12 週，微 CT 和組織學檢查顯示實驗組髓內減壓後的骨缺損區內形成的骨量少於對照組($p<0.05$)。壞死組骨缺損區分佈著大量的纖維結締組織，而正常組缺損區分佈正常的骨髓組織，壞死組的新生骨力學性能要低於與正常對照組相比。這些結果說明在激素性骨壞死的兔體內，髓內減壓後殘留的缺損不能準時癒合。

第四，驗證 PLGA/TCP/淫羊藿素混合支架材料治療激素性骨壞死髓內減壓後骨缺損的效果。仍然用兔建立激素性骨壞死模型，髓內減壓去除壞死骨形成骨缺損，植入 PLGA/TCP 和 PLGA/TCP/淫羊藿素支架材料。微 CT 和組織學結果顯示材料組形成的骨要多於無材料組($p<0.05$)，PLGA/TCP/淫羊藿素組形成的骨要多於 PLGA/TCP 組，兩組都可觀察到大量的新骨長入伴隨著材料本身的降解。同時也可以觀察到有新生血管長入支架材料內部。結果說明淫羊藿素的加入促進了壞死區骨缺損的癒合。

總結，PLGA/TCP/淫羊藿素混合支架材料具有良好的生物降解性、生物相容性和骨形成促進作用，這種混合支架可以提高激素性骨壞死髓內減壓後遺留骨缺損的修復效果。這說明這種多孔的支架材料有希望用於骨組織工程或者骨移植物，以促進局部骨修復。這是首次研究將中藥小分子藥物在材料製備階段

編織進入多孔混合支架材料。雖然在體內外的研究中觀察到這種混合中藥小分子淫羊藿素的多孔支架材料具有良好的骨形成促進作用，但是其作用的分子機制仍然不是非常明確，這將是以後研究的重點。

FLOWCHART OF THESIS OUTLINE

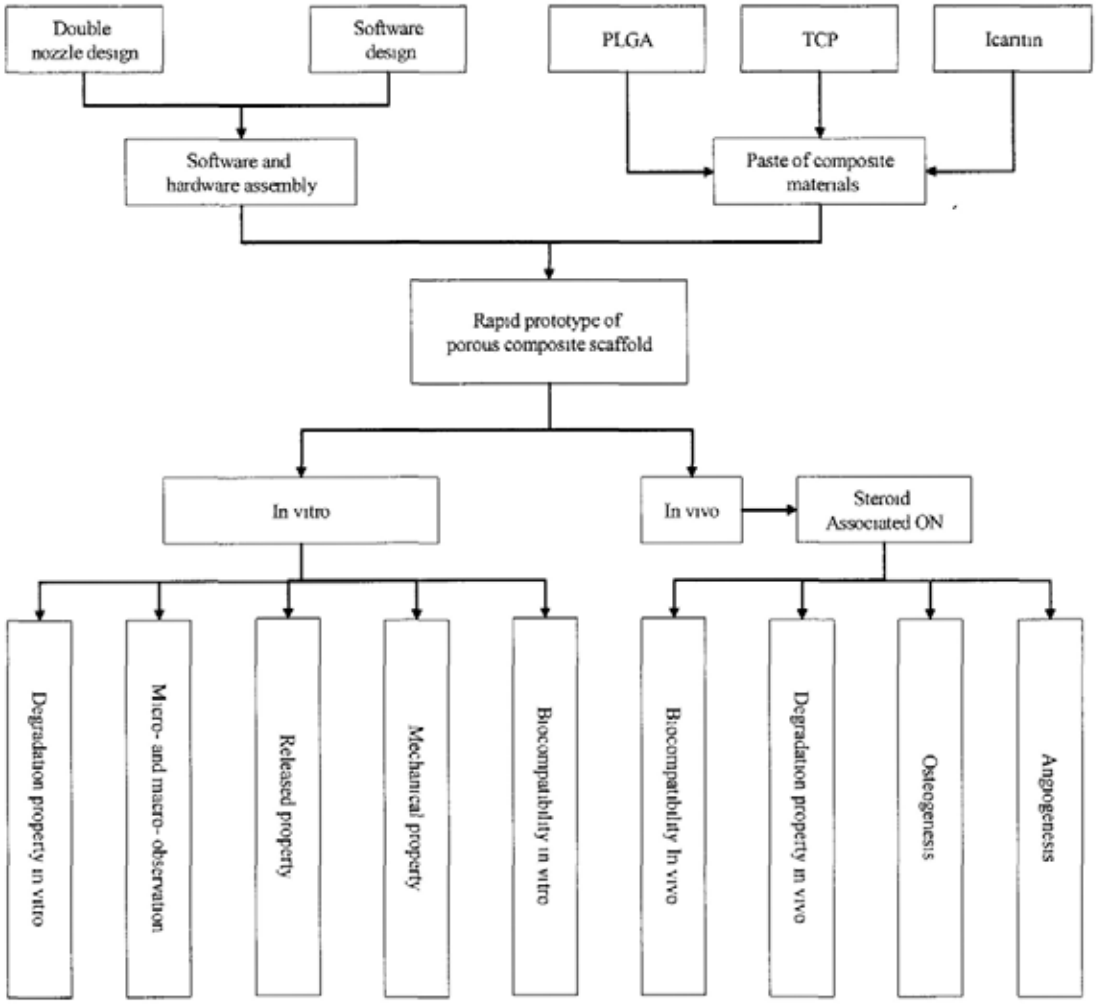

PUBLICATIONS

A: Journal Papers

1. **Xie XH**, Wang XL, Zhang G, He YX, Wang XH, Liu Z, He K, Peng J, Leng Y, Qin L. Structural and degradation characteristics of an innovative porous PLGA/TCP scaffold incorporated with bioactive molecular Icaritin. (Biomedical materials, under revision)
2. **Xie XH**, Zhang G, Wang XL, He YX, Wang XH, Liu Z, He K, Peng J, Ren FZ, Wang KF, Leng Y, Tang TT, Chen SH, Qin L. Production and characterization of a phytoestrogenic Icaritin releasing PLGA/TCP-based porous scaffold. (J Biomed Mater Res A, under review)
3. **Xie XH**, Wang XL, Zhang G, He YX, Liu Z, Yao D, Man CW, Hung LK, Hung V, Qin L. Impaired bone healing in rabbits with steroid-associated osteonecrosis. (Clinical and Experimental Rheumatology, under review)
4. Wang XL, **Xie XH** (co-fist author), Zhang G, Chen SH, He K, Wang XH, Yao XS, Leng Y, Fung KP, Leung KS, Qin L. Exogenous Phytoestrogenic Molecule Icaritin Incorporated into A Porous Scaffold for Enhancing Bone Defect Repair. (Submitted)
5. Zhang G, Wang XL, Sheng H, **Xie XH**, He YX, Yao XS, Li ZR, Lee KM, He W, Leung KS, Qin L. Constitutional flavonoids derived from *Epimedium* dose-dependently reduce incidence of steroid-associated osteonecrosis not via direct action by themselves on potential cellular targets. PLoS One. 2009 Jul 29; 4(7):e6419.

6. Zhang G, Sheng H, He YX, **Xie XH**, Wang YX, Lee KM, Yeung KW, Li ZR, He W, Griffith JF, Leung KS, Qin L. Continuous occurrence of both insufficient neovascularization and elevated vascular permeability in rabbit proximal femur during inadequate repair of steroid-associated osteonecrotic lesions. Arthritis Rheum 2009; 60:2966-77.
7. Zhang G, Qin L, Sheng H, Wang XL, Wang YX, Yeung DK, Griffith JF, Yao XS, **Xie XH**, Li ZR, Lee KM, Leung KS. A novel semisynthesized small molecule icaritin reduces incidence of steroid-associated osteonecrosis with inhibition of both thrombosis and lipid-deposition in a dose-dependent manner. Bone. 2009 Feb; 44(2):345-56.

B: Journal Supplements

1. **Xie XH**, Zhang G, Sheng H, Li G, Leung KS, Qin L. Adipose-tissue provides a stem-cell-rich alternative source for cytotherapy of steroid-associated osteonecrosis: An in vitro study. Bone 2008; 43:S95.
2. **Xie XH**, Zhang G, He YX, Wang XL, Sheng H, Wang XH, Li G, Leung KS, Leng Y, Qin L. Promotion of tissue repair of steroid-associated osteonecrosis lesion in rabbits by using PLGA/TCP/Icaritin composite biomaterials scaffold: An in vivo micro-computed tomography study. Bone 2009; 45:S107.
3. Wang XL, Zhang G, **Xie XH**, Yao XS, Qin L. Antagonistic Estrogen Receptor Beta Signaling Required in Promoting Periosteum Bone Formation and Inhibiting Osteoclastic Bone Resorption by Icaritin - a Novel Synthetic Small Molecule. Bone 2008; 43:S115.

4. Wang XL, Zhang G, **Xie XH**, Lee KM, Li G, Wang XO, Yao XS, Leng Y, Leung KS, Qin L. In vitro release of osteoinductive molecule Icaritin from porous PLGA/TCP/Icaritin scaffolds for repairing steroid-associated osteonecrosis lesion. Bone 2009; 45:S105.

C: Conference Presentations and Publications

1. **Xie XH**, Zhang G, Sheng H, Wang XL, Li Gang , Leung KS, Qin L. Adipose-tissue provides a stem-cell-rich alternative source for cytotherapy of steroid-associated osteonecrosis: An in vitro Study. International conference on osteoporosis and Bone research (ICOBR), Beijing 2008. Poster presentation.
2. **Xie XH**, Zhang G, He YX, Sheng H, Kumta KM, Wang XH, Lau Carol, Wang XL, Qin L. The growth properties of adipose-tissue derived stem cells seeded on scaffold biomaterials composed of PLGA/TCP/P-chitosan. Hong Kong Journal of Orthopaedic Surgery Vol. 12 Supplement p.128, Nov 2008. The 28th Annual Congress of the Hong Kong Orthopaedic Association. November 29-30th 2008, Hong Kong. Poster presentation.
3. **Xie XH** , Zhang G, He YX, Wang XL, Sheng H, Wang XH, Li G, Leung KS, Leng Y, Qin L. Promotion of Tissue Repair of Steroid-associated Osteonecrosis Lesion in Rabbits by Using PLGA/TCP/Icaritin Composite biomaterials Scaffold: An in Vivo Micro-computed Tomography Study. ICCBH5 2009, Cambridge, Poster presentation.
4. **Xie XH**, Zhang G, He YX, Wang XL, Sheng H, Li G, Leung KS, Qin L. A Novel Cell-based Osteogenic Strategy for Repairing Steroid-associated Osteonecrosis

Lesion in A Rabbit Model. 31st Annual Meeting of The American Society for Bone and Mineral Research (ASBMR). Denver, Colorado, USA. 2009. Poster presentation.

5. **Xie XH**, Zhang G, He YX, Wang XL, Sheng H, Wang XH, Li G, Leung KS, Leng Y, Qin L. Promotion of Tissue Repair of Steroid-associated Osteonecrosis Lesion in Rabbits by Using PLGA/TCP/Icaritin Composite biomaterials Scaffold: An in Vivo Micro-computed Tomography Study. 31st Annual Meeting of The American Society for Bone and Mineral Research (ASBMR). Denver, Colorado. USA. 2009. Poster presentation.
6. **Xie XH**, Zhang G, He YX, Wang XL, Wang XH, He K, Peng J, Leung KS, Leng Y, Qin L. PLGA/TCP/Icaritin Composite Scaffold Developed for Repair of Steroid-associated Osteonecrosis Lesion in Rabbits: An Pilot Study with Micro-computed Tomography. The 2nd International Symposium on Surface and Interface of Biomaterials (ISSIB-II), Hongkong, 4-6 January 2010. Oral presentation.
7. **Xie XH**, Zhang G, Wang XL, He YX, Wang XH, He K, Ren FZ, Wang KF, Leng Y, Tang TT, Qin L. Porous PLGA/TCP/Icaritin composite scaffold and its various changes during degradation in vitro. The 2nd International Symposium on Surface and Interface of Biomaterials (ISSIB-II). Hongkong, 4-6 January 2010. Oral presentation.
8. **Xie XH**, Zhang G, Wang XL, He YX, Wang XH, He K, Ren FZ,Wang KF, Leng Y, Tang TT, Qin L. Preparation of a novel osteopromotive porous

PLGA/TCP/Icaritin composite scaffold and its characteristics analysis. 29th Annual Congress of The Hong Kong Orthopaedic Association Hong Kong Convention & Exhibition Centre, Hong Kong, 28-29 November, 2009. Oral presentation.

9. **Xie XH**, Zhang G, Wang XL, He YX, Wang XH, Liu Z, He K, Peng J, Ren FZ, Wang KF, Leng Y, Tang TT, Qin L. A novel osteopromotive PLGA/TCP/Icaritin composite porous scaffold developed for orthopaedic applications. 56th Annual Meeting of the Orthopaedic Research Society. Morial Convention Center, New Orleans, Louisiana, USA. March 6 - 9, 2010. Poster presentation.

LIST OF ABBREVIATIONS

2D	Two-dimensional
3D	Three-dimensional
ALP	Alkaline phosphatase
ANOVA	Analysis of variance
AVN	Avascular necrosis
bFGF	Basic fibroblast growth factor
BMC	Bone mineral content
BMD	Bone mineral density
BMPs	Bone morphogenetic proteins
BMSCs	Bone mesenchymal stem cells
BSP	Bone sialoprotein
BV	Bone volume
Ca	Calcium
cDNA	Bomplementary deoxyribonucleic acid
CT	Computed tomography
DEA	Diethanolamine
DMEM	Dulbecco's modified eagle's medium
DMSO	Dimethyl sulphoxide
EF	*Epimedium*-derived flavonoid
EDS	Energy Disperse Spectroscopy

FBS	Fetal bovine serum
GAPDH	Glyceraldehyde phosphate dehydrogenase
GFP	Green fluorescent protein
H&E	Harry's hematoxylin and eosin
HA	Hydroxyapatite
HCL	Hydrogen chloride
HR-pQCT	High-resolution peripheral quantitative computed tomography
LIPUS	Low intensity pulsed ultrasound
LPS	Lipopolysaccharide
MPS	Methylprednisolone
MRI	Magnetic resonance imaging
mRNA	Messenger ribonucleic acid
MTT	3-(4, 5-Dimethylthiazol-2-yl)-2, 5-diphenyltetrazolium bromide
NaCl	Sodium chloride
OC	Osteocalcin
OD	Optical density
ON	Osteonecrosis
OPN	Osteopontin
P	Phosphate
PBS	Phosphate buffered saline
PCR	Polymerase chain reaction

PGA	Polyglycolic acid
PLA	Polylactic acid
PLGA	Poly-lactic glycolic acid
PNPP	Para-Nitrophenyl phosphate
R&D	Research and development
RA	Rheumatologic arthritis
RGR	The relative growth rate
ROI	Region of Interest
SAON	Steroid associated osteonecrosis
SARS	Severe acute respiratory syndrome
SEM	Scanning electron microscope
SLE	Systemic lupus erythematosus
Tb.N	Number of trabecular
Tb.Sp	Trabecular separation
Tb.Th	Thickness of trabecular
TCP	Tricalcium phosphate
TV	Tissue volume
VEGF	Vascular endothelial growth factor

Chapter 1

Introduction

1.1. Osteonecrosis

Osteonecrosis (ON) is a disabling clinical disease characterized by death of the osteocytes and the bone marrow, followed by resorption of the dead tissue by new but weaker osseous tissue which lead to a progressive destruction of bone architecture, subchondral fracture and collapse of femoral head, finally loss of joint function (Aaron R. 1998; Assouline-Dayan Y. et al. 2002; Malizos K. N. et al. 2007). Alexander Munro first identified this medical condition in 1738 and Cruveilhier firstly attributed this disorder to an aberration of circulation in the femoral head at the mid 1800's (Lavernia C. J. et al. 1999; Nogler M. 2004). The similar terms of ON include avascular necrosis (AVN), ischemic necrosis, subchondral avascular necrosis, aseptic necrosis of bone, and osteochondritis dissecans (Assouline-Dayan Y. et al. 2002). The terms AVN and ischemic necrosis were used to describe their vascular etiology and aseptic necrosis is used to indicate that the factor infection does not play an important role on osteonecrosis occurrence and its development. ON occurs mostly in large joints, such as hip (Fig.1) that may subsequently develop to joint collapse and end up with joint replacement surgery (Saito S. et al. 1989; Seyler T. M. et al. 2007).

1.1.1. Epidemiology

The number of new cases of ON at femoral head in the United States was between 10,000 and 20,000 per year and the ON accounts for 5-10% of total hip joint replacement (Lavernia C. J. et al. 1999; Malizos K. N. et al. 2007). In China, there are no accurate data for ON incidence and the number of total joint replacements, but

the number of ON patients is increasing (Sun W. et al.; Sun Y. et al. 2009b). Although ON can developed in any age groups, most patients are young adults and about 75% of patients with ON are between 30 and 60 years old, with the average age in the late 30's (D'Aubigne R. M. et al. 1972). 25% of ON patients are less than 25 years of age. Once one side of femoral head is affected by ON, up to 72% of another side of the femoral head may be involved in the next two years (Malizos K. N. et al. 2007). There are two types of ON involved: one is traumatic which is the most common and another is atraumatic (Aaron R. 1998). ON at hip result from trauma occurs in 10%, 15-30% and 10% for undisplaced femoral neck fractures, displaced femoral neck fractures and hip dislocations, respectively. 5-25% of patients with atraumatic ON are a result of steroid administration. At least 50% of patients with atraumatic hip ON will be suffered from bilateral ON. The prevalence of male to female ratio is about 7:3 for systemic lupus erythematosus (SLE) patients (Assouline-Dayan Y. et al. 2002). Except ON at femoral head, other bones are often involved in this disease such as knee (Griffith J. F. et al. 2005; Akgun I. et al. 2007), shoulder (Sarris I. et al. 2004), talus (Chiodo C. P. et al. 2004) and vertebral body (Young W. F. et al. 2002). The diagnosis of ON will not affect the life expectancy of patients, thus several hundred thousand patients are living with this disease.

1.1.2. Etiology

ON can be divided into two types: one is idiopathic (primary) ON in which there are no apparent etiologic or risk factor can be found; another is secondary ON in which the etiology is clearly identified (Malizos K. N. et al. 2007). According to

whether the traumatic factor is involved, ON can be divided into traumatic and non-traumatic ON. The traumatic factors include femoral neck fracture, hip dislocation, extensive burns, vessel trauma and iatrogenic injury. ON resulted from trauma is well known as the vascularity around the femoral head is severely damaged. Atraumatic ON has many risk factors including secondary conditions of hypercoagulation such as intake of steroids, alcoholism, myelodysplastic syndromes, pregnancy, contraceptive use, hyperlipidemia, collagen diseases, ehler-Danlos syndrome, raynaud's disease, diabetes mellitus and antiphospholipid antibodies (APLA); hematological diseases such as hemophilia, hemoglobinopathies and polycythemia; metabolic diseases, such as hyperparathyroidism, gout, cushing disease and gaucher disease; alimentary system diseases such as pancreatic, ulcerative colitis and Crohn's disease; other risk factors such as smoking, decompression disease, radiation and hemodialysis (Aaron R. 1998; Malizos K. N. et al. 2007; Gruson K. I. et al. 2009).

Of all the non-traumatic factors, the 2 mainly associated problems are corticosteroid use (Vestergaard P. et al. 2003; Yamamoto T. et al. 2006; Yildiz N. et al. 2008) and alcohol abuse (Rico H. et al. 1985; Yuan B. et al. 2009). The ON in large joint caused by corticosteroid use or alcohol abuse is usually associated with the worst prognosis (Devlin V. J. et al. 1988; Assouline-Dayan Y. et al. 2002; Berend K. R. et al. 2003; Nowicki P. et al. 2007). More than 400ml of alcohol abuse per week will usually cause ON and long time of heavy consumption will be more serious factor. Steroid-induced ON usually involves multiple sites of bone and nearly 100%

bilateral hip will be suffered with ON. The exact dose of steroid required to induce ON remains uncertain, but some studies indicate that higher doses, even in a single injection of corticosteroid into the hip joint, will result in histological observed ON (Yamamoto T. et al. 2006). Often, patients on steroids have other associated risk factors.

1.1.3. Classification

There are several staging systems currently used for femoral head ON, including Ficat classification (Ficat R. P. 1985), Steinberg staging system (Steinberg M. E. et al. 1984b; Maniwa S. et al. 2000), and International Classification of Osteonecrosis of the Femoral Head ((Association Research Circulation Osseus (ARCO)) (Gardeniers J. W. M. 1993; Zibis A. H. et al. 2007).

For Ficat classification, there are 5 stages included. Stage 0: No pain, normal radiographic findings, abnormal bone scan or magnetic resonance imaging (MRI) findings. Stage I: Pain, normal x-ray findings, abnormal bone scan or MRI findings. Stage II: Pain, cysts and/or sclerosis visible on x-ray, abnormal bone scan or MRI findings, without subchondral fracture. Stage III: Pain, femoral head collapse visible on x-ray, abnormal bone scan or MRI findings, crescent sign (subchondral collapse) and/or step-off in contour of subchondral bone. Stage IV: Pain, acetabular disease with joint space narrowing and arthritis (osteoarthrosis) visible on x-ray, abnormal MRI or bone scan findings (Ficat R. P. 1985).

For Steinberg staging system, there are 7 stages included. Stage 0: Normal or nondiagnostic radiographic, bone scan and MRI findings. Stage I: Normal

radiographic findings, abnormal bone scan and/or MRI findings. Stage II: Lucent and sclerotic changes in femoral head. Stage III: Subchondral collapse (crescent sign) without flattening. Stage IV: Flattening of femoral head. Stage V: Joint narrowing and/or acetabular changes. Stage VI: Advanced degenerative changes (Steinberg M. E. et al. 1984a; Steinberg M. E. et al. 1984b; Maniwa S. et al. 2000).

For ARCO staging system, there are 5 stages included (Fig.1.1). Stage 0: Bone biopsy results consistent with ON, other test results normal. Stage I: Positive findings on bone scan, MRI, or both. Stage II: Mottled appearance of femoral head, osteosclerosis, cyst formation, and osteopenia on radiographs; no signs of collapse of femoral head on radiographic or CT study; positive findings on bone scan and MRI; no changes in acetabulum. Stage III: Presence of crescent sign lesions classified on basis of appearance on Anteroposterior and lateral radiographs. Stage IV: Articular surface flattened; joint space shows narrowing; changes in acetabulum with evidence of osteosclerosis, cyst formation, and marginal osteophytes (Gardeniers J. W. M. 1993; Zibis A. H. et al. 2007).

The stage systems are beneficial for ON prevention, diagnosis, treatment and evaluation of therapeutic effects. According to all the classifications, the MRI is the most sensitive one to the necrotic region and can be used for early diagnosis before appearance of clinical symptoms. Of all the stage systems, the main changes in the last stage are joint space narrowing, acetabular changes and osteosclerosis, which usually mean that the patients need total hip joint replacement (Saito S. et al. 1989; Lieberman J. R. et al. 2003; Malizos K. N. et al. 2007; Nowicki P. et al. 2007;

Petrigliano F. A. et al. 2007; Seyler T. M. et al. 2007).

1.2. Steroid-associated osteonecrosis

Steroid-associated osteonecrosis (SAON) is a common orthopaedic problem caused by use of steroid which are initially prescribed for many non-orthopaedic medical conditions, including systemic lupus erythematosus (SLE), organ transplantation, asthma, rheumatologic arthritis (RA), and severe acute respiratory syndrome (SARS) (Assouline-Dayan Y. et al. 2002; Lieberman J. R. et al. 2003; Chan M. H. et al. 2006; Mont M. A. et al. 2006; Law R. K. et al. 2008). Steroids are now the second most common cause of ON after trauma and the prevalence in studies of ON varies between 3-38% (Assouline-Dayan Y. et al. 2002). In Hong Kong and the region, up to 20% ON incidence was reported for treating SLE patients (Mok C. C. et al. 1998; Mok C. C. et al. 2003), patients with organ transplantation (Marston S. B. et al. 2002) and SARS patients (Griffith J. F. et al. 2005; Chan M. H. et al. 2006; Cheng X. G. et al. 2006) using steroid. The ON appearances on MRI in patients with steroid were same to those caused by other etiologies or conditions. It was reported that at least one location with ON was found in 31%(138/448) of SARS patients after steroid therapy from Beijing Jishuitan Hospital of Beijing, China (Cheng X. G. et al. 2006). MRI screening revealed that the prevalence of SAON was quite high in SARS patients. SAON frequently occurred in multiple sites including the femoral head, knee, shoulder and ankle joints. Multiple joints involvement and bilateral occurrence were common (Mont M. A. et al. 1999). For patients with corticosteroid-induced humeral head ON, the rate of other joint involvement has

reached to 90% (Gruson K. I. et al. 2009).

The ON development was associated with dose and duration of administrating corticosteroids (Cheng X. G. et al. 2006). Usually, the chronic administration of high-dose steroids will result in the ON onset, but it is very difficult to predict which patient with steroid administration will finally develop to ON (Yamamoto T. et al. 2006; Kerachian M. A. et al. 2009) The interval between corticosteroid administration and ON onset was not certain. A retrospective study showed that the interval between steroid administration and the ON onset is from 6 months to more than 3 years. A prospective study using MRI to detect early ON of the femoral head showed that the initial changes of necrosis were found at 3.6 months after administration of steroid (Sakamoto M. et al. 1997).

Histopathologically, the ON formation was characterized by the diffuse presence of empty lacunae or pyknotic nuclei of osteocytes in bone trabeculae, accompanied by surrounding necrotic bone marrow (Yamamoto T. et al. 1997; Qin L. et al. 2006; Zhang G. et al. 2009b). Decreased trabecular width and increased number of osteoblasts and osteocytes apoptosis were also identified in patients with glucocorticoid administration (Weinstein R. S. et al. 1998). There are two types of repair can be found after ON is induced by steroid. Appositional bone formation with osteoblast-like cells around the necrotic lesion is classified as reparative osteogenesis, whereas granulation tissue creep linked to necrotic bone resorption is classified as destructive repair (Plenk H., Jr. et al. 2001; Zhang G. et al. 2009b). In form of destructive repair, the death of the bone will subsequently induce an

inadequate repair process, predominant resorption of necrotic bone exceeding bone formation frequently leads to subchondral collapse (Aaron R. 1998; Plenk H., Jr. et al. 2001). In form of reconstructive repair, reparative bone formation starts from subchondral fractures and/or the reactive interface, finally reduce the size of the necrotic area (Plenk H., Jr. et al. 2001).

The pathophysiology of SAON remained controversial (Aaron R. 1998). The recent advance in understanding the pathophysiological mechanism of the inadequate repair at early stage is that a decrease in activity of bone marrow stem cell (BMSC) pool (Hernigou P. et al. 1997; Hernigou P. et al. 1999; Gangji V. et al. 2005b; Hernigou P. et al. 2005), apoptosis of osteocytes, and trabecular bone matrix degeneration (Weinstein R. S. et al. 2000; Eberhardt A. W. et al. 2001). Steroids can induce differentiation of BMSCs into adipocytes linage and inhibit their osteogenic differentiation by down-regulating osteoblast transcription factor gene expression and up-regulating adipocytes transcription factor gene expression, thus result in increased lipid deposition including larger fat cells number and fat deposition area (Li X. et al. 2005; Yin L. et al. 2006; Sheng H. H. et al. 2007; Yeh C. H. et al. 2009). Increased fat cell hypertrophy will lead to venous sinusoidal compression which causes venous congestion, followed by intraosseous hypertension and impaired arterial inflow within the femoral head, finally resultant vascular collapse and local ischemia. Thus the increased intraosseous pressure will continuously promote the progress of necrosis regardless of etiology. If the death of the bone subsequently induces an inadequate repair process, the bone underlying the joint surface will be

weakened. In most patients, subchondral collapse changes the articular surface, leading to abnormal mechanics and arthritis to the joint. In addition, a fat embolism phenomenon with resultant vascular occlusion and a hyperlipidemic state also seems to be related to ON mechanism (Aaron R. 1998; Gruson K. I. et al. 2009).

1.3. Treatment of osteonecrosis

According to the different stages of the ON (ARCO), there are several treatments could be used, including the medical therapy and surgical therapy (Tab.1.1).

1.3.1. Prevention as the treatment strategy

It is very difficult to predict which patients receiving steroid administration will develop ON, though prevention of SAON is essential, e.g. already at the time of steroids treatment (Kerachian M. A. et al. 2009). Seldom evidence shows that the exact efficiency of prevention of the occurrence of SAON clinic. A retrospective report from Pritchett et al showed that the ON incidence was 1% in 284 patients who had received high dose corticosteroids while concurrently on a statin, which is significantly lower than the historical value of 3%-20% (Pritchett J. W. 2001). Muhammad Ajmal et al. analyzed the renal transplant database to determine if statin usage reduced the incidence of corticosteroid-related ON and identified 2,881 renal transplantation patients who met the entry criteria of ON. Among patients those used statins, 4.4% of patients developed ON, versus 7% of patients who were not on statins (Ajmal M. et al. 2009). The authors concluded that the statin usage did not appear to lower the risk of ON. Most experiments of prevention of SAON were

performed using animals at laboratory. It was reported that the herbal *Epimedium*-derived phytoestrogenic compound or its metabolic products (Qin L. et al. 2008; Sheng H. et al. 2008; Zhang G. et al. 2009a; Zhang G. et al. 2009c), vitamin E (Kuribayashi M. et al.), an anticoagulant (warfarin or enoxaparin) plus a lipid-lowering agent (probucol, lovastatin or pitavastatin) (Yamamoto T. et al. 2007; Nishida K. et al. 2008; Kang P. et al. 2010), electromagnetic fields (Ishida M. et al. 2008) and intra-bone marrow injection of autologous bone marrow cells (Asada T. et al. 2008) were able to exert partly beneficial effect on preventing SAON in rabbit model attributed to their osteogenic and anti-adipogenic effects as well as inhibition of both thrombosis and lipid-deposition in a dose-dependent manner. The prevention of SAON in another animal model (chicken) using statins (lovastatin) showed less adipogenesis and no bone death which indicated that lovastatin may be helpful in preventing the development of steroid-induced ON (Wang G. J. et al. 2000).

As both bone resorption and formation markers are unable to predict development of SAON (Chan M. H. et al. 2006) and patients only come to our orthopaedic clinics for ON diagnosis with joint pain symptoms, i.e. mostly already at ON stage I-II as diagnosed by MRI (Zibis A. H. et al. 2007), in order to avoid or delay the progression of the disease to the stage of the subchondral fracture and reduced the need for total hip replacement, the current consensus is an early surgical intervention for stage I-II ON patients (Malizos K. N. et al. 2007), according to Steinberg's classification (Steinberg M. E. et al. 1984a).

The clinical results were much better when surgery was performed at early

stages of avascular necrosis of the hip on long-term steroid treatment. The patients with stage I disease and 88.9% of stage II disease had excellent and good clinical results, but 66.7% of stage III disease and 50% of stage IV disease had poor clinical results. Considering the natural ON history of the hip, it was concluded that early surgical intervention was a viable treatment option in these difficult cases (Demirors H. et al. 2002).

1.3.2. Nonoperative treatment

Nonsurgical treatments of ON are limited and are commonly used at the early stage of ON and very small lesions, and the objects usually include relieving pain, preventing ON progression and improving the joint function (Gruson K. I. et al. 2009). Numerous medical and biophysical treatments have been reported including statins (Pritchett J. W. 2001; Ajmal M. et al. 2009), bisphosphonates (Lai K. A. et al. 2005), low molecular weight heparin (Glueck C. J. et al. 2005), stanozolol, iloprost, extracorporeal shock-wave therapy (Wang C. J. et al. 2008), hyperbaric oxygen, puerarin (herbal), and electromagnetic therapy (Steinberg M. E. et al. 1984a). Some of them showed some promise in treating at the early stage of disease.

1.3.3. Operative treatment

Operative treatment alternatives for femoral head ON mainly include osteotomy, core decompression sequestrectomy, bone and/or cells grafting and total hip arthroplasty. The age and general health of patients, ON stage particularly with collapse of the femoral head and/or acetabular involvement, size and location of lesion are commonly the determining factors for considering operation options (Mont

M. A. et al. 2006; Malizos K. N. et al. 2007).

1.3.3.1. Core decompression

Core decompression is one of the least invasive surgical procedures in early ON stages when the ON lesion is still small (Hungerford D. S. 1990; Stulberg B. N. et al. 1991; Mont M. A. et al. 1996; Plancher K. D. et al. 1997; Scully S. P. et al. 1998; Castro F. P., Jr. et al. 2000; Maniwa S. et al. 2000; Yuan B. et al. 2007; Sahajpal D. T. et al. 2008). It was described by Arlet and Ficatas in 1964 when they investigated painful hips in patients who had normal radiographic findings (Arlet J. et al. 1964). The operation is performed through a drilled bone tunnel made in the distal end of the greater trochanter (Fig.1.2) and about a 10-mm core of bone is removed from the necrotic lesion (Plancher K. D. et al. 1997). Core decompression is usually performed in Ficat stage II or earlier stages to prevent the subchondral collapse in SAON effectively. Biologically, core decompression helps to reduce intraosseous pressure and provide a conduit for angiogenesis to revascularize subchondral bone (Wang G. J. et al. 2000). Success rates with about 70% in stages before radiographic collapse and limited morbidity were observed which were better than those with conservative treatment (Stulberg B. N. et al. 1991). Mont and his collaborators reported a success rate of 84% patients with stage I lesions and 65% patients with stage II lesions for core decompression (Mont M. A. et al. 1996). Core decompression showed to be a highly effective treatment to delay the total joint replacement by 5 or more years. But concerns still do exist, including those related to incomplete reconstructive repair and its potential to weaken the trabecular bone

within and next to the necrotic region when the necrotic lesion was relatively large (Hungerford D. S. 1990; Scully S. P. et al. 1998; Castro F. P., Jr. et al. 2000; Malizos K. N. et al. 2007). What's more, once the femoral head develops a subchondral fracture, the efficacy of the core decompression will drop significantly. One of the reasons for incomplete reconstructive repair after SAON in the femoral head may be the decreased number of progenitor cells and the decreased osteogenic ability of BMSCs in the proximal extremity of the femur (Hernigou P. et al. 1997; Hernigou P. et al. 1999; Li X. et al. 2005; Yin L. et al. 2006; Sheng H. H. et al. 2007).

1.3.3.2 Core decompression with bone grafting

In order to reinforce the surgically bone defect resulted from core decompression sequestrectomy and delay the need for arthroplasty, several types of bone graft have been used to provide mechanical support for the affected joint in Ficat stage III or earlier stages (Fig.1.3). These include autogenous or allogenous cortical bone grafts of ilium, fibula or tibia alone, or alternatively, these procedures may be combined with core decompression (Chan T. W. et al. 1991; Assouline-Dayan Y. et al. 2002; Keizer S. B. et al. 2006; Hungerford D. S. 2007; Malizos K. N. et al. 2007). Free vascularized bone graft was used that showed some superior results as compared with most other procedures designed to preserve the femoral head collapse (Scully S. P. et al. 1998; Berend K. R. et al. 2003; Gonzalez Della Valle A. et al. 2005; Davis E. T. et al. 2006). However, such approach made total hip arthroplasty (THA) more difficult and prognosis was unsatisfactory (Davis E. T. et al. 2006). The autologous bone graft is used as a good substitute of the

necrotic site but the limitation include the insufficient supply and variation in the osteogenic potential of the graft material; the harvesting of host bone often result in some donor site morbidity (Laurie S. W. et al. 1984; Skouteris C. A. et al. 1989; Vail T. P. et al. 1996). Using homologous or heterologous grafts from bone bank can avoid the problem of autograft, but there will be potential risk of viral or bacterial infections and immune response (Stevenson S. 1987; Lord C. F. et al. 1988; Stevenson S. et al. 1996).

1.3.3.3. Core decompression with bone marrow or cells transplantation

Due to the decreased activity of mesenchymal stem-cell pool in the proximal femur or outside the necrotic zone in corticosteroid-induced ON (Hernigou P. et al. 1997; Hernigou P. et al. 1999). The additional mesenchymal stromal cells or bone marrow grafting are promised treatment option for ON for their differentiation properties, easy accessibility and proliferative capacity (Lee H. S. et al. 2003; Tzaribachev N. et al. 2008; Hernigou P. et al. 2009; Gao Y. S. et al. 2010). Clinically, good results were generously reported from treatment of ON using autologous bone marrow grafts combined with core decompression (Hernigou P. et al. 2002; Lee H. S. et al. 2003; Gangji V. et al. 2004; Hernigou P. et al. 2004; Gangji V. et al. 2005a; Gangji V. et al. 2005b; Hernigou P. et al. 2005; Tzaribachev N. et al. 2008; Wang B. L. et al. 2009). Most of the bone marrow were collected from the iliac crest but it was reported that the bone marrow near the site of ON could also be used (Lee H. S. et al. 2003). Their procedure was a less invasive surgery, but it might not be effective for large necrotic lesions because of larger marrow spacing were created after core

decompression sequestrectomy. In addition, a study in animal also showed that bone marrow mononuclear cells were benefit on vascularization and bone regeneration in steroid-induced ON of the femoral head (Sun Y. et al. 2009a).

1.3.3.4. Core decompression with growth factors

Growth factors such as BMPs and VEGF are osteogenic or angiogenic to promote the bone or vessel formation (Mont M. A. et al. 1998; Yuan B. et al. 2007). The bone morphogenetic proteins (BMPs) are osteoinductive agents that induce osteogenic cell differentiation *in vitro* and osteogenesis in bone healing *in vivo*. The growth factors can be used for treatment of ON directly or combined with bone graft after core decompression (Lieberman J. R. et al. 2004; Yuan B. et al. 2007; Stiehl J. B. et al. 2008). The growth factor gene could also be transduced into BMSCs and was capable of treating the ON in early-stage, e.g. demonstrated at femoral head in rabbit or goat model and the promoted osteogenesis and angiogenesis were observed (Tang T. T. et al. 2007; Wen Q. et al. 2008). In additional to its positive effect on osteogenesis, there are still some additional concerns related to the use of BMPs: (1) Need for non-physiologic large doses due to rapid degradation of unprotected protein(s). Unfortunately, much higher concentrations are needed in humans than in rodents and dogs because the concentration is species-dependent; (2) Their unstable chemistry will lead to difficulties with the incorporation in proper vehicles; (3) Short time of residence at the local site of the lesion; (4) Severe limitations in the gene therapy approaches apart from the direct cell transduction or the delivery of DNA by gene activated matrices; (5) whether they are useful in difficult fractures, nonunions

and large defects created from femoral head ON (Cancedda R. et al. 2007; Stiehl J. B. et al. 2008).

1.3.3.5. Tissue-engineered approach

Though the core decompression plus bone marrow stem cells could be used to treat ON, it might not be effective for large necrotic lesions or postcollapse cases. Due to the apoptosis of osteocytes, degeneration of trabecular bone matrix and osteocytes death in the femora (Weinstein R. S. et al. 2000; Eberhardt A. W. et al. 2001), the bone harvest would show decreased viability in the case of SAON. Recently, Kenji (Kawate K. et al. 2006) used the tissue-engineered approach for treating steroid-induced ON in femoral head, where cultured BMSCs/b-TCP(tricalcium phosphate) composite granules were implanted into the cavity that remained after curettage of necrotic bone, together with a subsequent free vascularized tibia grafting. But the limitation for practical application is that the cells should be cultured *in vitro* for 4 weeks before operation and potential risk of viral or bacterial infections apart. Other tissue-engineered technologies performed in animal model also provided an effective treatment result (Tang T. T. et al. 2007; Li Y. et al. 2009).

1.3.3.6. Total hip arthroplasty

Arthroplasty are usually used primarily for ON stages III and IV but occasionally used for stages I and II. Once the femoral head has collapsed and the hip joint has degenerated such that the articulation is compromised, the total hip replacement will be needed. The prognosis of joint replacement in SAON patents are

poor for patients with idiopathic or traumatic ON better post-surgical prognoses compared with those with steroid-induced ON (Assouline-Dayan Y. et al. 2002). Etiology does not affect the final outcome, but less favorable long-term results were found in the steroid-induced ON patients (Dudkiewicz I. et al. 2004). The patients with femoral head ON are generally young and total hip arthroplasty is often an unfavorable choice. Joint preservation is too difficult due to large pre-collapse lesions and post-collapse disease, so surgical alternatives for these patients may also include limited femoral resurfacing and bipolar hemiarthroplasty (Mont M. A. et al. 2006) .

According to the impaired osteogenic potential and activity of stem-cell-pool and degraded bone under influence of pulsed steroid as well as lack of platform for bone ingrowth after removal of large size necrotic bone after core-decompression-induced structural bone defect in SAON, the therapeutic strategy shall therefore provide sufficient precursor cells (osteogenic progenitors) and/or promote osteogenic ability of cells around necrotic region and/or eventually also within bone defect region (Wan C. et al. 2006; He Q. et al. 2007). It is also highly desirable to develop alternative approaches, e.g. to develop a biologically stable, easily applicable, and cost-effective osteoinductive composite porous bone substitute for core decompression to improve prognosis of early surgical repair of ON lesions. Biocompatible scaffold with required structure to fill the defect area after core decompression and osteogenic stimulator facilitating the repair of necrotic lesion for adequate repair of may meet the need for core decompression in early

stage of SAON.

1.4. Steroid-associated osteonecrosis animal models

To examine the mechanism or to identify the prevention or treatment efficiency of the biomaterials or some other therapy strategies for SAON, different animal models were built up such as rabbit (Yamamoto T. et al. 1995; Qin L. et al. 2006; Asada T. et al. 2008; Sun Y. et al. 2009a; Zhang G. et al. 2009a), rat (Drescher W. et al. 2006; Bitto A. et al. 2009; Okazaki S. et al. 2009; Takano-Murakami R. et al. 2009), mouse (Cui Q. et al. 2000; Yang L. et al. 2009), Bipedal chickens (Wang G. J. et al. 2000), pig (Drescher W. et al. 2001; Drescher W. et al. 2004), especially after outbreak of SARS in 2003 (Griffith J. F. et al. 2005; Chan M. H. et al. 2006; Cheng X. G. et al. 2006). Of all the animals, the rabbit is a commonly used animal model for SAON. The rabbit was provided to be an efficient animal for SAON model for high ON incidence.

To induce the SAON in rabbit, the administration of single methylprednisolone (MPS) (Yamamoto T. et al. 1997; Yamamoto T. et al. 2006; Asada T. et al. 2008) was proved to be an efficient method, but the incidence of ON was about 43%. Two injections of high-dose LPS combined with subsequent three injections of high-dose MPS (H-LPS×2+H-MPS×3) could improve the incidence of ON but had mortality up to 50% (Yamamoto T. et al. 1995). The LPS used here was to induce both hypercoagulable and hypofibrinolytic state which mimicking the clinic diseases (Irisa T. et al. 2001; Qin L. et al. 2006), and then followed the treatment with corticosteroid. we has developed a protocol by modifying the reported protocol with a single

low-dose LPS and followed by three times injection of MPS which had a high incidence of ON of up to 93% and low or no mortality (Qin L. et al. 2006; Sheng H. et al. 2009; Zhang G. et al. 2009a). Both static and dynamic imaging modalities were employed to study intra- and extra- vascular pathogenic events contributing to ON using a modified ON-inductive protocol. The results showed that intravascular thrombosis and extravascular lipid-deposition were the key pathogenic pathways in SAON (Qin L. et al. 2006; Sheng H. H. et al. 2007; Sheng H. et al. 2009). The extravascular pathway is attributed to lower osteogenic differentiation ability of the host BMSCs but significantly increased differentiation into adipocytes and its proliferation, resulting in increased local edema (Qin L. et al. 2006; Sheng H. H. et al. 2007). ON formation was found as early as week 2 post-induction. Histopathologically, a classical ON feature was found 4-6 weeks post-induction, i.e. necrotic bone with empty lacunae surrounded by necrotic marrow; that was further classified with either destructive repair (granulation tissue creep linked to necrotic bone resorption) or preparative ON with appositional bone formation, with a significant decrease in local blood perfusion confirmed by dynamic perfusion MRI (Sheng H. et al. 2009). For angiographic vasculature between week 4-6 post-induction, blocked trunk vessels surrounded by both disconnected small vessels and disseminated leakage substance was found in local ON lesion using micro-CT based angiography, suggesting a clear cell-molecule-structure-function mechanism of the neovascularization involved in its inadequate repair (Qin L. et al. 2006; Zhang G. et al. 2006).

1.5. Osteogenic Icaritin from *Epimedium*-derived flavonoids

Many Traditional Chinese herbs have been used for orthopaedic diseases, including ON and OP, for thousands of years in China. *Epimedium*, a kind of 'kidney-tonifying' herb, was used over thousands of years for treatment of bone and related diseases in oriental countries (Lu X. et al. 2005; Zhang G. et al. 2007b). Recent study showed that *Epimedium*-derived flavonoids (EF) exerted anabolic effects on osteoporotic bone and prevention effect on SAON due to its osteogenic and anti-adipogenic effects (Zhang G. et al. 2007a; Qin L. et al. 2008; Sheng H. et al. 2008; Zhang G et al. 2008; Songlin P. et al. 2009). In order to identify active compounds metabolized in vivo as an essential step to understand which part of the oral herbal compound reached to local target organ or tissues, the serum of patients treated with EF were recently examined. The results showed that instead of flavonoid compounds, small molecule Icariin, Icariside II and Icaritin were detected as an intestinal metabolite of a parent ring similar to phytoestrogen (Wang Y. K. et al. 2005; Wang X. L. et al. 2007; Wang X. L. et al. 2008) and their structure is showed at (Fig1.4). The *in vivo* studies suggested that icariin was able to promote the BMSCs' osteogenic ability by preventing its differentiation into adipocytes in steroid-treated animals (Chen K. M. et al. 2007; Sheng H. et al. 2008; Zhao J. et al. 2008) and it is also a potential osteoinductive compound for bone tissue engineering (Zhao J. et al. 2009). Icaritin is a flavonone that is hydrolyzed from icariin and these two hydrolytic metabolites may also be pharmacologically active (Tian L. et al. 2004; Huang J. et al. 2007). Using SAON model in rabbit, Icaritin was indeed

demonstrated the prevention effect on ON (Zhang G. et al. 2007a; Qin L. et al. 2008). It was also found that Icaritin could enhance the differentiation and proliferation of osteoblasts, facilitate matrix calcification, inhibit osteoclastic differentiation in both osteoblast-preosteoclast co-culture and osteoclasts progenitor cell culture, and reduce the motility and bone resorption activity of the isolated osteoclasts (Huang J. et al. 2007). The author indicated that Icaritin is more potent than icariin in these aspects. Our recent and on-going studies also show that Icaritin promotes ALP activity of UMR106 osteoblast-like cells (Wang X. L. 2008), promotes periosteum bone formation and inhibits osteoclastic bone resorption as well as facilitate BMSCs differentiate into osteoblasts (Wang X. L. et al. 2008; Xie X. H. et al. 2008; Zhang G. et al. 2008). Most recently, we also reported the role of Icaritin in promotion of the osteoporotic fracture repair in ovariectomized mice attributed to its osteopromotive effect (Zhang G et al. 2008).

Attributed to the prevention effect of Icaritin on SAON and its osteopromotive property, Icaritin could be considered to treat the bone defect after core decompression of SAON. In order to improve the long-term efficacy and reduce the dosage use of the drug, the local administration shall be a better way. In order to ensure that Icaritin could be located at the local treatment site and have a long-term effect, a drug delivery system or a controlled release system is needed for this object.

1.6. Biodegradable materials as drug delivery or bone substitute

A common approach in bone tissue engineering to promote osteogenesis is the three-dimensional (3D) scaffold that serves as a bone graft substitute for cell

interactions and to provide structural support for the new bone ingrowth. Scaffolds for bone regeneration should meet several criteria to make this function come true, including mechanical properties, biocompatibility and biodegradability at a rate commensurate with remodeling (Karageorgiou V. et al. 2005; Drosse I. et al. 2008). Both polymers and ceramics can be used for bone tissue engineering (Hollister S. J. 2005; Karageorgiou V. et al. 2005). Polymers are typically biodegradable and can be fabricated into scaffolds, such as PLA (Poly (glycolic acid)), PGA (poly (lactic acid)) and PLGA (Poly (L-lactide-co-glycolide). PGA is a highly insoluble polymer and PLA will also degrade in vivo from 1 to 6 years so it can be manufactured in screws or pins (Kacey G. M. 2005). The PLGA that consisted of PLA and PGA was shown to completely be resorbed in 12 months (Eppley B. L. et al. 1997). Ceramics comprise a group of biomaterials produced from the heating of natural mineral salts to very high temperatures (Ladd A. L. et al. 1999). Of the different ceramics, the TCP and HA (hydroxyapatite) are widely used for their similar architectural properties and surface chemistry when compared with bone (Hollinger J. O. et al. 1986). HA is a slow resorbing compound while TCP is a relatively fast resorbing ceramics and has been used in formulations to enhance fracture repair (Sanjeev K. et al. 2005). The PLGA and TCP are so well known biomaterials for their excellent biodegradability, biocompatibility and osteoconduction and they can be combined to form porous scaffold and to be used as drug delivery system such as BMP or as bone substitute in bone defect repair (Sherwood J. K. et al. 2002; Fan H. et al. 2006c; Ehrenfried L. M. et al. 2008; Hao W. et al. 2008; Miao X. et al. 2008; Yu D. et al. 2008; Jiang H. J. et

al. 2009; Schneider O. D. et al. 2009). The PLGA has disadvantage that their quick degradation will result in an acid micro-environment due to the formation of lactic and glycolic acid and the accumulation of acids could induce bacteria-free inflammation of the tissues around the implanted site in vivo (Jilek S. et al. 2004; Zhao X. et al. 2005; Chen V. J. et al. 2006; Zolnik B. S. et al. 2006; Kim M. S. et al. 2007; Yoon S. J. et al. 2008). Alkaline calcium phosphate can be introduced to reduce the acidity of the degradation products by neutralize acidity of the degradation acids (Ara M. et al. 2002; Loher S. et al. 2006). By using computer-controlled (rapid-prototype) technology (Fig.1.5), the PLGA and TCP could be fabricated into absorbable porous scaffold materials with desired porous structure such as porosity, pore size and pore connectivity (Wang X. et al. 2001; Wang X. et al. 2007; He K. et al. 2009).

1.7. Hypothesis of this study

Based on our previous and ongoing research as well as related research works of others, we formulate the following hypothesis that composite 3D scaffold material PLGA/TCP incorporated with Icaritin will facilitate its integration with host bone for achieving better significant surgical outcome after core decompression surgery, i.e., this novel composite material will offer structural reinforcement and promote osteogenic potential for adequate repair of SAON lesion in its early stage.

1.8. Objectives of this thesis work

The overall objectives of this thesis work were to evaluate the efficacy potential for adequate repair of SAON lesion in its early stage and its potential underlying

mechanisms. Specific objectives of the present study included both in vitro and in vivo part:

Firstly, Icaritin was incorporated into the PLGA/TCP using computer-controlled (rapid-prototype) technology to from a porous composite scaffold and its structural and mechanical characteristics were evaluated;

Secondly, the PLGA/TCP/Icaritin composite scaffold was put into the saline and its degradation characteristics were evaluated including the structural and the mechanical changes. The released property of Icaritin from scaffold was also examined at the same time.

Thirdly, the cytotoxicity, biocompatibility and the osteogenic properties of PLGA/TCP/Icaritin composite scaffold were evaluated by using L929 cells, BMSCs and UMR 106 cells.

Fourthly, a SAON rabbit model was established with combined administration of LPS and MPS and then the impaired bone healing was observed at the distal femora after a bone defect with 3mm in diameter was made. The osteopromotive effect of PLGA/TCP/Icaritin composite scaffold was evaluated by implanting the scaffold into the bone defect area. The micro-CT was used to evaluate the quantification of newly formed bone in bone tunnel and the histology was used to describe the histomorphology and observe the biological response of scaffold. The E-modulus and the compression strength of new bone in tunnel were evaluated by compression test.

1.9. Figures and Legends

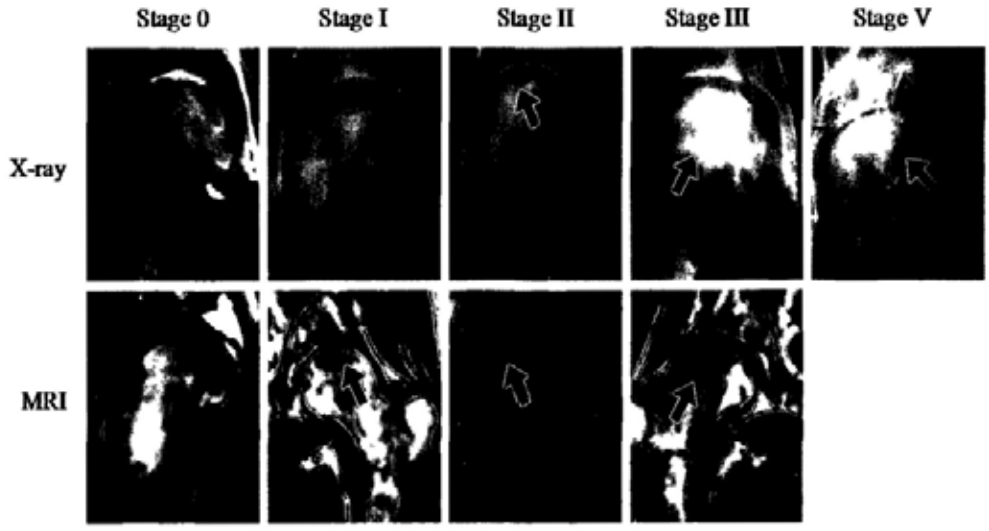

Fig.1.1. 5 stages of ON (arrow) from X-ray and MRI according to the ARCO staging system (Malizos K. N. et al. 2007).

Fig.1.2. Core decompression procedure (arrows) of femoral heads with corticosteroids induced ON (Assouline-Dayan Y. et al. 2002).

Fig.1.3. Left femoral head with ON was treated with bone graft (arrows) (Assouline-Dayan Y. et al. 2002)

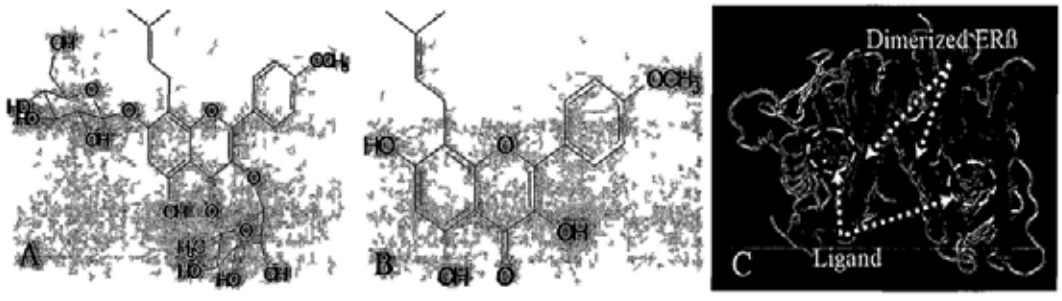

Fig.1.4. A: Structure of icariin; B: structure of Icaritin; C: Computer aided molecular design for ligand-receptor-docking also demonstrated Icaritin was the one with strong binding capability to estrogen-receptor-beta when compared to those seven EFs due to large size of those seven flavonoid molecules before intestinal metabolism of their side chain, which could not be put into the "pocket", i.e. ligand-binding-domain of receptor (Zhang G. et al. 2009c).

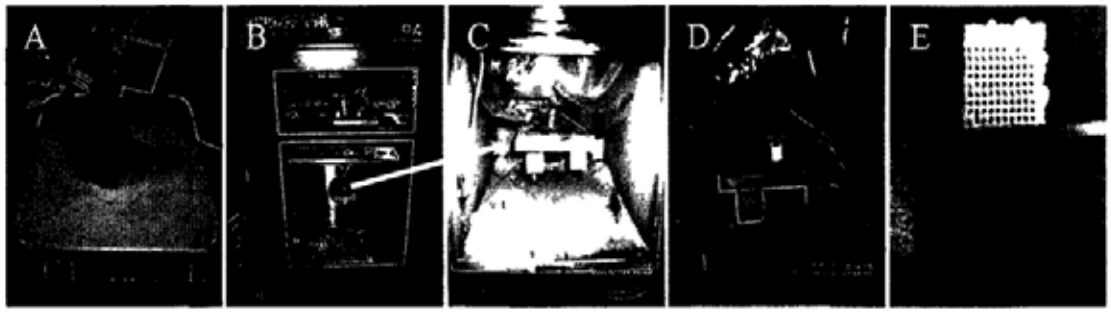

Fig.1.5. Process of preparation of PLGA/TCP scaffold. A: Mixture of PLGA/TCP; B: rapid-prototype machine; C: Computer-driven nozzle according to the predesigned model; D: The paste was spurted out layer-by-layer to form scaffold; E: The PLGA/TCP scaffold with porous structure.

1.10. Table

Tab.1.1. Approaches for diagnosis and stage-based interventions according to ARCO staging system.

	Diagnosis	Treatment
Stage 0	Bone biopsy, Bone scan, MRI	Prevention: Pharmacotherapy Physical therapy
Stage I	Bone scan, MRI	1. Nonoperative Treatment: Pharmacotherapy Physical therapy 2. Operative Treatment: Core decompression Core decompression with bone grafting Core decompression with bone marrow Core decompression with cells Core decompression with growth factors Tissue-engineered approach
Stage II	Radiographs or CT, Bone scan, MRI	Operative Treatment: Core decompression Core decompression with bone grafting Core decompression with bone marrow Core decompression with cells Core decompression with growth factors Tissue-engineered approach Osteotomy
Stage III	Radiographs	Operative Treatment: Core decompression with bone grafting Core decompression with bone marrow

		Core decompression with cells Core decompression with growth factors Tissue-engineered approach Osteotomy Arthrodesis Total hip arthroplasty
Stage IV	Radiographs	Operative Treatment: Arthrodesis Total hip arthroplasty

Chapter 2

Establishment of an innovative PLGA/TCP scaffold incorporating osteopromotive phytoestrogenic Icaritin

2.1. Introduction

Bone grafts are widely used in orthopaedic clinics, either as substitute or filler in repair of bone defect resulting from trauma, tumour or metabolic diseases, such as ON (Levin L. S. 2006; Hungerford D. S. 2007; Nishida J. et al. 2008; Zhang G. et al. 2009b). The autologous bone is considered the "gold standard" but harvesting or loss of host bone can result in donor site morbidity (Meland N. B. et al. 1992; Bodde E. W. et al. 2003). Using homologous or heterologous grafts from bone bank could avoid part of the problem associated with use of autograft, but there would be potential risks of viral or bacterial infections and immune response (Stevenson S. 1987; Lord C. F. et al. 1988; Stevenson S. et al. 1996; Ninin E. et al. 2001). PLGA (Fig.2.1) and TCP are well known for their excellent biodegradability, bio-absorbability and osteoconduction when fabricated in form of porous scaffold and used as bone substitute (Miao X. et al. 2008; Yu D. et al. 2008; He K. et al. 2009; Schneider O. D. et al. 2009).

However, the limitation of these inorganic synthetic polymer and organic bioceramics materials was lack of osteogenic potential or even osteoinductive potential. Endogenous growth factors, such as VEGF, TGF-β and BMPs, played an important role in tissue healing and they were loaded into composite scaffold biomaterials in vitro before implantation in vivo to promote bone or cartilage healing (Mont M. A. et al. 1998; Lieberman J. R. et al. 2004; Fan H. et al. 2006a; Tang T. T. et al. 2007; Fan H. et al. 2008). Porous beta-TCP loaded with BMP-2 gene-transducted BMSCs was tested to repair the bone defects, such as for repair of

ON lesions (Tang T. T. et al. 2007). Except the gene transfer technology, the usually used method was to dip the scaffold into growth factor(s) solution before their implantation in vivo. However, the shortcomings for these growth factors were difficulties with the incorporation of these proteins in proper vehicles or gene security (Cancedda R. et al. 2007).

Previous work showed that Icaritin, an exogenous small bioactive molecule from herbal compound *Epimedium*, was able to enhance the differentiation and proliferation of osteoblasts, facilitate matrix calcification, inhibit osteoclastic differentiation in both osteoblast-preosteoclast co-culture and osteoclasts progenitor cell culture (Huang J. et al. 2007). Our research also confirmed that Icaritin was the metabolite of *Epimedium* in serum that was able to stimulate osteogenesis and inhibit adipogenesis of BMSCs and promote periosteum bone formation (Zhang G. et al. 2007a; Qin L. et al. 2008; Wang X. L. et al. 2008; Zhang G. et al. 2009a; Zhang G. et al. 2009c). Icaritin could keep its bioactivity even when dissolved in organic solution dimethyl sulphoxide (DMSO) (Huang J. et al. 2007; Wang X. L. et al. 2008) and PLGA/TCP could be fabricated into absorbable porous scaffold materials using computer-controlled fine biospinning technology (Wang X. et al. 2001; Wang X. et al. 2007).

As porous PLGA/TCP has good osteoconduction and Icaritin can promote bone formation (osteopromotive effect), the work designed for this chapter aimed at fabricating an innovative porous osteopromotive PLGA/TCP scaffold incorporated with phytoestrogenic Icaritin, that might have designed porous structure with initial

mechanical stability.

2.2. Materials and Methods

2.2.1. Materials

Icaritin (Fig.2.1) was provided by the Institute of Traditional Chinese Medicine & Nature Product, Jinan University, China. The PLGA, 75:25 by mole ratio of lactide to glycolide, weight average molecular weights Mw = 115,000, number average molecular weight Mn = 96,000 and polydispersity Mw/Mn = 1.2) was purchased from the Institute of Biomaterials of Shandong, China. Amorphous TCP ceramic powders with 50μm in diameter were purchased from Beijing Organic Chemical Plant, China. All the chemicals were of analytical quality.

2.2.2. Preparation of porous PLGA/TCP/Icaritin composite scaffolds

The porous PLGA/TCP/Icaritin scaffolds were fabricated by a low-temperature spinning technique using a rapid prototyping machine (CLRF-2000-Ⅱ, Tsinghua university, Beijing, China) (Wang X. et al. 2006; Wang X. et al. 2007; He K. et al. 2009). The dose of Icaritin (74mg per 100g PLGA/TCP) was selected from an effective therapeutic dose reported previously (Shen P. et al. 2007; Wang X. L. et al. 2008). The PLGA was dissolved in 1, 4-dioxane to form a homogeneous solution and the TCP powders were added to the PLGA solution with a TCP : PLGA ratio of 1/4 (w/w) according to the established protocol for the proper consistency of mixture and proper mechanical property of scaffold (He K. et al. 2009). The Icaritin was also dissolved in 1, 4-dioxane to form a homogeneous solution. Then the two solutions were mixed and stirred using magnetic rotator for 10 minutes to form a uniform

liquid paste. The pure PLGA/TCP scaffold was used as reference scaffold material for comparison. After that, the paste was spurted out at the thickness and the distance of 500μm (default pore size) layer-by-layer by a computer-driven nozzle according to the predesigned model (Zein I. et al. 2002; Wang X. et al. 2006) to form scaffold block of 10x10x10mm^3. Such layer-by-layer fabrication technique granted a larger compression force in its axial direction, i.e. from top to bottom than the site in a lateral direction. This was confirmed by biomechanical machine as specified below. The fabrication temperature in the refrigerator was -28℃. Then the scaffolds were stored in a dry vacuum for 24 hours and sealed in plastic bag before evaluations specified below.

2.2.3. Characterization of PLGA/TCP/Icaritin composite scaffolds

2.2.3.1. Macroscopic observation

The macrostructures of four porous scaffolds were examined using a camera (COOLPIX 4500 Nikon, Japan) and then scanned by a high-resolution micro computed tomography (micro-CT).

2.2.3.2. Micro-CT evaluation

In order to quantify three-dimensional (3D) structure of the scaffolds, a high-resolution micro-CT (vivaCT40, Scanco Medical, Brüttisellen, Switzerland) was used with a spatial resolution of 20μm for scanning according to published protocol (Yeung H. Y. et al. 2005; Ho S. T. et al. 2006). The two-dimensional (2D) images were acquired directly from the scanning and the 3D structure was reconstructed by the volume of interest (VOI) where an optimized threshold was

used to isolate the scaffold materials. The size of pores was calculated in 2D images and the porosity of the scaffolds was calculated as the void volume of the biomaterials in 3D images as well as macropores interconnectivity, calculated as volume of interconnected pores/volume sum of interconnected and closed pores)×100% (Ho S. T. et al. 2006). After micro-CT scanning, the scaffolds were cut into small blocks for scanning electron microscope (SEM, JEOL JSM-6390, Tokyo, Japan) examination.

2.2.3.3. Surface morphology and composition evaluation

Porous scaffolds at a thickness of 2mm were prepared, freeze-dried and coated with gold using a Scancoat Six SEM sputter coater system using established conditions (Leng Y. et al. 2003; Fan H. et al. 2006b; Fan H. et al. 2006c). SEM was used to characterize both surface morphology and composition of PLGA/TCP/Icaritin porous scaffolds at 15 kV, 5.0mA. The scaffolds were analyzed using energy disperse spectroscopy (EDS).

2.2.3.4. Porosity analysis

The porosity of the PLGA/TCP/Icaritin scaffolds was determined using our published protocols (Zhang R. et al. 1999; Yeung H. Y. et al. 2005). Ethanol was used as the displacement liquid for its easy penetration into the pores (Zhang R. et al. 1999). The PLGA/TCP/Icaritin scaffolds (n = 6) were immersed into a 5ml ethanol (V1) in a test tube and the air inside the scaffolds was removed in a vacuum chamber. The total volume (V2) of ethanol and the ethanol-penetrated scaffolds was recorded. Then the ethanol-penetrated scaffolds were removed and the rest volume of ethanol

was recorded as V3. The volume of ethanol-penetrated scaffold was (V2 − V3) and the volume of ethanol penetrated into scaffold was (V1 − V3). Thus the porosity or space volume fraction of the PLGA/TCP/Icaritin porous scaffolds was calculated by following formula: Porosity (%) = (V1 − V3) / (V2 − V3) × 100%

2.2.3.5. Water absorption

To evaluate the hydrophilicity of materials, the PLGA/TCP/Icaritin porous scaffolds were respectively dipped into distilled water and the bubbles were pumped out in vacuum for facilitating the water to penetrate into the materials. Then the scaffolds were incubated at 37℃ for 48 hours. After that, the scaffolds were taken out from distilled water and the surface water was wiped off for weighting the wet mass (W_w). Then the same scaffolds were dried in vacuum for 24 hours. The scaffolds were then dried and weighted as W_d and then the water absorbability was calculated according to the following formula: Water absorption (%) = (W_w − W_d) / W_d × 100% (Yang F. et al. 2006; Yang Y. et al. 2008).

2.2.3.6. Mechanical properties

Mechanical properties of both PLGA/TCP and PLGA/TCP/Icaritin scaffolds (n = 6) were evaluated using our established indentation test (Lai Y. M. et al. 2005; Qin L. et al. 2005b; Leung K. S. et al. 2006). A 5mm diameter indentation rod was connected to a 250N load cell of a mechanical testing machine (H25K-S, Hounsfield Test Equipment, UK) and loaded onto the centre of the scaffolds block ($0.5\times0.5\times0.5cm^3$) at a compression speed of 5mm/min until the scaffolds yielded and get the F-λ graph. The compression directions included both axial and lateral one to

test potential difference in compression properties due to anisotropy of the scaffolds. The E-modulus (MPa), compressive strength (MPa), and energy (J) up to yield of the scaffold were recorded for comparison. The energy was calculated by the software attached to the mechanical test machine.

Compression strength: f=F/S

E-modulus: = (F/S)/(dL/L)

F: Failure load (N); S: Area of force (m2); dL: reduced length at failure load; L: Original length of scaffold.

2.2.4. Icaritin content in PLGA/TCP/Icaritin porous scaffolds

In order to confirm if the incorporated Icaritin would be remained in the PLGA/TCP/Icaritin scaffold after going through both preparation and fabrication processes, scaffolds in an average weight of 150mg (n=6) were prepared and dissolved in acetoacetate. After the sample was dried with nitrogen, 100μl methanol was added and vortex-mixed vigorously for 30 seconds. The Icaritin content in scaffold was evaluated using high performance liquid chromatography (HPLC, 166 NM UV Detector, Beckman). The concentration of Icaritin was detected at a wave length of 270nm and then converted into total released amount of Icaritin (Wang X. L. et al. 2009).

2.2.5. Statistical analysis

All quantitative data were expressed as mean ± standard error (SE). Unpaired Student's t-test was used to compare the difference between two groups using SPSS version 10.0 (SPSS, Chicago, IL, USA). Statistical significance was set at $p < 0.05$.

2.3. Results

2.3.1. Macroscopic observation

Both PLGA/TCP and PLGA/TCP/Icaritin scaffolds in a size of 10x10x10mm^3 showed uniform textures with regular macropores (Fig.2.2 A1 and B1). The PLGA/TCP scaffold was white while the PLGA/TCP/Icaritin was light yellowish. The distribution of Icaritin within PLGA/TCP was granted through liquid paste mixing procedure as described above in the methodology. 2D micro-CT images demonstrated macropores (Fig.2.2 A2 and B2) that were interconnected based on 3D reconstruction by a workstation of vivaCT (Fig.2.2 A3, A4, B3 and B4). The average size of macropores in PLGA/TCP and PLGA/TCP/Icaritin porous scaffolds did not differ statistically, with 492.8 ± 24.0μm and 477.5 ± 29.7μm in diameter, respectively (Tab.2.1). This was qualitatively confirmed by SEM (Fig.2.3 A1 and B1), suggesting that the incorporated Icaritin did not change the macrotexture of the PLGA/TCP scaffold.

2.3.2. Microstructure and composition analysis

The SEM demonstrated that the original surface of both groups was porous and TCP particles distributed homogenously on the trabeculae of the scaffolds (Fig.2.3 A1 and B1). When magnified, numerous micropores were observed that were distributed over the surface of trabeculae (Fig.2.3 A2 and B2). The micropores were hardly delineated by micro-CT due to their small pore size ranging from 2 to 15μm (Fig.2.3 A3 and B3). The micropores were interconnected, either ellipsoidal or round in shape in both groups. The surface composition of the scaffolds obtained by EDS

demonstrated the presence of C, O, P and Ca element (Tab.2.2). Qualitative EDS analysis showed that the weight percentage of C, O, P and Ca in PLGA/TCP group was 32.9 ± 3.1%, 51.9 ± 4.0%, 6.4 ± 1.0%, and 8.9 ± 1.0%, respectively, while in PLGA/TCP/Icaritin group was 34.9 ± 2.7%, 50.8 ± 1.8%, 5.5 ± 1.7%, and 8.8 ± 2.8%, respectively. The ratio of Ca to P was 1.67, which is similar to the ratio in human bone.

2.3.3. Quantification of scaffold porosity and interconnection

There was no significant difference found in quantitative data between the two groups. The absorbed volume of ethanol after immersing the scaffold was used to evaluate the average volume of pores in the scaffolds, with 74.9 ± 1.0% for PLGA/TCP and 75.0 ± 2.3% for PLGA/TCP/Icaritin ($p>0.05$) (Tab.2.1). The porosity measured by micro-CT was significantly smaller that ethanol immersion method, with 37.9 ± 2.1% for PLGA/TCP and 36.9 ± 1.9% for PLGA/TCP/Icaritin (Tab.2.1). The macropores interconnectivity was 100% for both PLGA/TCP and PLGA/TCP/Icaritin ($p>0.05$) (Tab.2.1).

2.3.4. Water absorption

Water absorption of scaffolds showed no statistical significant difference, with 197.6 ± 12.2% for PLGA/TCP group and 199.2 ± 9.7% for PLGA/TCP/Icaritin group (Tab.2.1).

2.3.5. Mechanical properties

All the specimens were tested to failure. Statistically, the E-modulus, the compressive strength and energy of the scaffold at yield, i.e. within the elastic region

for both axial and lateral compression directions did not differ between PLGA/TCP and PLGA/TCP/Icaritin scaffolds (Tab.2.3). These three parameters of the axial compression test in PLGA/TCP/Icaritin group were 44.7 ± 2.2MPa, 3.4 ± 0.5MPa and 29.6 ± 3.3 (10^{-3}J), which was significantly higher than that from the lateral compression test ($p < 0.05$ for all). The same results were seen in PLGA/TCP group.

2.3.6. Icaritin content in PLGA/TCP/Icaritin composite scaffolds

HPLC results showed that the actual Icaritin content was 68.6 ± 2.7mg per 100g PLGA/TCP/Icaritin scaffold which was similar to that predesigned. As negative control, no Icaritin was detected in PLGA/TCP scaffold.

2.4. Discussion

The work in this chapter was to report our multidisciplinary approach to fabricate an innovative phytoestrogenic Icaritin releasing PLGA/TCP-based porous scaffolds for potential bone tissue engineering. The results demonstrated that our novel scaffold had a desired pore structure, mechanical properties, and feature of slow release of exogenous osteopromotive Icaritin.

Scaffold biomaterials have been developed for various orthopaedic applications (Hollister S. J. 2005; Karageorgiou V. et al. 2005; Fan H. et al. 2006c; Rüegsegger P. et al. 2007; Place E. S. et al. 2009). Polymeric scaffold material such as PLGA was biodegradable and had good biocompatibility to support the cell attachment and growth (Ignatius A. A. et al. 1996). The biodegradable polymers with ceramics were examined in an attempt to improve the osteoconductivity of scaffolds (Dunn A. S. et al. 2001; Ignjatovic N. et al. 2006; Ehrenfried L. M. et al. 2008). The addition of TCP

to PLGA was able to buffer the pH to higher levels in vicinity of the sample which reduced the risk of inflammation in vivo, a means to obtain a fully absorbable sample with degradation properties that match in vivo requirements, while the mechanical properties of pure PLGA was also improved by the addition of TCP (Ehrenfried L. M. et al. 2008). As PLGA and TCP could be fabricated by a rapid prototyping technique (He K. et al. 2009), this provided us the excellent opportunity to incorporate exogenous phytochemical compounds into the PLGA/TCP. The slow-release property of osteopromotive agent from the porous scaffold is highly desirable for in vivo applications where sustainable presence of osteopromotive factors is essential to grant continuous osteogenesis and maximize the treatment efficiency. Our result revealed that up to post-dipping week 12, the percentage release of Icaritin from scaffold was about 72.01%. Though the in vitro release tests can not fully represent in vivo release dynamics of Icaritin, it is the essential step before moving into in vivo studies to confirm the osteopromotive effects potentially in a dose-dependent manner.

Porosity and pores size were important factors in development of scaffold materials for orthopaedic applications. The ideal scaffold should provide a temporary framework for angiogenesis and subsequent neovascularization, cell attachment and proliferation leading to new bone formation or regeneration. A typical pore diameter of at least 100μm is known to be compulsory for cell penetration due to cell size, migration requirements and a proper vascularization of the ingrown tissue; pore sizes around 300μm are also appreciated to enhance new bone formation and formation of

capillaries (Griffith L. G. 2002; Karageorgiou V. et al. 2005; Rezwan K. et al. 2006). Published experimental study demonstrated that small pores provided favorable hypoxic conditions and were able to induce osteochondral formation before osteogenesis, while large pores provided neovascularization, leading to direct osteogenesis, without preceding cartilage formation (Karageorgiou V. et al. 2005). In PLGA/TCP/Icaritin scaffold, two levels of pores were formed using computer-driven nozzle during fabrication at low temperature in the present study. As programmed, the macropores were formed with a size range between 450 to 500μm in diameter as measured by high-resolution micro-CT and the micropores within trabeculae were formed ranging from 2 to 15μm during vacuum drying process as shown by SEM. Porosity of PLGA/TCP/Icaritin was about 75.0% measured by ethanol immersion method while micro-CT and SEM confirmed interconnection of both macro- and micro- pores inside of scaffold. As the incorporation of Icaritin into PLGA/TCP did not change the porosity, pores interconnectivity and the structure of PLGA/TCP scaffold, such optimal structural features would benefit local nutrition exchange (Kruyt M. C. et al. 2003; Ivirico J. L. et al. 2009). As compared with ethanol immersion method, the lower percentage of porosity data found in micro-CT data was explained by its scanning resolution set at 20μm where pores with size smaller than this threshold were not detectable, while the organic solvent ethanol with a molecular size of 0.44nm could penetrate and fulfill those micropores (Lalik E. et al. 2006). The water absorption reflected the extent of hydrophilicity of scaffold materials and the hydrophilicity of scaffold was not changed by incorporating Icaritin.

High hydrophilicity was reported beneficial for scaffold to absorb more nutrition from environment to the whole volume of the scaffold (Ivirico J. L. et al. 2009).

As mentioned in the results, the element of PLGA/TCP scaffold remained unchanged when Icaritin was incorporated. The average ratio of Ca to P was 1.5-1.6 which was similar to that in human bone. PLGA and TCP mimic the inorganic and organic component respectively for bone. Calcium phosphate in the materials would enhance the bone regeneration and graft material resorption in bone defects (El-Ghannam A. et al. 2004). During degradation, soluble Ca and P ions released from the porous scaffolds would give rise to both intracellular and extracellular responses at the interface of the materials with its cellular environment and give an ideal environment for colonization, proliferation and differentiation of the cells to form new bone that had a mechanically strong bond to the implant surface (Hench L. L. et al. 2002).

For potential clinical applications, porous scaffold materials must meet local mechanical demands as well. It is known that the properties of synthetic composite scaffold may vary with their crystallinity, grain size, porosity, and composition (Rezwan K. et al. 2006). In this study, the E-modulus and the compression strength of PLGA/TCP/Icaritin porous scaffold in axial direction were 44.7 ± 2.2MPa and 2.4 ± 0.5MPa, respectively. Taken the axial loading properties for comparison with other popular orthopaedic scaffold materials, the E-modulus and compression strength were 2-7.5MPa and 0.1-0.2MPa in PLGA/HA (Guan L. et al. 2004), 51.0MPa and 0.4MPa in PLGA/bioglass (Lu H. H. et al. 2003) as compared with 100-500MPa and

4-12MPa reported for cancellous bone (Giesen E. B. et al. 2001).. The mechanical properties of PLGA/TCP/Icaritin approached that of cancellous and were superior to those reported biomaterials. Like cancellous bone, the mechanical property of PLGA/TCP/Icaritin was anisotropy. The E-modulus, compression strength and energy at yield in axial direction was about 4.6, 2.3 and 9.0 times higher than those tested in a lateral direction, as it was already predetermined by its spinning alignment principle, i.e. the materials were layered from bottom to top (Zein I. et al. 2002; Wang X. et al. 2006; He K. et al. 2009). This implies that attention must be paid to its placement into bony defect during clinical application, i.e. to orientate scaffold material with its principle axis vertically towards the loading direction of the treated skeletal site.

Icaritin is a small molecule which was found as an intestinal metabolite with a parent ring similar to phytoestrogen that had the potential to treat the osteoporotic fracture (Wang X. L. et al. 2007; Zhang G et al. 2008). It also has the ability to keep the BMSCs' osteogenic ability by preventing its differentiation into adipocytes in SAON in animals (Chen K. M. et al. 2007; Qin L. et al. 2008). The confirmed content of Icaritin in PLGA/TCP/Icaritin porous scaffold might suggest its potential applications for enhancement of bone repair.

2.5. Conclusion

In conclusion, we successfully incorporated a phytoestrogenic molecule Icaritin into PLGA/TCP to form an innovative osteopromotive porous scaffold in this chapter. The incorporation of Icaritin did not alter both structural and mechanical properties

of the porous PLGA/TCP scaffold and the content of Icaritin in scaffold was consistent with that predesigned. The regular porous structure, the capability of carrying with bioactive molecular and the proper mechanism of the scaffold indicated its potential application in orthopaedics. Biodegradation is an important property for biomaterials in tissue engineering or as bone substitute, accordingly, the next chapter will be investigating the effect of the release of the incorporated Icaritin during degradation of this composite scaffold in vitro.

2.6. Figures and legends

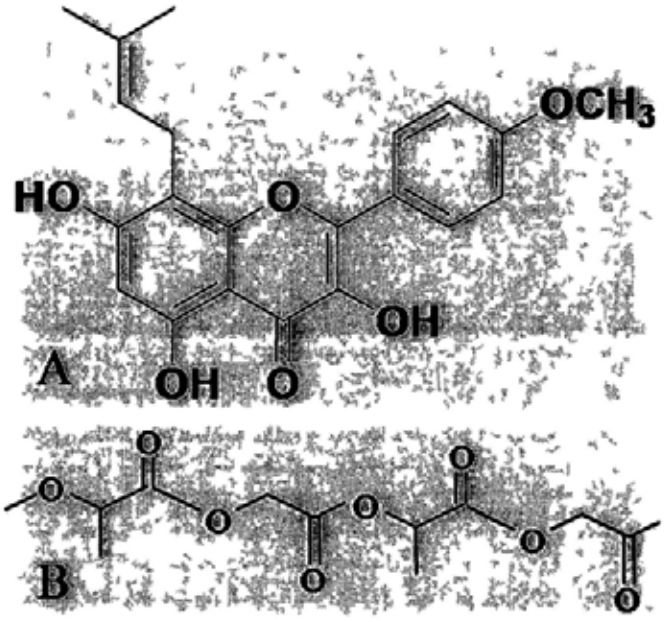

Fig.2.1. A: Structure of Icaritin from *Epimedium*-derived flavonoids with parent rings that demonstrated benefit effect on promotion of osteogenesis due to its phytoestrogenic nature (Chen K M. et al. 2007; Zhang G. et al. 2009a); B· Structure of PLGA (Kacey G. M. 2005).

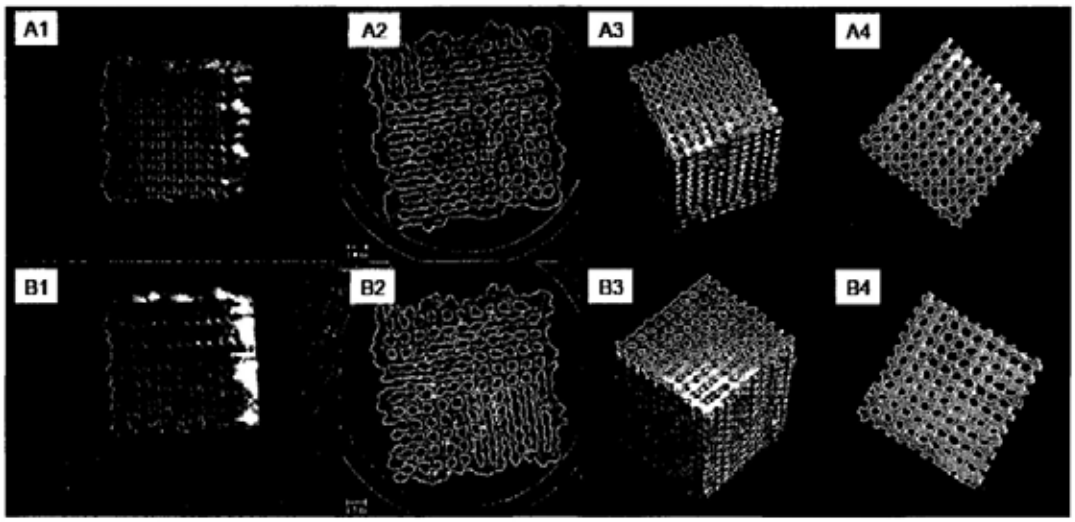

Fig.2.2. Comparison of PLGA/TCP with PLGA/TCP/Icaritin scaffolds. Macroscopic observation of scaffolds: (A1) PLGA/TCP scaffold in white; (B1) PLGA/TCP/Icaritin scaffold with homogonously distributed Icaritin in light yellowish as Icaritin powder is yellow in colour before mixing into PLGA/TCP. 2D structure of the porous scaffolds by micro-CT: (A2) PLGA/TCP scaffold; (B2) PLGA/TCP/Icaritin scaffold (Arrows point to the maropores). 3D structure of the porous scaffolds by micro-CT: (A3) PLGA/TCP scaffold; (B3) PLGA/TCP/Icaritin scaffold. Interior section from 3D structure of the scaffold: (A4) PLGA/TCP scaffold; (B4) PLGA/TCP/Icaritin scaffold.

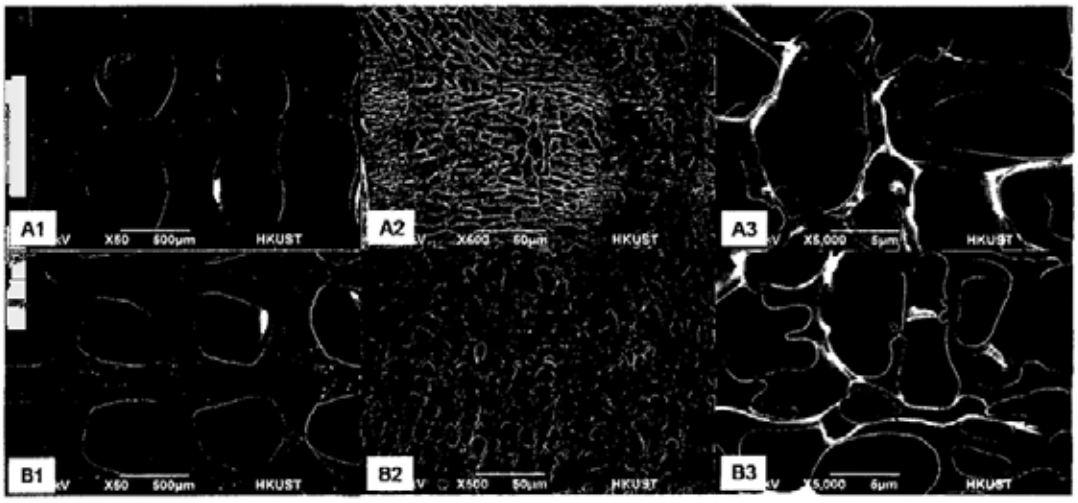

Fig.2.3. Surface morphology of the porous scaffolds by SEM (1: 50×; 2: 500×; 3: 5000×): (A) PLGA/TCP scaffold; (B) PLGA/TCP/Icaritin scaffold. (A1 and B1: Arrows point to the TCP particles and frames are region of interests that are magnified and shown in A2 and B2; Frames in A2 and B2 are magnified and shown in A3 and B3, with arrows pointing to the micropores in A3 and B3).

2.7. Tables

Tab.2.1. Macropore size, porosity and water absorption of PLGA/TCP and PLGA/TCP/Icaritin scaffolds.

	PLGA/TCP (n = 6)	PLGA/TCP/Icaritin (n = 6)
Macropore size (μm)	492.8 ± 24.0	477.5 ± 29.7
Porosity by ethanol immersion (%)	74.9 ± 1.0	75.0 ± 2.3
Porosity by micro-CT (%)	37.9 ± 2.1	36.9 ± 1.9
Macropores connectivity (%)	100	100
Water absorption (%)	197.6 ± 12.2	199.2 ± 9.7

Tab.2.2. The surface composition of PLGA/TCP and PLGA/TCP/Icaritin scaffolds by EDS.

Groups	C (%)	O (%)	P (%)	Ca (%)	Ca/P ratio
PLGA/TCP	32.9 ± 3.1	51.9 ± 4.0	6.4 ± 1.2	8.9 ± 1.0	1.5 ± 0.3
PLGA/TCP/Icaritin	34.9 ± 2.7	50.8 ± 1.8	5.5 ± 1.7	8.8 ± 2.8	1.6 ± 0.2

Tab.2.3. Mechanical properties of PLGA/TCP and PLGA/TCP/Icaritin for axial and lateral compression test.

	PLGA/TCP (n=6)		PLGA/TCP/Icaritin (n=6)	
	Axial	Lateral	Axial	Lateral
E-modulus (MPa)	44.4 ± 2.4*	8.6 ± 0.8	44.7 ± 2.1*	9.7 ± 0.8
Compression strength (MPa)	3.3 ± 0.8*	0.9 ± 0.2	3.4 ± 0.5*	1.0 ± 0.1
Energy of yield (10^{-3}J)	31.9 ± 2.1*	10.8 ± 1.1	29.64 ± 3.3*	10.4 ± 1.0

* $p < 0.05$ as compared between axial and lateral directions.

Chapter 3

Structural and degradation characteristics of the innovative PLGA/TCP/Icaritin composite scaffold in vitro

3.1. Introduction

The concept of tissue engineering is to use degradable porous material scaffolds integrated with biofactors, such as cells, genes, molecules and/or proteins, to regenerate the damaged tissues (Langer R. et al. 1993; Hollister S. J. 2005; Place E. S. et al. 2009). The biodegradable bone graft substitute included the inorganic synthetic polymer and organic bioceramics (Griffith L. G. et al. 2002; Hench L. L. et al. 2002). They can be combined to form porous scaffold and to be used as drug delivery system or as bone substitute in bone defect repair (Sherwood J. K. et al. 2002; Fan H. et al. 2006c; Ehrenfried L. M. et al. 2008; Hao W. et al. 2008; Yu D. et al. 2008; He K. et al. 2009). The combination of TCP-based ceramics with biodegradable polymers is a promised approach that yields composites materials with desirable controlled degradation (Kacey G. M. 2005). In order for a tissue engineering scaffold to be successful for a long time, the scaffold materials must have a rate of degradation that acts in concert with the new tissue ingrowth. Ideally, the scaffold would degrade slowly enough to maintain structural support during the initial stages of bone formation, but fast enough to allow space for continuous growth of new bone in vivo (Hedberg E. L. et al. 2005).

Although scaffold mimicking the porous structure of bone has been shown to promote favorable cellular activity, the directly influence of scaffold on the cell behavior can be improved through the delivery of growth factors and other bioactive molecules (Richardson T. P. et al. 2001; Porter J. R. et al. 2009; Tabata Y. 2009). Controlled release of bioactive molecules or drugs from biodegradable

scaffolds was proved to be an ideal administration methods in which the rapid diffusion from the target site would be avoid (Biondi M. et al. 2008). Because of the hydrolytically unstable linkages in their backbone and tunable biodegradation rate, polymers have been proved as the most successful materials in controlled delivery of bioactive molecules (Porter J. R. et al. 2009).

In chapter 2, we have successfully incorporated Icaritin into the PLGA/TCP to form a porous composite scaffold. The scaffold incorporated with Icaritin had the regular porous structure and mechanical property, which indicated its potential future clinical applications. But whether Icaritin will influence the biodegradation property of composite scaffold and whether Icaritin could be released from the scaffold is unknown. So it is essential to understand its rate of degradation in vitro and the release kinetics of the osteopromotive Icaritin before application in vivo. In this part, we used physiological saline to mimic in vivo chemical environment of body fluid, and incubated the scaffolds incorporated with different dosages of Icaritin to observe the degradation of the PLGA/TCP/Icaritin at various concentrations in vitro. The dosing effect of the incorporated Icaritin on degradation and structural characteristics of the porous PLGA/TCP/Icaritin composite scaffold as well as the released kinetics of Icaritin from the PLGA/TCP/Icaritin scaffolds were systemically evaluated.

3.2. Materials and methods

The PLGA/TCP/Icaritin and PLGA/TCP scaffolds were incubated in 0.9% saline as degradation medium at 37℃ for 12 weeks. Changes in volume, weight, diameter of macropores, pH value of degradation medium and Ca^{2+} released from the

scaffold were investigated weekly. After 12 weeks, the surface morphology and the element changes were examined by SEM and EDS.

3.2.1. Preparation of PLGA/TCP/Icaritin composite scaffolds

In this part, the different dosages of Icaritin were used to add into the scaffold. The PLGA/TCP/Icaritin composite scaffolds were fabricated by a rapid prototyping machine as the same process as that in chapter-2 (Wang X. et al. 2006; Wang X. et al. 2007; He K. et al. 2009).The dose of incorporated Icaritin was 74mg, 7.4mg and 0.74mg per 100g PLGA/TCP i.e. in PLGA/TCP/Icaritin-H, M and L groups, respectively, based on the level of therapeutic dose reported previously (Shen P. et al. 2007; Wang X. L. et al. 2008). The pure PLGA/TCP scaffold was used as control. After that, the paste was spurted out at the thickness and the distance of 500μm by a computer-driven nozzle to be deposited layer-by-layer into specific positions from bottom to top according to the predesigned model (Zein I. et al. 2002; Wang X. et al. 2006) with a block of $10\times10\times10mm^3$. Then the scaffolds were then stored in dry vacuum conditions for 24 hours and sealed in plastic bag before being used.

3.2.2. In vitro degradation of PLGA/TCP/Icaritin composite scaffolds

PLGA/TCP and PLGA/TCP/Icaritin scaffolds were cut into block with $10x10x10mm^3$ and the original weight of the scaffolds was calculated. 6 samples were used for degradation observation and 6 for Icaritin release evaluation in each group. Another 12 samples with $5x5x5mm^3$ in each group were used for mechanical test. The in vitro degradation was carried out by dipping the specimens into saline which worked as degradation medium and the degradation time lasted 12 weeks. The

scaffold was put into the test tube respectively and the degradation medium was 10 times the volume of the scaffold. The tubes were fixed in warm room with 37℃ and the incubation medium was changed by the fresh saline weekly. The penicillin/streptomycin (Invitrogen, USA) with the end concentration 1% (w/v) was added into saline to prevent the bacterial infection. In each week, the scaffolds were used for characterization.

3.2.3. Characterizations

3.2.3.1. PH value changes of degradation medium

The pH value of degradation medium in tubes was measured with a PH meter (S20-K, USA) before degradation and every week after the scaffolds were immersed into saline with the initial pH value about 7.2.

3.2.3.2. Lactic acid released from the scaffolds

The PLGA was hydrolyzed and released lactate during the degradation, so the lactate released accumulatively into the medium was also be measured by lactate assay kit (K607-100, BioVision, USA) at 1, 6 and 12 weeks, respectively. 10μl medium and the calcium standard were added in wells in a 96-well plate, up to the total volume to 50μl with lactate assay buffer. 50μl of the reaction mixture (46μl lactate assay buffer, 2μl lactate probe and 2μl lactate enzyme mix) were added subsequently to each well containing standards and samples. After being mixed gently and incubated reaction for 30 minutes at room temperature and protect from light, the samples were measured the OD at 570nm. The lactate concentration in the test samples was calculated by the formula C=La/Sv, where La was the lactate acid

amount (nmol) from the standard curve and Sv was the sample volume (ml) added into the well. The accumulated lactate acid concentration for 1, 6 and 12 weeks was calculated.

3.2.3.3. Volume changes of the scaffolds

The length, width and height of each sample were measured with a vernier caliper (BS-H074) before and every week after the degradation. The volume change of the scaffold was calculated by the following equation: The volume change (%) = $(V_0 - V_t)/V_0 \times 100$. The V_0 and V_t were stand for the volume of the scaffold before and after degradation for the t time respectively.

3.2.3.4. Macropores size changes of the scaffolds

To determine the internal structure changes of the scaffolds before and after degradation, a high-resolution micro-computed tomography (vivaCT40, Scanco Medical, Brüttisellen, Switzerland) was used with a spatial resolution of 20μm for scanning according to our published method (Siu W. S. et al. 2004; Yeung H. Y. et al. 2005). 2D images were acquired directly from the scanning and 3D structure was reconstructed by VOI in which an optimized threshold was used to isolate the scaffold materials from the background. The average size of macropores and the porosity of the scaffolds were calculated by vivaCT40 workshop station.

3.2.3.5. Weight changes of the scaffolds

Weight change of the composite scaffolds before and every week after degradation was measured. It change, expected as weight loss of scaffolds was calculated by the equation: weight loss (%) = $(W_0 - W_t)/W_0 \times 100$. the W_0 and W_t

were stand for the weight of the scaffolds before and after degradation at each week respectively.

3.2.3.6. Ca^{2+} released from the scaffolds

In each week, the Ca^{2+} concentration in the replaced degradation medium was measured by calcium colorimetric assay kit (K380-250, BioVision, USA). 10μl medium and the calcium standard were added in wells in a 96-well plate. Bring the total volume to total 50μl with dH2O. 90μl of the chromogenic reagent and the 60μl of the calcium assay buffer were added subsequently to each well containing standards and samples. After being mixed gently and incubated reaction for 5 minutes at room temperature, the samples were measured the OD at 575nm. The calcium concentration in the test samples was calculated by the formula C=Sa/Sv, where Sa was the calcium sample amount (in μg) from standard curve and Sv was the sample volume (ml) added into the sample well. The accumulated Ca^{2+} concentration for each week was calculated.

3.2.3.7. Surface morphology and composition changes of the scaffolds

To observe the surface morphology and composition changes of PLGA/TCP/Icaritin composite scaffolds, the normal scaffolds and those immersed into saline for 12 weeks were sliced into section 2mm in thickness for SEM operated at 15 kV, 5.0mA combined with EDS. Before scanning the samples were freeze-dried and coated with gold using a Scancoat Six SEM sputter coater system.

3.2.3.8. Changes of mechanical property of the scaffolds

6 scaffold specimens with block $5\times5\times5mm^3$ in each group were immersed into

saline for 12 weeks. Mechanical property of the PLGA/TCP/Icaritin composite scaffolds before and after degradation were evaluated using our established indentation test (Qin L. et al. 1997; Qin L. et al. 2005b; Leung K. S. et al. 2006). 250N load cell was used and a 5mm diameter indentation rod connected to a mechanical testing machine (H25K-S, Hounsfield Test Equipment, UK) was loaded on the centre of the scaffolds with a compression speed at 5mm/min until the materials yielded. The compression direction was along the axial direction of scaffolds. The E-modulus, the compressive strength and energy for yield of materials were recorded for comparison. The total energy for half compression of the PLGA/TCP/Icaritin composite scaffolds was also recorded.

3.2.4. Icaritin release from PLGA/TCP/Icaritin composite scaffolds

The in vitro release of Icaritin was carried out over a period of 12 weeks and the cumulative released Icaritin was calculated for each group. Approximately 150mg of PLGA/TCP/Icaritin scaffold was dipped into a tube with 5ml saline. The resultant mixture was placed in an orbital shaker bath at 37℃, 120rpm. 5ml of sample mixture was extracted at every week from each test tube and the equal volume of SBF was supplemented. Icaritin in SBF was extracted with equal volume of ethyl acetate for three times. After the sample was dried with nitrogen, 100μl methanol was added and vortexes. High performance liquid chromatography (HPLC, 166 NM UV Detector, Beckman, USA) with our established protocol was used to detect the concentration of Icaritin at a wave length of 270nm and then the accumulated released amount of Icaritin from composites scaffolds were calculated.

3.2.5. Statistical analysis

All quantitative data were expressed as mean ± standard deviation (SE) and one-way ANOVA was used to compare the difference between two groups using SPSS version 10.0 (SPSS, Chicago, IL, USA). The level of significance was set at $p < 0.05$.

3.3. Results

3.3.1. pH value

The results showed that the pH value of degradation medium of all four groups decreased over time while that of saline did not (Fig.3.1 A). The higher Icaritin concentration in the scaffold, the less decreased speed of pH was observed during degradation. The pH value decreased fast in all scaffolds groups at the first week and then decreased moderately. After 10 weeks, the pH value decrease became faster again and the pH value was measured at 7.0, 5.4, 5.7, 5.9 and 6.0 in saline, PLGA/TCP, PLGA/TCP/Icaritin-L, PLGA/TCP/Icaritin-M, and PLGA/TCP/Icaritin-H groups at 12 weeks, respectively.

3.3.2. Lactic acid released from the scaffolds

Fig.3.1B showed that the lactic acid concentration in degradation medium of 4 groups decreased over time. The lactic acid concentration was about 100.7nmol/ml, 107.2nmol/ml, 99.6nmol/ml, and 84.9nmol/ml in PLGA/TCP, PLGA/TCP/Icaritin-L, PLGA/TCP/Icaritin-M, and PLGA/TCP/Icaritin-H groups at the first week, respectively, following those about 156.0nmol/ml, 148.8nmol/ml, 135.9nmol/ml and 127.7nmol/ml at 6 weeks, 256.6nmol/ml, 236.2nmol/ml, 221.7nmol/ml and

209.6nmol/ml at 12 weeks.

3.3.3. Volume and macropores size changes

Both the volume and macropores size of the scaffolds decreased with degradation over time (Fig.3.2 A). At the first week, the volume decreased fast to 77.8%, 86.1%, 89.6%, and 90.8% of the original volume in PLGA/TCP, PLGA/TCP/Icaritin-L, PLGA/TCP/Icaritin-M, and PLGA/TCP/Icaritin-H groups, respectively. The higher Icaritin concentration in the scaffolds, the less was its reduction in volume over time. At 12 weeks, the volume decreased to about 18.6%, 25.6%, 48.4% and 51.3% of original volume in PLGA/TCP, PLGA/TCP/Icaritin-L, PLGA/TCP/Icaritin-M, and PLGA/TCP/Icaritin-H group, respectively. The decrease in volume was more obvious in PLGA/TCP and PLGA/TCP/Icaritin-L groups than that in PLGA/TCP/Icaritin-M and PLGA/TCP/Icaritin-H groups after 8 weeks ($p<0.05$). There was no obvious difference in volume change between PLGA/TCP/Icaritin-M and PLGA/TCP/Icaritin-H groups, as well as between PLGA/TCP and PLGA/TCP/Icaritin-L groups after 10 weeks.

It was shown in Fig.3.2B that the average pores size were about 492.8μm, 492.4μm, 465.4μm and 477.6μm in PLGA/TCP, PLGA/TCP/Icaritin-L, PLGA/TCP/Icaritin-M, and PLGA/TCP/Icaritin-H groups before degradation, respectively. The pores size in all the scaffolds decreased slightly at the first 6 weeks, but after that, the pores size decreased quickly in PLGA/TCP and PLGA/TCP/Icaritin-L groups than that in PLGA/TCP/Icaritin-M and PLGA/TCP/Icaritin-H groups. At 12 weeks, the average pores size was about

296.5μm, 311.3μm, 329.8μm and 376.7μm in PLGA/TCP, PLGA/TCP/Icaritin-L, PLGA/TCP/Icaritin-M, and PLGA/TCP/Icaritin-H groups, respectively.

3.3.4. Weight loss

It was shown in Fig.3.2C that all the scaffolds in four groups tended to decrease their weight over time, but the amount of weight loss in PLGA/TCP and PLGA/TCP/Icaritin-L groups was higher than that in PLGA/TCP/Icaritin-M and PLGA/TCP/Icaritin-H groups. At the end of the degradation, the weight of the scaffolds decreased obviously, especially in PLGA/TCP and PLGA/TCP/Icaritin-L groups. The weight remained about 78.8%, 82.0%, 88.9% and 88.8% of the original scaffolds in PLGA/TCP, PLGA/TCP/Icaritin-L, PLGA/TCP/Icaritin-M, and PLGA/TCP/Icaritin-H groups at 12 weeks, respectively.

3.3.5. Ca^{2+} released from the scaffolds

Ca^{2+} released into degradation medium increased in all groups over time (Fig.3.2 D), with 66.0μg/ml, 51.6μg/ml, 53.2μg/ml and 43.5μg/ml in PLGA/TCP, PLGA/TCP/Icaritin-L, PLGA/TCP/Icaritin-M, and PLGA/TCP/Icaritin-H groups at the first week, respectively. The value of Ca^{2+} released in PLGA/TCP group was higher than that in other three groups during degradation and that in PLGA/TCP/Icaritin-L group was higher than that in PLGA/TCP/Icaritin-M and PLGA/TCP/Icaritin-H groups after 8 weeks ($p<0.05$). There was no difference in value of Ca^{2+} released from scaffold between PLGA/TCP/Icaritin-M and PLGA/TCP/Icaritin-H groups.

3.3.6. Surface morphology and composition changes

The morphology changes of composite scaffolds before and after degradation were shown in Fig.3.3. The initial surface of scaffolds in four groups was uniform in porosity before degradation in an inorganic-organic composition (Fig.3.3 A1, B1, C1 and D1) and some TCP particles were observed on the wall of the scaffolds. After 12 weeks, the surface of PLGA/TCP and PLGA/TCP/Icaritin-L was relatively smooth, yet with decrease in number and size of micropores (Fig.3.3 A2 and B2), while the surface of PLGA/TCP/Icaritin-M and PLGA/TCP/Icaritin-H scaffolds partly kept their porous morphology (Fig.3.3 C2 and D2).

The surface composition of the scaffolds obtained by EDS clearly revealed the presence of C, O, P and Ca element. Qualitative EDS analysis showed that the weight percentage of Ca in PLGA/TCP, PLGA/TCP/Icaritin-L, PLGA/TCP/Icaritin-M, and PLGA/TCP/Icaritin-H groups at baseline was 8.3%, 9.3%, 10.6%, and 9.8%, respectively while that 12 weeks after degradation was 3.1%, 4.3%, 3.3%, and 5.2%, respectively (Fig.3.3 E). The weight percentage of P in PLGA/TCP, PLGA/TCP/Icaritin-L, PLGA/TCP/Icaritin-M, and PLGA/TCP/Icaritin-H groups at baseline was 5.5%, 6.2%, 6.5%, and 6.5%, respectively while that 12 weeks after degradation was 0%, 0.8%, 0%, and 0.4%, respectively (Fig.3.3 F). The percentage of both P and Ca element decreased remarkablely in four groups after degradation ($p<0.05$). Another change in composite of the scaffold surface was that there was no Na element was observed at the surface of the scaffolds at baseline, while that was about 1.0%, 0.7%, 0.8%, and 0.8% in PLGA/TCP, PLGA/TCP/Icaritin-L, PLGA/TCP/Icaritin-M, and

PLGA/TCP/Icaritin-H groups 12 weeks after degradation.

3.3.7. Mechanical properties

Fig.3.4 showed the mechanical properties of the composite scaffolds in PLGA/TCP, PLGA/TCP/Icaritin-L, PLGA/TCP/Icaritin-M and PLGA/TCP/Icaritin-H groups before and after degradation, respectively. There was no obviously difference observed in E-modulus, compressive strength and energy at yield among four groups before degradation, while those decreased in PLGA/TCP/Icaritin-L, PLGA/TCP/Icaritin-M and PLGA/TCP/Icaritin-H groups and increased in pure PLGA/TCP group. The mechanical changes before and after degradation were remarkable in pure PLGA/TCP, PLGA/TCP/Icaritin-M and PLGA/TCP/Icaritin-H groups ($p<0.05$).

3.3.8. Slow-release property of Icaritin

The percentage of Icaritin released from scaffolds into degradation medium was shown in Fig.3.5. No Icaritin was detectable in PLGA/TCP/Icaritin-L group. For PLGA/TCP/Icaritin-M group, no Icaritin was measured in the first two weeks but detected slightly from 2 to 7 weeks and rapidly from 7 to 12 weeks, with 65% release of Icaritin from the scaffold during 12-week degradation. In PLGA/TCP/Icaritin-H group, there was no bust release of incorporated Icaritin within the first week of degradation, but released slowly afterwards to 5 weeks, followed by a rapid release from 6 weeks to 10 weeks, and ended up with a total of 70% of Icaritin released from PLGA/TCP/Icaritin scaffold at the end of 12 weeks.

3.4. Discussion

Both biodegradation and porous structure of scaffolds are important variables when used for bone tissue engineering. Therefore in this chapter, we evaluated the degradation properties of the novel PLGA/TCP/Icaritin in vitro and the release of Icaritin from scaffold before making suggestions for in vivo applications.

In order to evaluation the changes of scaffolds during degradation in vitro, the 0.9% NaCl solution was used as the degradation medium instead of the common phosphate buffer solution (PBS) to avoid the effect of buffer solution that would neutralize the alteration of pH value. The result showed that the pH value of the degradation medium in four groups decreased with time, but that in saline remained unchanged. It was considered that the decreased pH value was result from the formation of the acidic degradation products and their release from scaffolds to the degradation medium (Yang F. et al. 2006). Since the degradation products of PLGA consist of lactic acid and glycolic acid, we observed that the concentration of lactic acid in degradation medium was increased during degradation. Though the accumulation of acids could induce bacteria-free inflammation of the tissues around the implanted site in vivo (Kim M. S. et al. 2007), the lactic acid in vivo could also be hydrolyzed into water and the carbon dioxide. In addition, the degradation of scaffolds in vitro was under static conditions so the true harmful effect of the acid would be reduced in vivo due to circulating body fluid to transport away the acid products, which was confirmed by the in vitro test under dynamic conditions (Yang Y. et al. 2008). The pH value with scaffold with high concentration Icaritin decreased slowly than that in the pure PLGA/TCP group. Accordingly, we observed higher

concentration of lactic acid in the medium in pure PLGA/TCP group. Pure PLGA degraded much rapidly in medium (Chen V. J. et al. 2006; Zolnik B. S. et al. 2006), alkaline calcium phosphate was introduced to reduce the acidity of the degradation products by neutralize acidity of the degradation acids (Ara M. et al. 2002; Loher S. et al. 2006). This suggested that the decreased pH value was related to the concentration of Icaritin in the composite scaffolds that might alter the degradation rate of porous PLGA/TCP/Icaritin scaffolds, with slower change of pH value and release of lactic acid in the PLGA/TCP/Icaritin-H group as compared with other groups.

The present study showed that volume, dry weight, and macropores size of the porous scaffolds decreased obviously during degradation, especially around 8 weeks. The decrease in volume of scaffolds implied that the scaffolds shank during this degradation process, especially with prolonged time as reported previously (Yang F. et al. 2006). This also explained the decreased macropores size of scaffolds instead of commonly believed pores size enlargement during degradation. The percentage decrease in scaffold volume was proportionally larger than the decrease in pores size. The loss in material weight was attributed to the degradation of the PLGA and partially also of the TCP component in scaffolds, that was explained by the release of Ca and degraded lactic products from the scaffolds into the degradation medium over time in the present in vitro study. As compared with PLGA/TCP control, we also found that PLGA/TCP incorporated with Icaritin slowed down the deformation of its scaffold structure in terms of volume, weight and pores size. This unique

characteristics of our novel composite material would physically benefit cell migration, bone ingrowth and neovascularization in vivo as reported by others (Hollister S. J. 2005; Butler M. J. et al. 2007; Henry J. A. et al. 2009).

Effect of porosity and pores size of porous scaffolds on osteogenesis in vitro and in vivo has been demonstrated by others (Karageorgiou V. et al. 2005). Interconnection of pores is also essential to improve cell seeding, migration, and tissue ingrowth (Hollister S. J. 2005). Most of the previous studies only reported material structural and mechanical properties of porous scaffold before implantation in vivo. However, such properties may alter after implantation that may affect the desirable treatment effects. In order to provide such information, the present study used in vitro model to monitor changes with degradation and our SEM results revealed that the surface morphology changes were related with Icaritin concentration. The middle and high Icaritin concentration group maintained its initial structure significantly longer, implying that the incorporation of Icaritin retarded the rate of PLGA degradation. The EDS result showed that the percentage of P and Ca element at scaffold surface decreased, implying its potential local osteogenic and osteopromotive effects reported by in vivo study of others (Jones J. R. et al. 2007).

The present study showed that the mechanical property in PLGA/TCP/Icaritin group declined 12 weeks after in vitro degradation, even inferior to that of pure PLGA/TCP group. This was explained by two associated physic-chemical actions. Firstly, there was a moderate shrinkage of the scaffolds with relatively high Icaritin concentration during degradation. Secondly, it might be related to the deposition of

the sodium for more Na element found at the surface of PLGA/TCP scaffold. We found that the scaffolds in PLGA/TCP and PLGA/TCP/Icaritin-L groups was more brittle and easy to crack into pieces under mechanical test while those in PLGA/TCP/Icaritin-M and PLGA/TCP/Icaritin-H groups was rather durable and tough. However, the in vitro condition would not the same as compared with in vivo. Lin et al. found that the optimally designed PPF/TCP scaffolds with a modulus of 140MPa degraded to a modulus of 38MPa without bone ingrowth but scaffolds had a modulus of 65MPa at eight weeks after bone regeneration (Lin C. Y. et al. 2005). This is explained by the factor that the new bone formed within the interconnected pores would augment the mechanical property of scaffold during in vivo degradation. Yet, the limitations of in vitro experiments were also obvious that degradation taking place without enzyme and macrophage involvement, as they actively involved in the process of biodegradation (Lu L. et al. 2000; Hedberg E. L. et al. 2005). As local mechanical loading condition would also influence the implanted scaffold degradation behaviour, in vivo studies with specific experimental designs are desirable for future research.

The ideal scaffold for tissue engineering should have a feature of bioactivity apart from good degradation properties and mechanical function. Controlled-release strategies are frequently adopted to overcome the short half-life and residence of free growth factors in solution (Hollister S. J. 2005; Cancedda R. et al. 2007). As an osteopromotive exogenous phytoestrogenic factor, our multidisciplinary research group incorporated Icaritin successfully into PLGA and TCP to form

PLGA/TCP/Icaritin scaffold for the first time using computer-controlled technology. The unique feature of slow-release was that during 12-week degradation, there was no initial burst release of the incorporated Icaritin at the first week. But the concentration of Icaritin released from composite scaffold was higher in PLGA/TCP/Icaritin-H group than that in other groups. So according to the promoted effect of the composite scaffold on bone healing at the early time after implantation in vivo, the high dosage of Icaritin in the scaffold would be preferred. The Icaritin released into degradation medium increased slowly thereafter up to about 70% at week 12. This controlled-released property would benefit bone forming marrow cells to be stimulated by the released phytoestrogenic Icaritin for longer period of time when implanted in vivo, such as for potential treatment of difficult large bone defect repair.

3.5. Conclusion

The studies in this chapter evaluated the degradation characteristics of porous PLGA/TCP scaffold incorporating bioactive molecule Icaritin at different concentrations which was investigated using standard in vitro testing systems. Findings suggested that the porous composite scaffolds had the ability to degrade in physiological saline and the incorporated Icaritin delayed the degradation rate of porous scaffold dose-dependently, in favor of maintaining the porous structural and mechanical properties with higher Icaritin concentration. The slow release of osteopromotive molecule Icaritin from our innovative composite scaffold suggested its potential application as bone filler or bone substitute for bone defect repair. As

the composite scaffold was confirmed biodegradable in vitro and Icaritin could be released slowly from composite together with its degradation, the next work in the following chapter would focus on the cytotoxicity of this degradable composite scaffold and its bioactivity.

3.6. Figures and legends

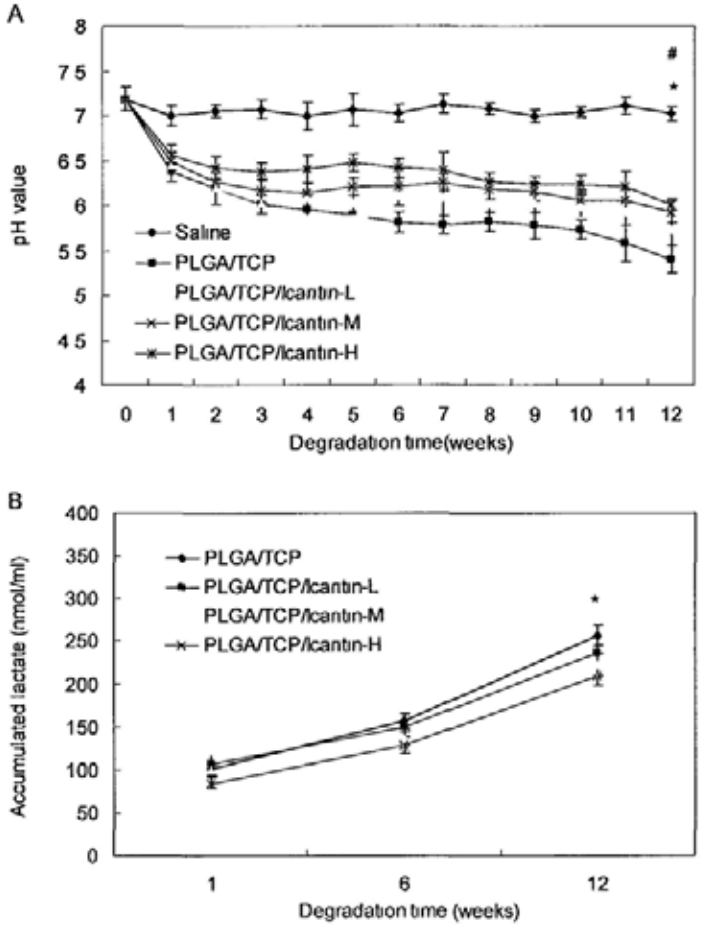

Fig.3.1. Dose-dependent degradation feature of an innovative PLGA/TCP/Icaritin composite porous scaffold. A: pH value changes of the degradation medium during 12 weeks; B: Accumulated lactic acid in degradation medium at 1, 6 and 12 weeks during degradation. * $p<0.05$ as compared between 0 and 12 weeks. # $p<0.05$ as compared between PLGA/TCP and PLGA/TCP/Icaritin-H groups.

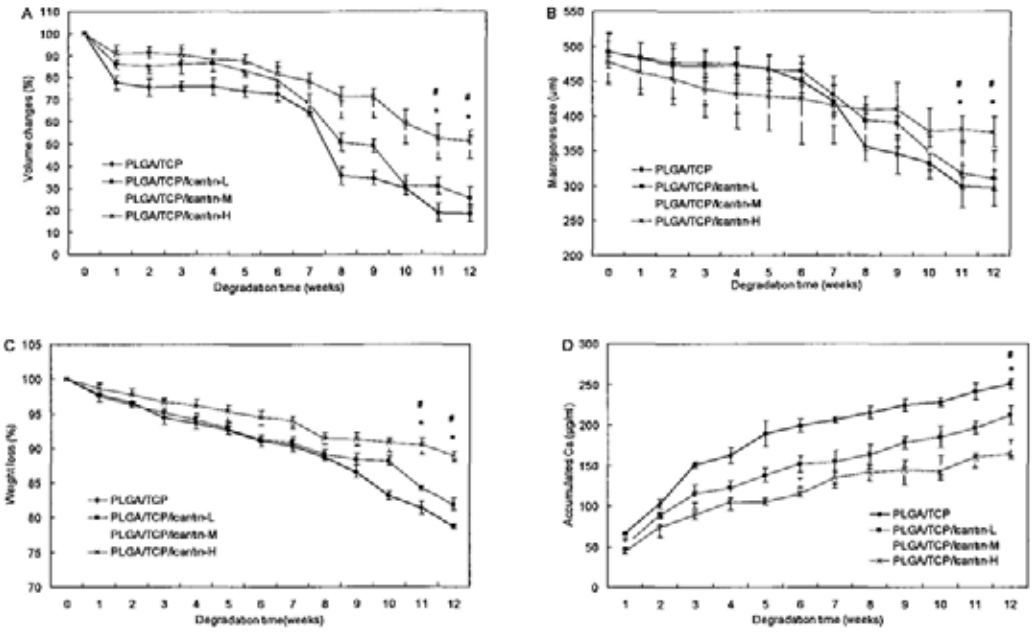

Fig.3.2. Dose-dependent degradation feature of an innovative PLGA/TCP/Icaritin composite porous scaffold. A: Changes in volume; B: Changes in macropores size; C: Changes in weight loss; D: Accumulated Ca release. *: $p<0.05$, compared with results of 0 week. # $p<0.05$, compared between PLGA/TCP and PLGA/TCP/Icaritin-H groups.

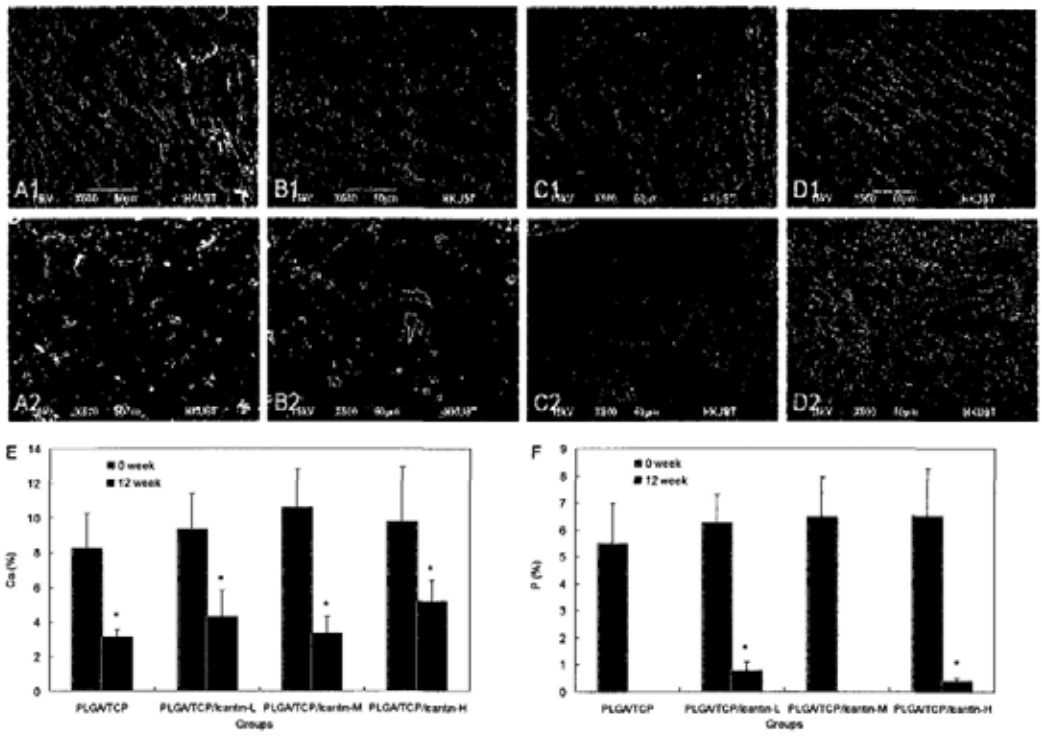

Fig.3.3. SEM micrograph (A, B, C and D. 500×) and EDS (E, F) analysis of the surface of the scaffolds in PLGA/TCP group, PLGA/TCP/Icaritin-L group, PLGA/TCP/Icaritin-M group and PLGA/TCP/Icaritin-H group at 0 and 12 weeks during degradation. (1: 0 week; 2: 12 weeks. A: PLGA/TCP; B: PLGA/TCP/Icaritin-L; 1: PLGA/TCP/Icaritin-M; D: PLGA/TCP/Icaritin-H) E: Calcium (Ca) element changes; F: Phosphate (P) element changes. *: $p<0.05$, compared between 0 and 12 weeks.

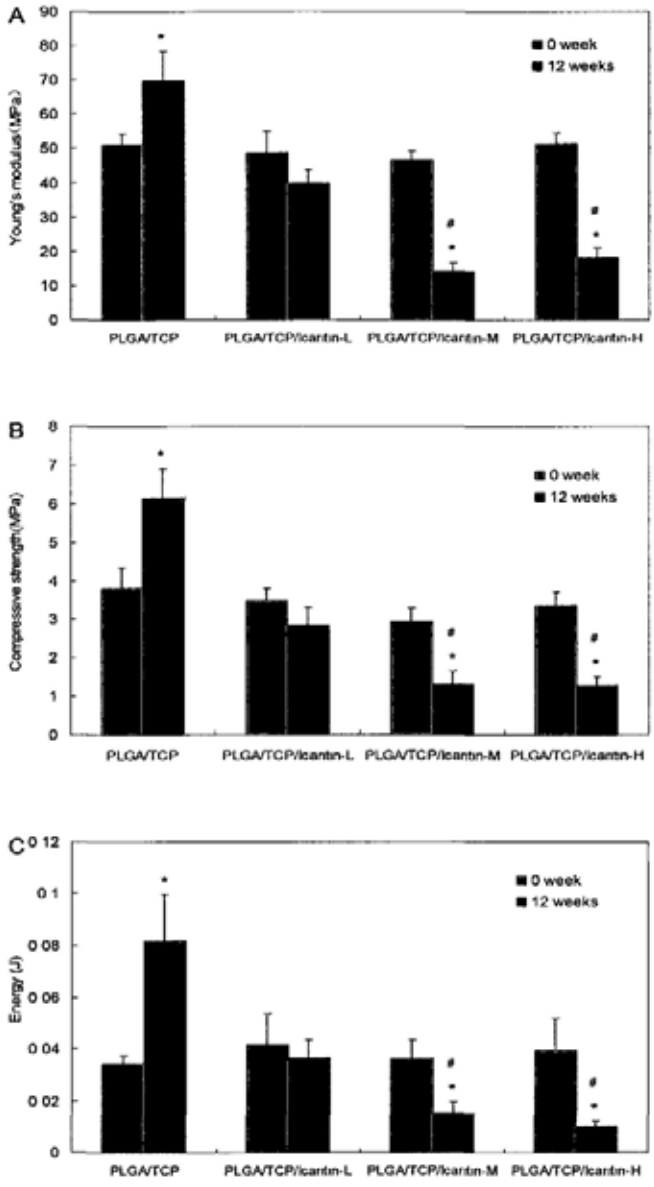

Fig.3.4. The changes of mechanical properties of the scaffolds in PLGA/TCP group, PLGA/TCP/Icaritin-L group, PLGA/TCP/Icaritin-M group and PLGA/TCP/Icaritin-H group before and after degradation, respectively. A: E-modulus; B: the compressive strength; C: energy for yield of materials.*: $p<0.05$, compared between 0 and 12 weeks. #: $p<0.05$ when compare with PLGA/TCP group and PLGA/TCP/Icaritin-L group.

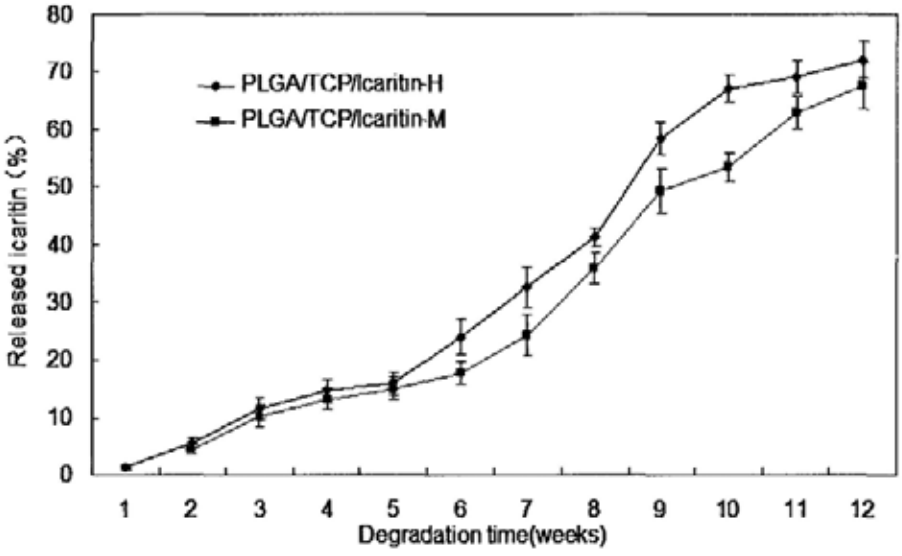

Fig.3.5. The accumulated Icaritin released from PLGA/TCP/Icaritin porous scaffolds into degradation medium. A: PLGA/TCP/Icaritin-H group; PLGA/TCP/Icaritin-M group.

Chapter 4

Biocompatibility and osteopromotion of innovative porous PLGA/TCP/Icaritin composite scaffold

4.1. Introduction

For several reasons such as bone defect size, infection, and many others, injured or diseased bone can not repair itself by means of mechanical fixation alone which often results in non-union (Porter J. R. et al. 2009). Composite biomaterials have potential ability for bone tissue reparation and augmentation. Polymer/ceramic composite biomaterials can be successfully applied with bone tissue reparations due to their osteoconductive, biodegradable and biocompatible properties. Addition of calcium based ceramic with biodegradable polymer such as PLGA/TCP is a good way to yield the composite materials with desirable properties such as controlled degradation, increased bioactivity and proper mechanical strength (Sherwood J. K. et al. 2002; Fan H. et al. 2006c; Ehrenfried L. M. et al. 2008; Hao W. et al. 2008; Yu D. et al. 2008; He K. et al. 2009). A better synthetic implant designed for reconstructing of bone defect is usually composed of a combination of biocompatible materials and biological factors (Hollister S. J. 2005; Place E. S. et al. 2009). Controlled growth factors to be released from bone substitute can create a fine approach for bone regeneration. Incorporation of growth factors with bone tissue engineering therapies simulates the natural bone micro-environment and may enhance the bone healing.

As a replacement material, it should satisfy a serious of criteria such as 3D porous structure, interconnected pores, biodegradation, osteoconduction or osteoinduction, biocompatibility and non-toxicity (Hollister S. J. 2005; Karageorgiou V. et al. 2005; Ignjatovic N. et al. 2006; Place E. S. et al. 2009). In chapter 2, we have developed the PLGA/TCP/Icaritin composite scaffold using the computer-controlled

fine biospinning technology. The Icaritin, a biological factor, was incorporated into this scaffold due to its osteogenic ability (Zhang G. et al. 2007a; Qin L. et al. 2008; Wang X. L. et al. 2008; Songlin P. et al. 2009; Zhang G. et al. 2009a; Zhang G. et al. 2009c). The scaffold had pores with 300-500μm in diameter and the pores were interconnected. More important was that this scaffold had proper biodegradable property as specified in Chapter 3 and Icaritin could be released slowly and maintained for long time which may contribute to the osteogenesis of this composite scaffold. Though Icaritin alone had the osteopromotive effect in vitro, this effect of composite biomaterials incorporated with Icaritin needed to be confirmed in vivo for understand its treatment efficacy.

Biocompatibility testing involves biological testing of medical devices or materials to identify their potential hazards and ensure that these products do not have adverse effect on patient. The biocompatibility and the cytotoxicity of biomaterials played important roles on the attachment, migration and proliferation of cells, which thus influenced the reconstruction of tissue around the materials (Ignjatovic N. et al. 2006). PLGA and TCP, gained FDA approval for human use in biomedical fields (Hao W. et al. 2008; Liu H. et al. 2008; Coimbra M. E. et al. 2009), were proved to have good biocompatibility and osteoconduction to be widely used in tissue engineering (Fan H. et al. 2006c; Hao W. et al. 2008; Kang Y. et al. 2008; Yu D. et al. 2008). However, the PLGA also have the disadvantages that their degradation will result in an acid micro-environment due to the formation of lactic and glycolic acid and the accumulation of acids could induce bacteria-free inflammation of the

tissues around the implanted site in vivo (Jilek S. et al. 2004; Zhao X. et al. 2005; Kim M. S. et al. 2007; Yoon S. J. et al. 2008). Pure PLGA degraded much rapidly in medium (Chen V. J. et al. 2006; Zolnik B. S. et al. 2006), alkaline calcium phosphate was introduced to reduce the acidity of the degradation products by neutralize acidity of the degradation acids (Ara M. et al. 2002; Loher S. et al. 2006). Though the degradation study we did in Chapter 3 have proved the mildly decreased pH value in PLGA/TCP/Icaritin group when compared with that in PLGA/TCP group, more information was needed about the biological response of the degradation products of PLGA/TCP/Icaritin. For biodegradable materials, the materials and their biodegradable products should be evaluated for their in vitro cytotoxicity by employing cultures. The advantage of the tests is that each biomaterial could be evaluated on cytotoxicity on the basis of its influence on cell growth and division in the given cell cultures. Any bone substitute will be in contact with around soft tissues and these tissues are generally considered to show a more severe inflammatory response than the bone. Hence the biocompatibility of the bone substitute material has to be evaluated in the soft tissue environment as well (Velayudhan S. et al. 2005).

In this part, the cytotoxicity test in vitro and biocompatibility in vivo were performed for PLGA/TCP/Icaritin composite scaffold. Cell culture studies using mouse fibroblast cell line (L929) were used to assess the in vitro cytotoxicity and intramuscular implantation studies on rabbits were performed to assess the in vivo biocompatibility of the composite materials. Moreover, the osteogenic potential of PLGA/TCP/Icaritin scaffold was also evaluated by using BMSCs from rabbit and

osteoblast-like UMR 106 cells.

4.2. Materials and methods

4.2.1. Preparation of the PLGA/TCP/Icaritin composite scaffold

In this part, the PLGA/TCP/Icaritin composite scaffolds were fabricated using a rapid prototyping machine and the same manufacturing process as described in both Chapter 2 and 3. The composite scaffolds with high dosage of Icaritin (74mg Icaritin per 100g PLGA/TCP) were used for cytotoxicity, implantation in muscles and osteopromotion studies as this high dose was selected because of its better biological activities from in vitro studies where scaffolds with different dosages of Icaritin for cell seeding and proliferation were tested.

4.2.2. Cytotoxicity - testing on an extract

Materials: L929 cell line; DMEM (Dulbecco's modified eagle's minimum essential medium) + 10% FBS (fetal-inactivated fetal calf serum); penicillin and streptomycin (Sigma, USA); PLGA/TCP/Icaritin composite scaffold; Phenol and tissue culture grade polystyrene (13mm in diameter); 5mg/ml MTT (3-(4,5-dimethylthiazol-2-yl)-2,5-diphenyltetrazolium bromide) stock solution, 25mg of MTT was dissolved in 5ml PBS; Acid isopropanol (1N HCL 300μm + 100ml isopropanol); Phenol solution at 6.4mg/ml (128mg phenol + 20ml culture medium); DMSO (dimethyl sulphoxide); 96-well dish;

Cell culture: The in vitro cytotoxicity of PLGA/TCP/Icaritin scaffold was evaluated by testing on an extract according to a standard procedure ISO-10993-5 using L929 cells (ISO 1992). The cells were maintained in DMEM containing 10%

FCS (HyClone Logan, Utah, USA) and 100 IU/ml penicillin and 100μg/ml streptomycin (Sigma, USA). Cultures were maintained at 37℃ in incubator containing 5% carbon dioxide with a medium change at an interval of 3 days. When the adherent cells reached subconfluence, they were digested from the dish with 0.05% trypsin and subcultured in DMEM for standby.

Preparation of extracts: The PLGA/TCP/Icaritin composite scaffold extracts were prepared by incubating 0.8 g of the composite scaffold in 4ml culture medium. Tissue culture grade polystyrene extracts were prepared by incubating 4 slices of polystyrene of surface 1.33 cm2 into 2ml culture medium, which worked as positive control. They were incubated into 37℃ for 48 hours. After that, the extracts were taken into the centrifuge tubes and kept in the fridge for reserve. Phenol was used as the negative control.

MTT assay of cytotoxicity: The assay is founded on the ability of living cells to reduce MTT, a water-soluble yellow dye, to a water-insoluble purple formazan crystals product by mitochondrial succinate dehydrogenases. The assay has been developed as a quick effective method for testing mitochondrial impairment by drugs correlating well with cell proliferation. It could be also modified as a method for evaluating in vitro cytotoxicity of soluble synthetic polymers (Ignatius A. A. et al. 1996). The MTT stock solution was diluted to 0.5mg/ml with PBS. Prepare the dilution of phenol following the Tab.4.1. Prepare the dilution from the scaffold extraction according to the Tab.4.2. 24 hours after L929 cells were seeded onto 96-well plates at a density of 5×10^3 per well, the medium in plate was carefully

removed with the automatic pipette without touching the cells at the bottom of the wells. Phenol and scaffold dilutions (200μl) were added into each well according to the Tab.4.3 (each concentration for 6 wells) and cytotoxicity was assessed qualitatively after cultured at 37℃ in a humidified 5% CO_2 atmosphere for 48 hours. Then the old medium in the 96-well plate were discarded and 200μl MTT solution were added into each well respectively. After incubated at 37℃ 4 hours in dark, the MTT solution was removed and the crystals were diluted in DMSO. Then it was kept at room temperature for 15-30 minutes (not more than half an hour) and the shaker was used to homogenize the mixture. The optical density (OD) was measured at 570nm by microplate reader. To ensure that the extracts themselves did not contribute to the result, the different extract dilutions were also assayed in a microtitre plate by the MTT assay. The relative growth rate (RGR, %) was calculated by the following equation:

$$RGR = (OD_{\text{scaffold extracts}} / OD_{\text{positive group}}) \times 100\%$$

The cytotoxicity of scaffold was evaluated by scoring system (Zhang Y. S. et al. 2005) and the non-cytotoxicity of materials will be certified by grade 0 or 1 (Tab.4.4).

4.2.3. Intramuscular implantation studies

Intramuscular implantation studies were carried out to evaluate the local responses to the composite material (Velayudhan S. et al. 2005). 4 healthy New Zealand white rabbits with body weight about 4kg were anesthetized with xylazine (2mg/kg) and ketamine hydrochloride injection (50mg/kg) intramuscularly. PLGA/TCP/Icaritin and PLGA/TCP scaffolds were implanted randomly at the

bilateral thigh muscles of the rabbits (Fig4.1 A). The dimensions of the scaffolds were 10mm×10mm×10mm. The rabbits were placed in their own cages after surgery and allowed to move without restriction. They were sacrificed at one month after implantation. Each implant with surrounding muscles was taken out and fixed in 10% buffered formalin for 24 hours (4 samples in each group). After fixation, the samples were dehydrated in graded alcohol from 70% to 100%, cleared in chloroform, impregnated and embedded in paraffin wax. Sections with 5μm in thickness were cut using paraffin machine and stained with Harry's hematoxylin and eosin (H&E) followed by examine under a light microscope (Leica DMLS, Germany) equipped with a digital camera (0.63X, Leica, Germany). A semi-quantitative histological analysis of the retrieved specimens was carried out such as necrosis, cells infiltration, calcification, haemorrhage, oedema, collagen fibers and new blood vessel (Turner J. E. et al. 1973; Velayudhan S. et al. 2005).

4.2.4. Attachment and proliferation of BMSCs on composite scaffold

Isolation and culture of BMSCs: Mature New Zealand White rabbits (12 weeks old, 2.5-3 kg) were anaesthetized. The bone marrow from the iliac crest was obtained and mononuclear cells were separated by centrifugation in a Ficoll-Hypaque gradient (Sigma Co., St. Louis, USA), suspended in DMEM containing 10% fetal bovine serum (FCS) (HyClone Logan, Utah, USA) and seeded at a concentration of 1×10^6 cells/cm^2. Cultures were maintained at 37 °C in incubator containing 5% carbon dioxide. When the adherent cells reached subconfluence, they were digested from the dish with 0.05% trypsin and subcultured in DMEM for standby (Fan H. et al.

2006c).

Preparation of scaffold for cell culture: In order to facilitate the cell-seeding procedure, the four kinds of scaffolds (PLGA/TCP, PLGA/TCP/Icaritin-L, PLGA/TCP/Icaritin-M and PLGA/TCP/Icaritin-H groups) were cut into pieces of $5\times5\times3mm^3$, to fit the well size of 96-well plates. The scaffold was sterilized with 75% ethanol and washed with sterilized PBS before put into a dish and exposed to ultraviolet for 30 minutes before used.

Seeding efficiency of BMSCs on scaffolds: BMSCs were trypsinized and suspended at a density of 1×10^5 cells/ml in DMEM. 200μm cell suspensions were then seeded directly onto the scaffolds in 96-well dish and cultured for 4 hours at 37°C, 5% CO2 and the cells plated into wells without scaffold worked as total number of seeded cells. After that, the BMSCs/PLGA/TCP/Icaritin composites were removed to a new 96-well dish and covered with fresh DMEM. The cells not adhering to the scaffold after cell seeding and the cells plated in wells without scaffold were washed with PBS and then measured by MTT method for seeding efficiency (the percentage of attached cells of the total number of seeded cells) (Minamiguchi S. et al. 2008). Cell attachment on scaffold was examined by SEM. In brief, the scaffolds with cells were cut into 2mm in thickness and rinsed in PBS and fixed in 2.5% glutaraldehyde at 4℃ for 24 hours. Then the samples were put in 0.1% osmium acid at 4℃ for 2 hours. The scaffold was then rinsed three times using PBS, dehydrated in a gradient series of ethanol, critical point dried, sputter coated with gold, and examined on SEM (Yang J. et al. 2009).

The proliferation of BMSCs on scaffolds: On 1, 3, 5, and 7 days after cell seeding, the culture medium was removed and the cells were trypsinized using 0.25% trypsin/EDTA. After centrifugation (1,200 rpm for 10 minutes), the cell pellets were suspended and the supernatant was discarded. The cell numbers in composite scaffolds were assayed by MTT method. The cells on the PLGA/TCP/Icaritin-H scaffold were labeled with green fluorescent protein (GFP) and observed under fluorescent microscope (LEICA DM IRB, Germany; Moticam 2300 camera, Canada).

4.2.5. ALP activity of BMSCs on PLGA/TCP/Icaritin scaffold

In order to evaluate the osteogenic effect, the PLG/TCP and PLGA/TCP/Icaritin-H scaffolds were used and cut into pieces of $10\times10\times5mm^3$ to fit the well size of 24-well plates. BMSCs were trypsinized and suspended at a density of 1×10^5 cells/ml in DMEM. 1ml cell suspensions were then seeded directly onto the scaffolds and cultured for 4 hours at 37°C, 5% CO_2. After culturing for 2 and 5 days, the scaffolds were taken out and the cells were digested by 0.25% trypsin (Invitrogen, USA) and centrifuged at 1500rpm for 5 min, the cells were then collected for ALP activity analysis. In brief, the cell pellets were washed with PBS 3 times and then lysed in 200μl diethanolamine (DEA) lysis buffer. The cellular material was homogenized in the cool room at 4℃ for 15 minutes and then returned to room temperature. ALP activity was determined with p-nitrophenylphosphate as the substrate. Sample volumes of 30μl were added to 170μl p-nitrophenylphosphate. The p-nitrophenol release was monitored by measuring the optical density (OD) at 405nm

by using universal microplate reader (measure kinetics for 10 minutes with 1 minute interval). ALP activity was expressed as normalized by the content of protein. The protein concentrations of cells lysates were determined biochemically using the Bradford protein assay (Bio-Rad, USA) according to the manufacturer's protocol. Data were fitted by Gaussian distribution by GraphPad Prism software Version 5.0 (GraphPad Software, Inc, USA). 6 samples were included in each group. ALP activity was expressed as IU/L.

4.2.6. Cell mineralization in LGA/TCP/Icaritin scaffold

On days 14, the extracellular calcium deposit was evaluated using the method reported by others (De Ugarte D. A. et al. 2003; Hao W. et al. 2008). In brief, the cells were collected in both groups as before. The cell pellets were washed with PBS for 3 times and incubated with 1ml of 0.5N HCl for 12 hours. The extracts were centrifuged for 5 minutes at 1000rpm and the Ca^{2+} ions in the samples were measured by calcium colorimetric assay kit (K380-250, BioVision, USA) as before and expressed as $\mu g/10^5$ cells. 6 samples were included in each group.

4.2.7. Quantitative real time PCR for osteogenic gene expression

5000 cells/well of UMR 106 cells were seeded onto PLGA/TCP or PLGA/TCP/Icaritin-H composite scaffold in 96-well plates and incubated in the cultured DMEM medium and the medium was changed every day. The gauge of the scaffold is $5\times5\times3mm^3$. After culturing for 4 days, the scaffolds were taken out and the cells were digested by 0.25% trypsin (Invitrogen, USA) and centrifuged at 1500 rpm for 5 minutes, the cells were collected for real time PCR analysis. Total RNA

was isolated at 4 days after seeding to the scaffolds using the RNeasy total RNA extraction kit from Qiagen (Cat. No. 74106, Hilden, Germany) (Shimizu E. et al. 2004) . 1μg of the total RNA was reverse-transcribed to cDNA as the starting material using previously described protocol (Viereck V. et al. 2005). Quantitative real-time PCR was performed using the following primer sets: OC-R-T forward, 5'-CTCACTCTGCTGGCCCTGAC-3'; OC-R-T reverse, 5'-CCTTACTGCCCTCCTGCTTG-3'; BSP-R-T forward, 5'-AGAAAGAGCAGCACGGTTGA-3'; BSP-R-T reverse, 5'-CCCTCGTAGCCTTCATAGCC-3'; OPN-R-T forward, 5'-AGCAGCAGGACTGAAGGAGC-3'; OPN-R-T reverse, 5'-ACAGGAGGCAAGGCCGAACA-3'; GAPDH-R-T forward, 5'-CAAGTTCAACGGCACAGTCA-3'; GAPDH-R-T reverse, 5'-CCATTTGATGTTAGCGGGAT-3' using the SYBR Green qPCR kit. The 10μl volume of the final reaction solution contained 1μl of the diluted cDNA product, 5μl of 2X Power SYBR® Green PCR Master Mix (Applied Biosystems, CA, USA), 0.5μl each of forward and reverse primers and 3.5μl nuclease-free water. The amplification conditions were: 50°C for 2 minutes, 95°C for 10 minutes, 40 cycles of 95°C for 15 sec, 60°C for 1 minute. The fluorescence signal emitted was collected by ABI PRISM® 7900HT Sequence Detection System and the signal was converted into numerical values. Expression of the cDNA of interest was measured relative to the expression of the housekeeping gene GAPDH by the comparative threshold-cycle method as described earlier (Raddatz D. et al. 2004).

4.2.8. Statistics

All values were presented as means ± standard error. Differences among four experimental groups were assessed by ANOVA and considered statically significant when $p<0.05$. Student's T test was performed to compare the amount of new bone formation between PLGA/TCP group and PLGA/TCP/Icaritin group.

4.3. Results

4.3.1. In vitro cytotoxicity

In vitro cytotoxicity studies carried out on PLGA/TCP/Icaritin showed that the extraction of composite material was non-cytotoxic to L929 cells (Tab.4.5). The RGR was 110%, 105%, 94% and 83% separately for the 1%, 10%, 50% and 100% extraction of PLG/TCP/Icaritin scaffold, while that in negative group was very low. The cytotoxicity score was 0-I grade which indicated that the PLGA/TCP/Icaritin had a good biocompatibility.

4.3.2. Biocompatibility in vivo

For intramuscular implantation studies, all the rabbits showed to tolerate the surgery after intramuscular implantation. No cases of mortality, infection, oedema or paralysis were found during one-month observation period. The area of implantation healed without any complications. When the samples were taken out, the muscles around the scaffolds in both PLGA/TCP and PLGA/TCP/Icaritin groups were obviously normal (Fig.4.1 B). The histology showed that the muscles had good healing response to the scaffold at one month after implantation in both groups (Fig.4.2 A and B). Summary of light microscopy observations around the composite

scaffold materials at one month post-implantation were showed in Tab.4.6 and there were no obvious difference between PLGA/TCP and PLGA/TCP/Icaritin scaffolds. Fibrous connective tissues were observed between the muscles and the scaffolds as a capsule and they were also exited at the inner pores of scaffolds combined with mild degradation of composite materials. Many fibroblasts and fibrocytes were present in the capsule combined with obvious neovascularization ingrowth (Fig.4.2). There were no necrosis, oedema and haemorrhage could be found at the site of muscles around the scaffolds in both groups. No calcification, oedema and fatty infiltration were found at the area of scaffolds. There were many macrophages and lymphocytes could be found to penetrate into the scaffolds in both groups. The most of the macrophages were close to the edge of the materials or spread at the inner of the materials which was related with the degradation of the scaffolds.

4.3.3. Cells attachment in scaffold

Fig.4.3 showed the attachment of BMSCs to scaffolds in PLGA/TCP, PLGA/TCP/Icaritin-L, PLGA/TCP/Icaritin-M and PLGA/TCP/Icaritin-H groups 4 hours after seeding. The initial cell seeding efficiency was 65.6 ± 7.8%, 67.8 ± 6.2%, 70.4 ± 5.8% and 73.6 ± 7.2% for PLGA/TCP, PLGA/TCP/Icaritin-L, PLGA/TCP/Icaritin-M and PLGA/TCP/Icaritin-H groups, respectively. The seeding efficiency showed no obvious difference among four groups. Attachment and the morphology of BMSCs on scaffolds were confirmed by direct visualization under SEM (Fig.4.4). The cells were attached to the scaffolds tightly and spread at the surface of the scaffold according to the micro-shape of materials.

4.3.4. Cells proliferation in scaffold

The proliferation curve of BMSCs on scaffolds in four groups from day 1 to 7 was shown at Fig.4.5 by MTT method. The cell number increased in four groups with time development after cell seeding. The proliferation of BMSCs in PLGA/TCP/Icaritin-H increased quickly when compared with that in PLGA/TCP group, especially at day 5 and 7 ($p<0.05$). When labeled with GFP, the cells at the surface of the scaffolds could be observed under fluorescent microscope. Fig.4.6 showed the proliferation of BMSCs at the surface of PLGA/TCP/Icaritin-H scaffold which was confirmed by the MTT method. When the scaffold was cut into half, the cells were found to penetrate from surface to centre of the scaffold along the trabeculae of scaffold at the sectional drawing under fluorescent microscope and the depth of the cells ingrowth into the scaffold was at least three pores (Fig.4.7). The cells number gradually decreased with the distance away the surface of the scaffold.

4.3.5. Osteogenic effect in vitro

To certify the potential osteogenic ability of BMSCs in PLGA/TCP and PLGA/TCP/Icaritin-H scaffold in vitro, ALP activity and extracellular calcium deposition were determined. At day 7, the ALP activity in PLGA/TCP/Icaritin-H group was higher than that in PLGA/TCP group (Fig.4.8, $p<0.05$). At day 14, the calcium deposition in PLGA/TCP/Icaritin-H group was higher than that in PLGA/TCP group (Fig.4.9, $p<0.05$),

As it is technically not feasible to delineate the original osteogenic gene expression of the BMSCs from rabbit due to the absence of primer in gene bank of

PubMed, several genes related to osteogenesis (OC, BSP and OPN) were selected to perform real time PCR using UMR 106 cells. 4 days after seeding of UMR 106 cells on the porous scaffolds, mRNA expression of OC and BSP in PLGA/TCP/Icaritin-H group was higher than those in PLGA/TCP group ($p<0.05$), yet no difference in OPN mRNA expression was found between two groups (Fig.4.10).

4.4. Discussion

Biocompatibility of bone substitute was indeed important in clinical applications because the materials with toxicity would result in cells death and host tissue necrosis followed by a high rate of sterile inflammation response and osteolytic reactions (Bostman O. et al. 1992). Though the biocompatibility of PLGA, TCP and Icaritin was well proved (Sherwood J. K. et al. 2002; Fan H. et al. 2006c; Hao W. et al. 2008; Yu D. et al. 2008), once a new composite material was fabricated for practice, it was necessary to assess the biocompatibility of the new materials, even if the individual materials were proved to be biocompatible before (Lawrence W. H. 1999.263-73). In this study, MTT assay was used to examine the relative growth rate of L929 cells on the extract of PLGA/TCP/Icaritin. Though the cell growth in medium extraction with 100% and 50% dilutions was inhibited slightly, no obvious cytotoxicity to L929 cells was found about these extracts. The cytotoxicity of the scaffold seemed to be dependent on the degradation of the polymer (Ignatius A. A. et al. 1996). Faster degradation resulted in lower pH value of degradation medium and higher concentration of degradation products such as L- or D-lactic and glycolic acid, thus the cytotoxicity was found on the L929 cells. The

molecular weight of polymer played an important role on the degradation of materials and that the PLGA with molecular weight 10000-20000 was more soluble. In this study, the molecular weight of PLGA we used was about 800000, which made the materials hardly degrade in short time. What's more, the incorporated Icaritin also moderated the speed of degradation of composite scaffold in study before.

The in vivo biocompatibility was performed by implanting the scaffold in muscles, which could provide a comprehensive understanding on the relationship between biologic response and composite biomaterials. This study strategy was reported to be a good way to access the biocompatibility of biomaterials in vivo by other investigators (VandeVord P. J. et al. 2002; Velayudhan S. et al. 2005). The biocompatibility of implanted materials was usually based on the features of "fibrous capsule" that enveloped at the around or inner of the materials (Behling C. A. et al. 1986). The fibrovascular invasion from the surrounding tissues rapidly induced by materials was important for subsequently incorporated into and replaced by bone tissues. In this study, fibrous connective tissues with fibroblasts and fibrocytes were formed at the interface of the muscles and the scaffolds as a capsule with obvious neovascularization ingrowth in both groups. They also invaded into the inner pores of porous scaffolds with mild degradation of composite materials. A number of macrophages were found around the degraded composite materials which indicated that the cells participated in the degradation process of materials. The cell-mediated degradation result was confirmed by the findings from other in vitro and in vivo studies (Visscher G. E. et al. 1985; Satturwar P. M. et al. 2003; Xia Z. et al. 2006).

The shortcoming of in vivo biocompatibility study is that the result would be influenced by many factors such as incision of muscle, hemorrhage and surgical implantation. The wound formed during surgical process itself could initiate the inflammatory response. When the materials were implanted into the body, the compatibility reaction involved both the effects of the material on the host and that of the host on the material (Marchant R. E. 1989). Inflammation, wound healing, and foreign body responses are generally considered as parts of the tissue or cellular host responses to injury. A moderate inflammatory response would be evoked at the site of surgery characterized by recruitment of neutrophil and lymphocytes at early stage after injury or implantation and followed by the appearance of macrophages after that (Satturwar P. M. et al. 2003). Though the inflammation cells exited one month after implantation in this study, it was just a normal biological response to the degradation of materials because this reaction did not damage the normal muscle around the materials and the wound healing. The connective capsule and collagen fibers formed at the sit of implantation represented the end stage of a healing process (repair phase), which usually follows the initial inflammatory phase (Velayudhan S. et al. 2005). We believed that this innocuousness reaction would help the degradation of the composite materials and be disappeared when the materials absorbed completely by host body.

Osteoconduction is defined as the ability to stimulate the attachment, migration, and distribution of vascular and osteogenic cells within the graft material. The material with a 3D structure and an interconnected pore system permit the transport

of substances and cell ingrowth. The surface must also facilitate the cell attachment and growth (Hutmacher D. W. 2000; Ignjatovic N. et al. 2006). In this study, well initial cell attachment and the higher proliferation of BMSCs were observed on PLGA/TCP/Icaritin-H scaffold, suggesting a better osteoconduction and biocompatibility of the novel PLGA/TCP/Icaritin. Once the scaffold was implanted in vivo, the first step was the attachment of stem cells from local site or migrated from elsewhere. Only by this way, the cells could proliferate at the surface of composite scaffold and then differentiate into osteoblast to form new bone. It was reported that various biodegradable osteoconductive porous materials seeded with viable BMSCs or osteogenic cells can be promising alternatives to an autogenic cancellous bone graft (Ignatius A. A. et al. 1996; Gugala Z. et al. 2005; Morgan S. M. et al. 2007; Fang B. et al. 2009; Heo S. J. et al. 2009; Ivirico J. L. et al. 2009; Yang J. et al. 2009; Ye L. et al. 2009). Several physical characteristics can affect the graft osteoconductivity, including porosity, pore size, and 3Darchitecture (Gugala Z. et al. 2005; Hollister S. J. 2005; Karageorgiou V. et al. 2005). The present study showed that there was no difference for the seeding efficacy among four groups due to their similar surface morphology in our previous work. The increased cell proliferation in PLGA/TCP/Icaritin scaffold may due to the biological effect of Icaritin because Icaritin could be released slowly from the composite scaffold during the cell culture. The additional advantages of using bone graft substitutes based on scaffolds from bioresorbable polymers include the easily controlled sized and shape to match the geometry of the implantation site; the progressively resorption to be replaced by new

bone tissue, and the easily follow-up of bone healing simply using a radio-graphic evaluation due to their radiolucency.

In this study, the cells were found to penetrate into the interior of scaffold from the section of the materials and the cells number gradually decreased with the distance away from the surface of the scaffold. It indicated that the cells seeded on the PLGA/TCP/Icaritin could migrate along the trabeculae of the scaffold into the inner pores of the composite materials. The decreased number at the centre of the scaffold was due to the limitation of the static culture such. Static seeding using a cell suspension lead to high seeding efficiency but poor uniformity, especially lacking of cells integrating in the central of scaffold during the whole culture process (Yang J. et al. 2009). Flow perfusion culture can not only supply nutrients and oxygen for cells and remove the metabolic wastes in the scaffolds by transport of medium throughout the scaffolds but also induces the osteoblastic differentiation of marrow stromal cell-scaffold constructs in the absence of dexamethasone (Holtorf H. L. et al. 2005; Yang J. et al. 2009). Though high seeding efficiency and proliferation of BMSCs could be found at the PLGA/TCP/Icaritin scaffold in this study, it was necessary to use the flow perfusion culture to help the migration and proliferation of cells at the centre of the scaffold in future.

Osteoinduction refers to the ability to stimulate the proliferation and differentiation of pluripotent activated BMSCs into bone-forming cells, resulting in the induction of new bone. In this in vitro study, Icaritin incorporated into the scaffold seemed to promote the ALP activity and extracellular calcium deposition of

BMSCs and osteogenic gene expression of the osteoblast-like UMR 106 cells, which indicated that the PLGA/TCP/Icaritin was able to promote the osteogenic differentiation ability for BMSCs or osteoblast-like cells. Though we could not conclude that the PLGA/TCP/Icaritin composite scaffold had osteoinductive effect due to absence of calcification or ectopic bone formation when the scaffold implanted into the muscles, we also considered that the scaffold had the osteopromotive effect. The osteopromotive refers to factors that facilitate bone formation but are insufficient to drive bone formation like osteoinductive factors such as bone morphogenetic protein BMP-2.

The selection of Icaritin derived from the herb *Epimedium* as bone stimulating or osteopromotive factor was based on our previous studies that showed its effective prevention of estrogen-depletion-induced osteoporosis and SAON (Zhang G. et al. 2007b; Songlin P. et al. 2009; Zhang G. et al. 2009a). By analyzing the main metabolites (Icaritin and Icariin) of EF, Icaritin was biologically more potent than Icariin in differentiation of osteoblastic like cell line, which confirmed previous in vitro studies that serum taken from rats administered with *Epimedium* extract could stimulate proliferation and differentiation of osteoblasts (Chen K. M. et al. 2004) and BMSCs (Songlin P. et al. 2009), while the *Epimedium* extract itself exhibited modest effects. Our in vitro results also demonstrated that Icaritin stimulated proliferation, differentiation and mineralization of BMSCs that might explain potential underlying mechanism of traditional Chinese medicine (TCM) with *Epimedium* as main component of oral herbal drugs for effective treatment of bone metabolic and related

diseases (Chen K. M. et al. 2004).

4.5. Conclusion

Based on our findings in this chapter, we concluded that the PLGA/TCP/Icaritin composite scaffold was non-cytotoxic and the scaffold facilitated the cells attachment, proliferation and osteogenic differentiation. The intramuscular implantation study indicated that the scaffold exhibited an acceptable healing pattern for biocompatible materials. It might be a promising biomaterials applied in bone tissue engineering, e.g. for repair of bone defect. In the next, we will evaluate the osteopromotion effect of this composite scaffold in vivo.

4.6. Figures and legends

Fig.4.1. A: Implantation of the composite scaffold materials (arrow) with 10 mm×10mm×10mm in muscles of rabbit. B: The scaffold (arrow) was sampled from muscle and the muscle around the implant was obviously normal.

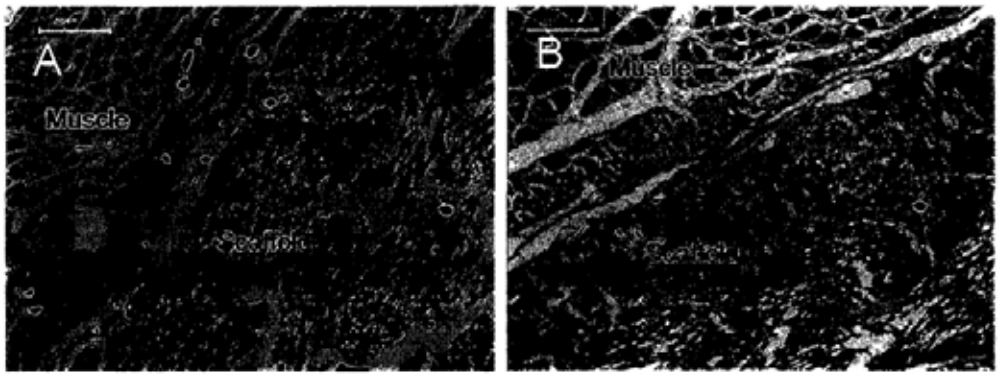

Fig.4.2. Histological observation (H&E) of PLGA/TCP (A) and PLGA/TCP/Icaritin (B) scaffolds in muscles one month after implantation (10×).

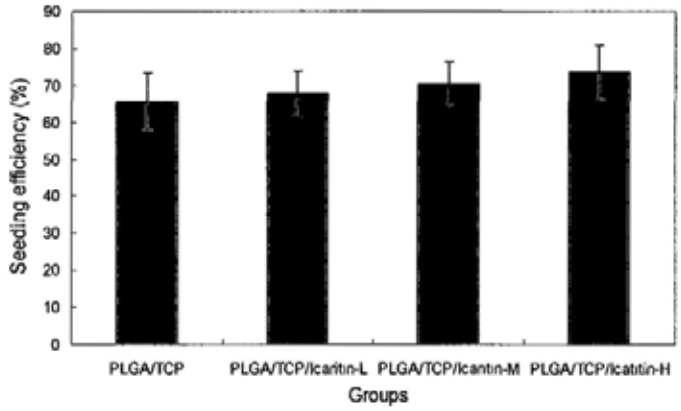

Fig.4.3. Seeding efficiency of BMSCs on scaffolds in PLGA/TCP, PLGA/TCP/Icaritin-L, PLGA/TCP/Icaritin-M and PLGA/TCP/Icaritin-H groups 4 hours after seeding. No difference was found.

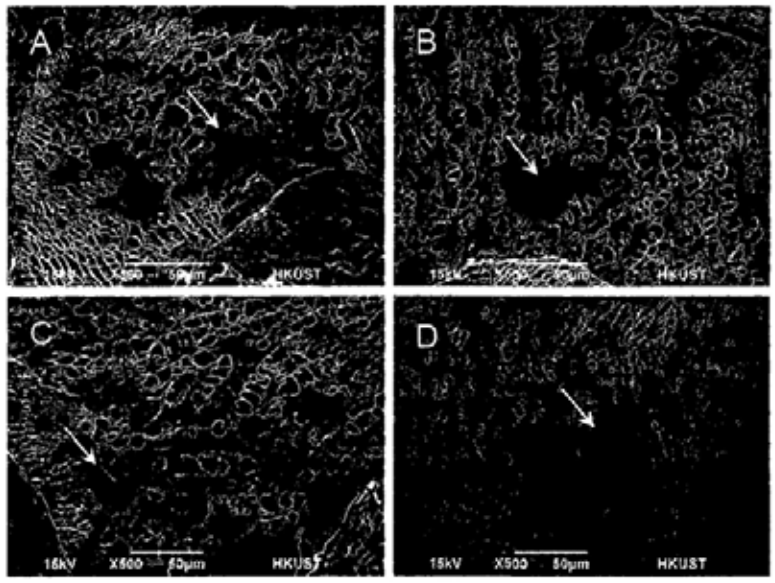

Fig.4.4. SEM observation for attachment of BMSCs (arrow) on scaffolds in PLGA/TCP (A), PLGA/TCP/Icaritin-L (B), PLGA/TCP/Icaritin-M (C) and PLGA/TCP/Icaritin-H (D) groups 4 hours after cells seeding.

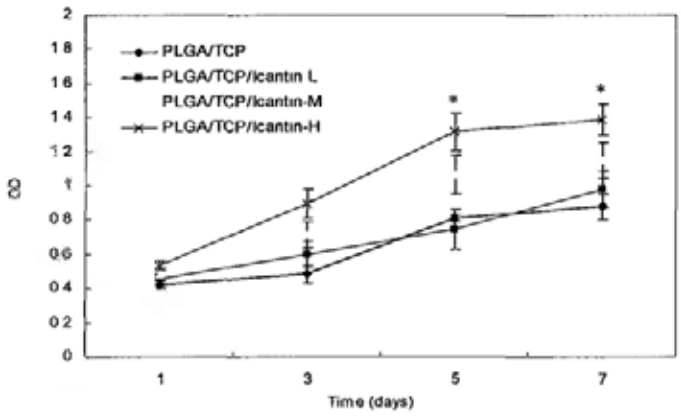

Fig.4.5. Cell proliferation of BMSCs on scaffolds in PLGA/TCP, PLGA/TCP/Icaritin-L, PLGA/TCP/Icaritin-M and PLGA/TCP/Icaritin-H groups. *: $p<0.05$ when compared between PLGA/TCP and PLGA/TCP/Icaritin-H groups.

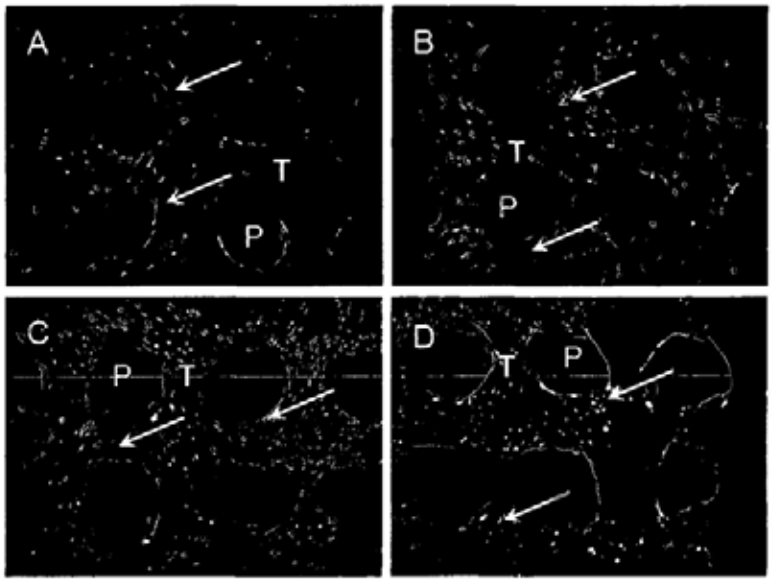

Fig.4.6. Proliferation of BMSCs (arrows) on PLGA/TCP/Icaritin-H scaffolds at day 1, 3, 5 and 7 under fluorescent microscope (5×). A: 1 day; B: 3 days; C: 5 days; D: 7 days. The cells were labeled with GFP. T: trabeculae of scaffold; P: pores of scaffold.

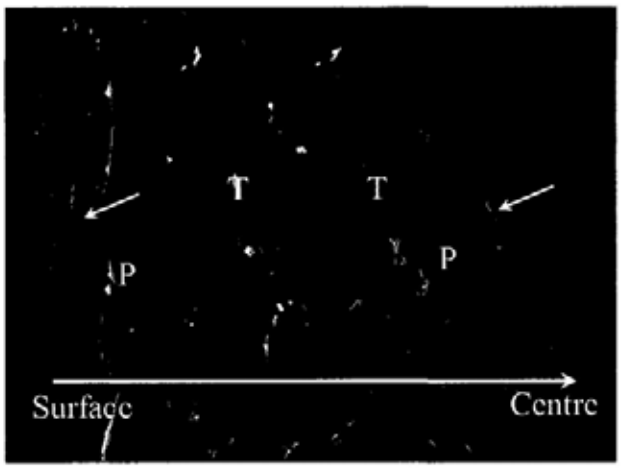

Fig.4.7. Penetration of BMSCs (short arrows) into the inner of PLGA/TCP/Icaritin-H scaffold from sectional drawing (from surface to centre) at day 7 under fluorescent microscope (5×). The cells were labeled with green fluorescent protein. T: trabeculae of scaffold; P: pores of scaffold.

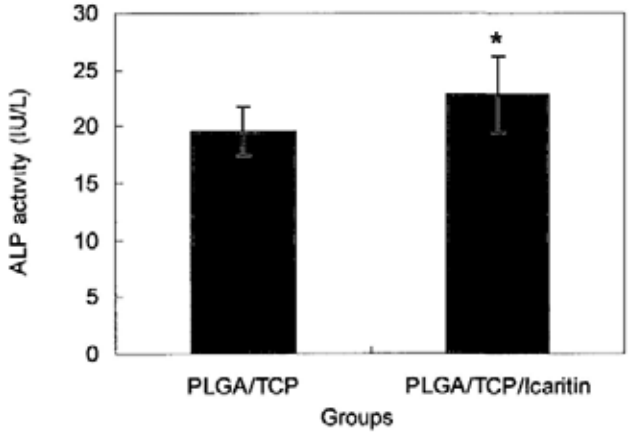

Fig.4.8. ALP activity of cells in PLGA/TCP and PLGA/TCP/Icaritin-H groups 7 days after culture. *: $p<0.05$ when compared between PLGA/TCP and PLGA/TCP/Icaritin-H groups.

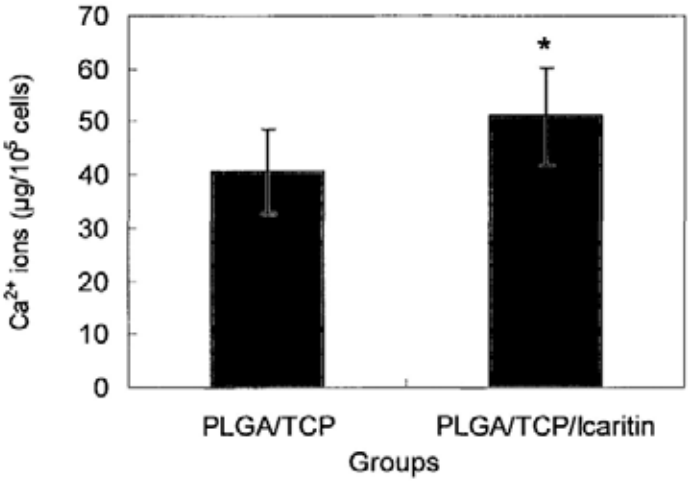

Fig.4.9. Deposit of extracellular calcium in PLGA/TCP and PLGA/TCP/Icaritin-H groups at day 14 after cell culture. *: $p<0.05$ when compared between PLGA/TCP and PLGA/TCP/Icaritin-H groups.

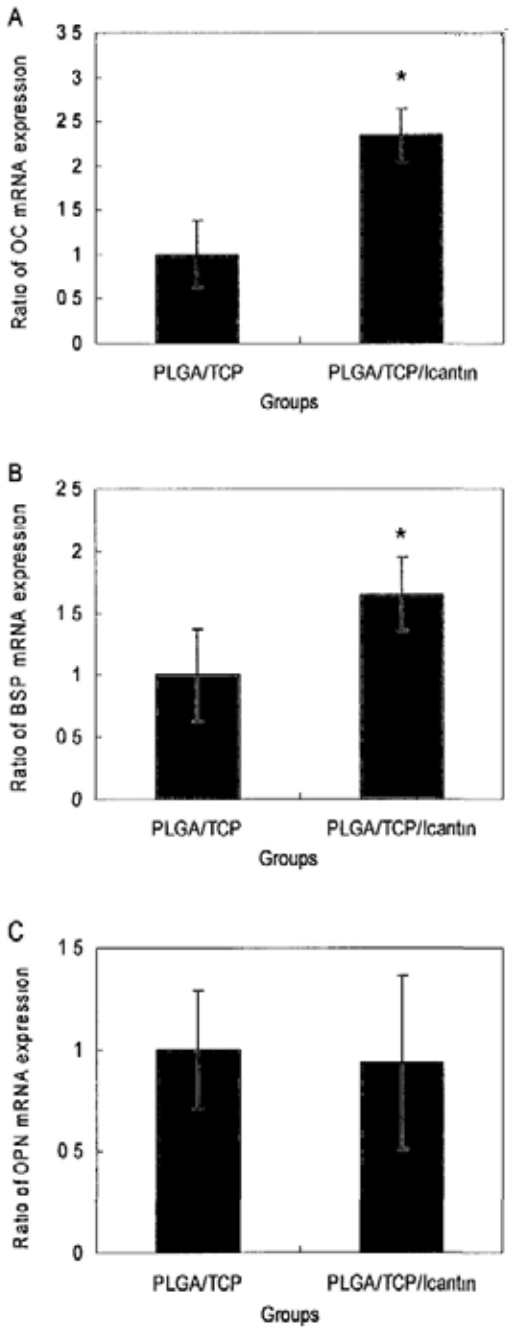

Fig.4.10. Osteocalcin (OC), bone sialoprotein (BSP) and osteopontin (OPN) mRNA of UMR 106 cells on PLGA/TCP and PLGA/TCP/Icaritin scaffolds. *: $P<0.05$ when compared between PLGA/TCP and PLGA/TCP/Icaritin-H groups.

4.7. Tables

Tab.4.1. Preparation of the dilution of phenol

	1%	10%	15%	25%
Phenol solution(ml) at 6.4mg/ml	0.02	0.2	0.3	0.5
Medium (ml)	1.98	1.8	1.7	1.5

Tab.4.2. Preparation of the dilution from the scaffold extraction

	1%	10%	50%	100%
Scaffold extracts (ml)	0.02	0.2	1.0	2.0
Medium (ml)	1.98	1.8	1.0	0

Tab.4.3. Phenol and PLGA/TCP/Icaritin scaffold dilutions (200μl) added at 96-well plate

	Dilutions of medium extraction (%)				Dilutions of phenol (negative group) (%)				Polystyrene extraction (positive group)	Medium
1	2	3	4	5	6	7	8	9	10	11
A										
B	1	10	50	100	1	10	15	25	Polystyrene	Medium
C	1	10	50	100	1	10	15	25	Polystyrene	Medium
D	1	10	50	100	1	10	15	25	Polystyrene	Medium
E	1	10	50	100	1	10	15	25	Polystyrene	Medium
F	1	10	50	100	1	10	15	25	Polystyrene	Medium
G	1	10	50	100	1	10	15	25	Polystyrene	Medium
H										

Tab.4.4. Scoring system for estimating cytotoxicity

Cytotoxicity grade	The relative growth rate (RGR) (%)
0	≥100
1	75-99
2	50-74
3	25-49
4	1-24
5	0

Tab.4.5. Effects of PLGA/TCP/Icaritin extracts on cell viability of L929 cells.

	Dilutions of medium extraction (%)				Dilutions of phenol (negative group) (%)				Polystyrene extraction (positive group)	Medium (%)
	1	10	50	100	1	10	15	25	Polystyrene	Medium
RGR	110	105	94	84	81	41	11	1	100	103

RGR (%): The relative growth rate

Tab.4.6. Summary of light microscopy observations around the composite scaffold materials at one month after muscular implantation

Parameters	PLGA/TCP	PLGA/TCP/Icaritin
Necrosis	0	0
Neutrophils	+	+
Macrophages	++	++
Lymphocytes	++	++
Fibroblasts	+++	+++
Fibrocytes	+++	+++
Fatty infiltration	0	0
Calcification	0	0
Haemorrhage	0	0
Oedema	0	0
Collagen fibers	+++	+++
Neovascularization	++	++

(0) item not present; (±) item occasionally present; (+) item present to a mild degree; (++) item present to a moderate degree; (+++) item present to an appreciable degree (Velayudhan S. et al. 2005).

Chapter 5

Impaired bone healing in steroid-associated osteonecrosis

5.1. Introduction

We have identified that the PLGA/TCP/Icaritin composite scaffold had the proper biodegradation, biocompatibility and osteopromotion, which indicated its potential application in bone defect due to trauma or other disease such as ON.

Steroid-associated osteoporosis (OP) and ON are common that increase both fracture risk and fracture incidence (Naganathan V. et al. 2000; Lane N. E. 2006; Li E. K. et al. 2010). The pathogenesis and pathophysiology of steroid-associated OP and ON are well studies (Assouline-Dayan Y. et al. 2002; Yeap S. S. et al. 2002; Asada T. et al. 2008). Histopathologically, SAON is the death of the bone, which subsequently induces an inadequate repair process that frequently leads to subchondral collapse (Aaron R. 1998; Zhang G. et al. 2009b; Zhang G. et al. 2009c). Therefore, core decompression a commonly used method to treat the early stage of SAON at either proximal or distal long bone, such as at hip was introduced to remove necrotic bone for facilitate bone healing for avoiding later joint collapse (Steinberg M. E. et al. 1984a; Marker D. R. et al. 2008; Sahajpal D. T. et al. 2008; Babhulkar S. 2009; Stronach B. M. et al. 2009).

Although the use of corticosteroid increases the risk and incidence of vertebral or hip fractures (Naganathan V. et al. 2000; Tsugeno H. et al. 2002; Vestergaard P. et al. 2003; Lane N. E. 2006), the effect of these compounds on bone defect healing is not well known. Only few studies reported adverse effect of corticosteroids on fracture or bone defect repair at long-bone shaft (Waters R. V. et al. 2000; Gaston M. S. et al. 2007). Several experimental models or protocols were developed to study

fracture healing typically at long-bone shaft, such as using tibia shaft in rabbits and femoral shaft in rats or mice (Manigrasso M. B. et al. 2004; Komatsubara S. et al. 2005; Sumitomo N. et al. 2008). One of the most appreciated bone healing models to study bone healing at trabecular bone dominant region is a drill-hole bone defect model at metaphysical region of long bone end with advantages of healing without influence of mechanical instability to the healing bone (Zhang R. et al. 2004). This is in fact the model mimicking core decompression. Biologically, core decompression helps to reduce intraosseous pressure and provide a conduit for angiogenesis to revascularize subchondral bone (Wang G. J. et al. 2000). But the residual bone and marrow next to the bone tunnel after core decompression might also be impaired under the influence of corticosteroids that subsequently affected the tunnel repair.

In order to test the hypothesis that the steroid therapy might adversely affect the bone defect healing in trabecular bone, we used an established bone defect model in rabbits with SAON for investigation of bone healing at trabecular dominant skeletal site, i.e. within bone tunnel after core decompression at the distal femora of rabbits.

5.2. Materials and methods

5.2.1. Animal model

Ten 28-week-old male New Zealand white rabbits were used in this study and housed in an environmentally controlled animal care laboratory. The experimental protocol was approved by Animal Experiment Ethics Committee of the Chinese University of Hong Kong (09-472 in DH/HA&P/8.2.1 Pt.10). 5 rabbits were used for establishing the SAON model according our published ON-induction protocol (Qin L.

et al. 2006). One injection of 10μg/kg of LPS was given intravenously. 24 hours later, three injections of 20mg/kg of MPS were given intramuscularly at a time interval of 24 hours. Two weeks after ON-induction, ON would happen at multi-skeletal sites including both distal and proximal femora (Qin L. et al. 2006). Then under general anesthesia, core decompression, i.e. a bone tunnel was created at the coronal plane at bilateral distal femora i.e. CD-ON group. Other 5 rabbits without steroid administration served as controls, i.e. CD-normal group. The consideration for using distal femora for this study was that this region was surgically easier to approach and to monitor osteogenesis and remodeling within the bone tunnel using micro-CT in vivo over time as specified below. Briefly, under general anesthesia with xylazine (2mg/kg body weigh) and ketamine (50mg/kg body weight) a 5mm incision was made laterally through the skin next to the central part of bilateral femoral condyles under fluoroscopy. A 3.0mm trephine was drilled through the distal femora, from the attachment of the medial collateral ligament to the contralateral cortex, parallel to the coronal plane of knee joint. Then the wound was carefully sutured and analgesic was given when needed. Micro-CT evaluation, histological, histomorphometrical and biomechanical analysis were performed.

5.2.2. Micro-CT analysis on new bone formation in bone tunnel

The samples (n=10 in each group) were scanned using a in vivo micro-CT, i.e. a high-resolution peripheral CT (XtremeCT, Scanco Medical, Brüttisellen, Switzerland) with a spatial resolution of 40μm according to the published protocol (Qin L. et al. 2006). The structure of the newly formed trabecular bone in VOI (volume of interest,

including the entire tunnel of 3mm in diameter was defined (Fig.5.1) for evaluation of histomorphometric parameters reported previously (Yeung H. Y. et al. 2005; Ho S. T. et al. 2006). Images of the new bone were reconstructed using proper threshold (range from 130-1000). Average volumetric bone mineral density (vBMD, mg/cm^3), bone mineral content (BMC, mg), bone tissue volume density (BV/TV, %), connectivity density (Conn.D, $1/mm^3$), trabecular number (Tb.N, 1/mm), trabecular thickness (Tb.Th, mm), Trabecula Separation (Tb.Sp, mm) and Structure Model Index (SMI) in bone tunnel were measured. Finite element models were constructed directly from the micro-CT data. The bone tissue around the bone tunnel about 160 slices was reconstructed into 3D image and an element-by-element finite element solver was used to perform uniaxial compression simulations (Fig.5.1 B) for finite element analysis (FEA). Under the application of a 10000MPa in compression strength along the femora axis, two variables in each sample were computed for calculation of both the stiffness and failure load (Donahue T. L. et al. 2002; Bourne B. C. et al. 2004).

5.2.3. Descriptive Histology

After micro-CT scanning, the samples were cut into half along the axial by hacksaw. The medial half of samples were decalcified in the 9% buffered formalin acid. Then all the decalcified samples were embedded in paraffin and longitudinal sections of specimens (each 7μm thick) were prepared using paraffin slicing machine and stained with Hematoxylin and Eosin (H&E). Sections were examined using a light microscope (Leica DMLS, Germany, a digital camera of 0.63X, Leica,

Germany) with polarized light to evaluate both new bone matrix (mineral pattern, collagen alignment and bone cellular events) and marrow composition within the bone tunnel and in the residual bone around the bone tunnel as well as in subchondroal area (Zhang G. et al. 2009a). As collagen is an anisotropic material and when collagen fibers are aligned perfectly transverse to the direction of the light propagation, the change in the refraction of light can be observed when the specimen is exited showing the maximum brightness (Bromage T. G. et al. 2003). The number of osteoclasts (Oc.N) and the osteoblast perimeter percentage (Ob.Pm%) in bone tunnel were calculated under microscope. 10 slices in each sample were observed under microscope with 40 times magnification and 10 regions in bone tunnel were randomly selected, the osteoclasts were counted and the average Oc.N in bone tunnel was calculated. The average Ob.Pm% was calculated by the ratio of length of trabecular surface covered by osteoblast to the whole length of trabecular surface in bone tunnel.

5.2.4. Mechanical test analysis

The lateral half of the specimens of each group were prepared with an identical thickness vertical to the axis of bone tunnel for compression test to obtain the surrogate index of surrounding and ingrowth tissue into the bony tunnel using an indenter of 2.5mm in diameter (Qin L. et al. 2005a; Qin L. et al. 2005b). After positioning the bone tunnel under X-ray, a material test machine (H25K-S, Hounsfield Test Equipment, UK) was used to compress the bone at the bone tunnel at a rate of 10mm/min with a 2.5mm diameter indenter to get the F-λ graph and record

the E-modulus (Mpa), compression stiffness (N/mm) and energy (J) using our established custom-made testing jag (Siu W. S. et al. 2004; Deng H. W. et al. 2005) (Fig.5.6 C).

5.2.5. Statistical analysis

All quantitative data were expressed as mean ± standard error (SE). ANOVA was used to compare the temporal change in new bone within the bone tunnel over time that was measured in vivo at 3 time points and Student t-test was used to compare the difference in mechanical data between the two groups using SPSS version 10.0 (SPSS, Chicago, IL, USA). The level of significance was set at $p < 0.05$.

5.3. Results

No animal died during the entire study period. There were no inflammation and swelling observed at the area of surgery.

5.3.1. Micro-CT quantification of bone repair in whole bone tunnel

Fig.5.1 C and D showed the 3D structures of the new bone formed in the bone tunnel (Fig.5.1 A) of 3mm in diameters at 4, 8 and 12 weeks after core decompression. Fig.5.2A showed the histomorphometry of new bone within bone tunnel of two groups. At week 4, new bone started to form in the tunnel but mainly next to the residual bone around the edge of the tunnel in both groups. Post hoc analysis showed that at week 4, though the BMD, BV/TV, Conn.D and Tb.Th in CD-normal group were higher than those in CD-ON group, such difference was no statistically significant. At week 8, the BMC, BV/TV, Conn.D and Tb.Th increased in both groups when compared with those at week 4 and the BV/TV, Conn.D and Tb.Th

in CD-normal group were significantly higher than those in CD-ON groups ($p<0.05$). At week 12, there was no difference for BMD, BMC and TB.Sp between two groups but the BV/TV, Conn.D, Tb.N, and Tb.Th in CD-normal group were significantly higher than those in CD-ON group (8.80 ± 0.56 vs. 6.49 ± 1.07 for BV/TB (%); 0.65 ± 0.13 vs. 0.37 ± 0.12 for Conn.D ($1/mm^3$); 0.64 ± 0.03 vs. 0.55 ± 0.03 for Tb.N (1/mm); 0.22 ± 0.01 vs. 0.18 ± 0.01 for Tb.Th (mm); $p<0.05$). The SMI in CD-normal group was lower than that in CD-ON group (2.14 ± 0.12 vs. 2.63 ± 0.21, $p<0.05$).

New bone formation increased toward to centre of the tunnel with healing over time up to 12 weeks in CD-ON group and CD-Normal group (Fig.5.2 A). Within each group, the BMD, BMC, BV/TV and Tb.Th were higher at week 12 than those at week 4 ($p<0.05$).

5.3.2. Compression results of finite element analysis using micro-CT

When the simulated compression performed along the femoral axis from distal to proximal direction, the results (Fig.5.2 B) showed that the stiffness (57.6 ± 1.8×10^3N/mm) and the failure load (1316.6 ± 24.2N) of the distal femora in CD-normal were higher than those (54.9 ± 1.3×10^3N/mm) for stiffness and 1253.9 ± 24.8N for failure load)) in CD-ON group ($p<0.05$).

5.3.3. Descriptive histomorphology of new bone formed within bone tunnel

The histomorphological observation on bone healing within the bone tunnel at week 12 was shown in Fig.5.3. The bone tunnel in CD-normal group was filled with normal bone marrow at the centre of tunnel and new formed bone mostly

accumulated at the area about 1mm from the edge of tunnel (Fig.5.3 A). The new bone was thick and well connected with the bone out of the tunnel and had the normal structure with osteocytes in the bone trabeculae and some osteoblasts spreading at the surface of that. There was no empty lacunae was found in the bone trabeculae. For CD-ON groups, the bone tunnel was filled with a lot of fibrous connective tissues, bone marrow infiltrated with a number of mononuclear cells, more osteoclasts and some scattered new bone fragments (Fig.5.3 B). Though no empty lacunae were found, the new formed bone was thin and accompanied by more active osteoblasts and active resorptive activities by osteoclasts. The bone histomorphometry showed that the average number of osteoclasts and the osteoblast perimeter percentage in bone tunnel in CD-normal were lower than those in CD-ON group (Fig.5.3 C and D, $p<0.05$). The arrangement of collagen fibers in bone under polarized light was showed in Fig.5.3 A4 and B4. The collagen fibers showed coherent alignment along the direction of new formed bone in CD-normal group while disordered arrangement of collagen fibers was found in CD-ON group.

5.3.4. Descriptive histomorphology of the residual bone around the bone tunnel

With regard to the bone around the bone tunnel in distal femora of rabbits at week 12, we selected the around area about 1mm distance away from the edge of the bone tunnel (Fig.5.3 A1 and B1). Normal bone and normal bone marrow were observed in CD-normal group (Fig.5.4 A). Osteocytes in bone trabeculae and osteoblasts at the surface of that were observed and the collagen fibers were arranged regularly and parallel with the direction of bone (Fig.5.4 A3). As observed in bone

tunnel, the bone arrow around the tunnel was infiltrated with a number of mononuclear cells and few osteoclasts in CD-ON groups (Fig.5.4 B). But the empty lacunae were found in the bone trabeculae combined with the reparative osteogenesis around them. The collagen fibers were arranged regularly and parallel with the direction of bone (Fig.5.4 B3), which was different with that in bone tunnel in CD-ON group.

5.3.5. Descriptive histomorphology of the subchondral bone

With regard to the subchondral bone near the bone tunnel in distal femora of rabbits at week 12, no fracture and the collapse were found (Fig.5.5). But a number of empty lacunae and seldom osteocytes were observed in bone trabeculae with few osteoblasts spread at the surface of bone in CD-ON group. In CD-normal group, many living osteocytes and osteoblasts were found at the subchondral bone and almost no empty lacunae were observed.

5.3.6. Mechanical test

Before compression test, X-ray of the samples were taken to assist the positioning the bone tunnel and the new bone was visualized in the bone tunnel in both groups (Fig.5.6 A and B). At week 12, the E-modulus (14.8 ± 1.1MPa) and the compression stiffness (68.4 ± 13.4N/mm) in CD-normal group were higher than those (6.2 ± 2.5MPa for E-modulus and 22.2 ± 3.0N/mm for compression stiffness) in CD-ON group ($p<0.05$).

5.4. Discussion

The work designed for this chapter employed in vivo micro-CT, histology and

histomorphometry, radiography and mechanical test to investigate the bone repair within bone tunnel after core decompression in rabbits with SAON to confirm our study hypothesis an overall impaired bone healing under the influence of corticosteroid administration. The LPS used in this study was to induce both hypercoagulable and hypofibrinolytic state which mimicking the clinic diseases, and then followed the treatment with corticosteroid (Qin L. et al. 2006).

In this study, as compared with CD-normal group, BV/TV, Conn.D, Tb.N and Tb.Th of the new bone in tunnel were found significantly lower and SMI was found higher in CD-ON group ($p<0.05$). Histologically, impaired and delayed osteogenesis and remodelling within bone tunnel was demonstrated in CD-ON group, characterized with less and thinner trabeculae surrounded by more osteoblasts and more osteoclasts, significant number of mononuclear cells and insensitive fibrous connective tissues within marrow space. The bone defect was performed in distal femora of rabbits in this study because the SAON also happened in the distal femora (Miyanishi K. et al. 2005). The empty lacunae and the reparative osteogenesis at the surrounding area of bone tunnel in distal femora proved the SAON that occurred, which would impair the bone healing in tunnel at the early stage after administration of steroid. It was reported that the glucocorticoid-induced direct impairment of osteoblast, osteocyte, and osteoclast function leaded to reduced bone remodeling and diminished repair of microdamage in bone (Patschan D. et al. 2001). We also found that the osteogenic ability of marrow mesenchymal stem cells decreased during early SAON development from our previous work and also by others (Li X. et al. 2005;

Yin L. et al. 2006; Sheng H. H. et al. 2007). So the less volume and the thickness of new bone in the bone tunnel in CD-ON group at the early stage might be due to the decreased osteogenic ability and the reduced bone remodelling around bone tunnel.

It was well know that the bone healing in normal bone or osteoporotic bone have been extensively examined clinically and experimentally (Schneider E. et al. 2005; Cancedda R. et al. 2007; Zhang G et al. 2008; Alemdaroglu K. B. et al. 2009). Though the systemic administration of corticosteroids caused OP and ON and increased risk of fracture, few studies have been performed to study the corticosteroids on fracture healing or bone defect repair (Gaston M. S. et al. 2007), especially at the epiphysial and metaphysial regions with dominant trabecular bone where we reported high incidence of steroid-associated fractures (Li E. K. et al. 2010). In long-bone, Waters et al. found that prolonged systemic administration in the presence of defects in long bones small enough to heal spontaneously in a rabbit model led to an 85% rate of nonunion compared with 18% in the control group. Systemic corticosteroids was also reported to inhibit bone healing in a rabbit ulnar osteotomy model (2000). However, few other studies showed that the short-term administration of prednisolone in rats with standardized bone defects (2mm in diameter) in the middle of the femora or intramedullary pinned osteotomies of rat femora did not show any inhibitory effects on long bone healing (Hogevold H. E. et al. 1992; Aslan M. et al. 2005). Such difference may be explained by dosage and duration of steroid administration. In the present study, short-term and pulsed steroid administration was tested that induced ON in the early stage (2 weeks) after

induction in rabbits but the tunnel healing after core decompression was evaluated at 12 weeks after steroid induction. The results revealed that the bone volume, the thickness and the connectivity density of new formed bone in bone tunnel in CD-ON group were lower than those in CD-normal group at week 4, 8 and 12, which could be explained by the decreased osteogenic ability of existing mesenchymal stem cells (Li X. et al. 2005; Yin L. et al. 2006; Sheng H. H. et al. 2007). Thus the steroid could also inhibit the bone healing in trabecular bone defect.

Though we observed that the quality and quantity of new formed bone in CD-ON group were inferior to those in CD-normal group, we also noted that the bone volume, thickness and bone density in CD-ON group increased with the time, which suggested that the bone healing was not completely inhibited. The thin trabeculae with more osteoblasts and more osteoclasts in bone marrow in bone tunnel indicated the active on-going bone formation as compared with mature bone where thicker trabecular with more osteocytes but less lying cells on the bone surface were observed in the CD-normal groups. Extensive fibrous connective tissues were found in the bone tunnel in CD-ON group while normal bone marrow was revealed in the CD-normal group. The aggregated fibrous connective tissues would prevent the ingrowth of new bone which was similar as that happened clinically (Gonzalez Della Valle A. et al. 2005). So it revealed that the SAON indeed delayed the bone healing in general but that of bone defect after core decompression in particular, suggesting the needs for intervention or argumentation of bone healing in patients under the influence of corticosteroid, especially those with fractures at trabecular dominant

skeletal sites (spine and hip) or ON patients after core decompression.

In this study, a bone defect with 3mm in diameter was created in distal femora of rabbit after the core decompression. Accordingly, CD-ON group revealed significant inferior mechanical properties in terms of compression load and elastic modules as compared with that of CD-normal group, which was also supported the simulated compression test at the distal femora using FEA of micro-CT.The mechanical test showed that the stiffness of new bone in bone defect in CD-ON group was significant lower than that in CD-normal group. Though we used the compression test in this study which represented the mechanical properties of interface between new bone in tunnel and the residual bone around the tunnel, it could indirectly indicate the poor mechanical properties for the new formed bone in bone tunnel in CD-ON group, which could explain the trend to collapse easily after core decompression treatment in clinic when the relatively large necrotic bone was removed. From the mimic compression test using FEA which was similar to the loading direction in vivo, the stiffness and the failure load of distal femora of rabbits in CD-ON group were lower than those in CD-normal groups. The results in this study seemed similar as those from clinic studies in which the ON patients had a significantly higher rate of mechanical failure than those without ON (Ortiguera C. J. et al. 1999). Low bone volume formed in bone tunnel and the relatively low BMC might explain the inferior mechanical properties.

According to the follow-up results using micro-CT at week 4, 8 and 12, the new bone grew into the bone tunnel gradually with the time development but most of

them concentrated at the area 1mm away from the edge of the tunnel and few bone penetrated into the centre of the tunnel, which could be confirmed by the histology observation results. From the 3D images from micro-CT, we found the bone volume at the two ends of the bone tunnel (area near the cortical bone) was more than that at the middle (area among the trabecula bone) of the bone tunnel. This might be explained by stronger osteogenic ability of peripheral periosteum next to the bone tunnel (Malizos K. N. et al. 2005). The little bone at the centre of the bone tunnel could be the result of lacking the platform to conduct the bone ingrowth, so bone graft or different bone substitute were needed for augmentation of bone repair after core decompression.

5.5. Conclusion

In conclusion, the experimental study designed in this part confirmed that bone healing was impaired or delayed in a trabecular bone defect model in rabbits with SAON. This animal model formed a foundation for developing therapy strategies for enhancing treatment prognosis of difficult fracture or bone defect repair resulted from administration of steroid that was designed for confirmation in the next Chapter (Chapter 6).

5.6. Figures and legends

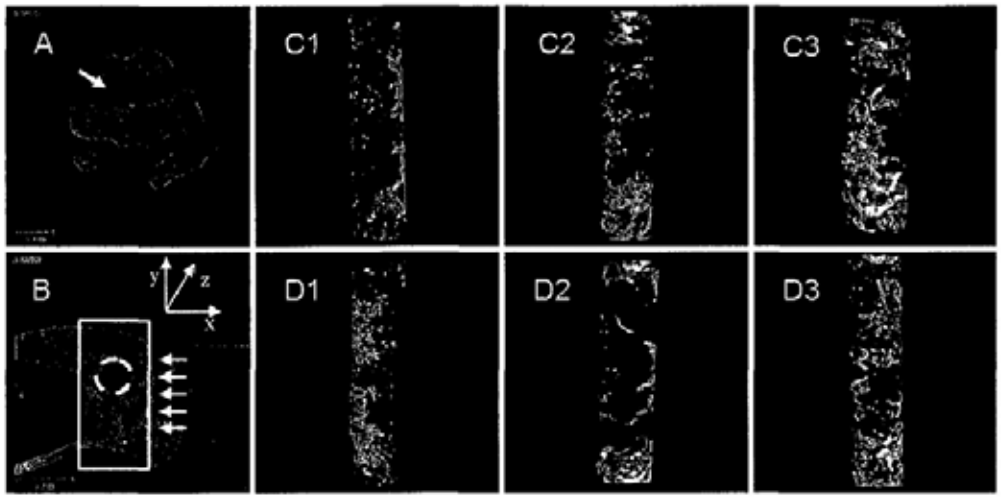

Fig.5.1. Bone tunnel after core decompression and its micro-CT evaluation. A: 2D micro-CT image of bone tunnel (arrow) in a coronal view; B: 2D micro-CT image at sagittal view with drill hole for refining ROI (dotted cycle) of new bone formed in the bone tunnel where finite element analysis was perform to simulate uniaxial compression along the x-axis (arrows) towards the bon tunnel (rectangular frame). C and D: representative micro-CT 3D images of the new bone formed within the bone tunnel of 3mm in diameters of CD-normal group (C1-3) and CD-ON groups (D1-3) at week 4, 8 and 12 after core decompression, respectively.

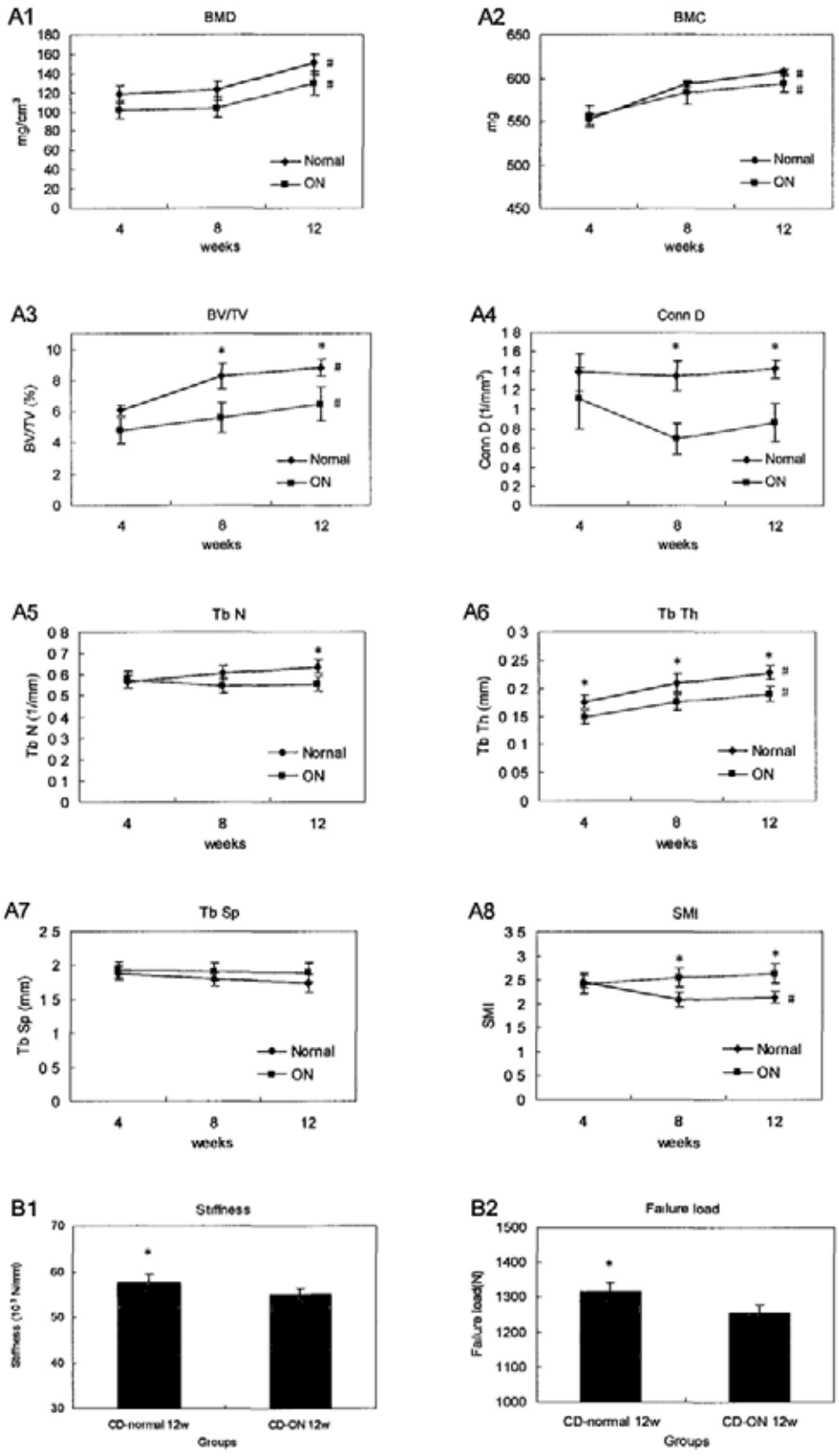

Fig.5.2. Micro-CT quantitative analysis. A: Bone mineral and structural data of the newly formed bone tissue within bone tunnel of 3mm in diameter in the CD-normal

group (n=10) and CD-ON group (n=10) at week 4, 8 and 12 after core decompression (A1-8). *: $p<0.05$ when compared to CD-ON group; #: $p<0.05$ when compared at week 4, 8 and 12 in each group. B: Finite element analysis for the distal femora in direction along the axis of femora in CD-normal group and CD-ON groups 12 weeks after core decompression. B1: Stiffness compared between CD-normal group and CD-ON group (*: $p < 0.05$); B2: Failure load compared between CD-normal group and CD-ON group (*: $p < 0.05$).

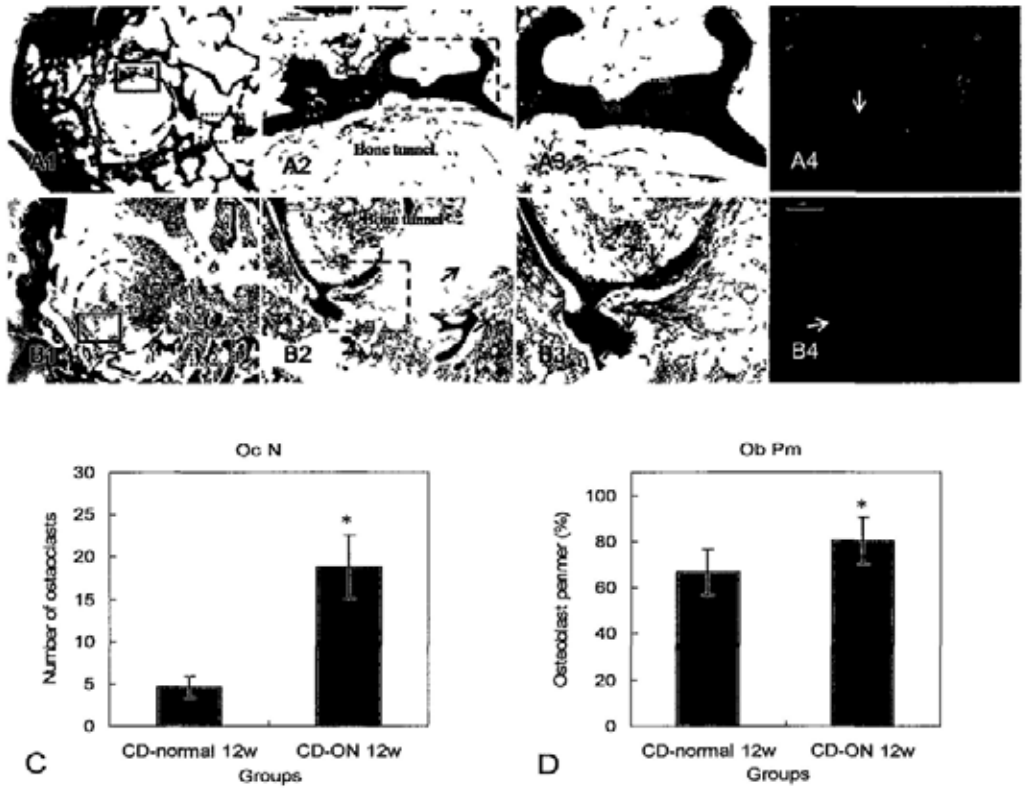

Fig.5.3. Representative histology of bone tunnel in CD-normal group (A) and CD-ON (B) group. 12 weeks after core decompression or 14 weeks after ON induction (H&E staining: A1-A3 and B1-B3; Polarized microscopy: A4 and B4). A1: New bone (included in black circle) formed within bone tunnel in CD-normal group (1.6×), the dotted rectangular frame was magnified to Fig.5.4.A; A2: ROI magnified from the rectangular frame of A1, showing new formed bone marrow and trabecular bone with normal structure (10×); A3: ROI magnified from the dotted rectangular frame of A2, showing normal new bone formation, with numerous osteoblasts lying along the trabecular surface (black arrows) with regular bone marrow fat cells (20×); A4: Trabeculae observed under polarized light of A3, showing regular and parallel or lamellar-type collagen fibers (20×); B1: New bone (included in black circle) formed within bone tunnel in CD-normal group (1.6×), the dotted rectangular frame was

magnified to Fig.5.4.B; B2: ROI magnified from the frame of B1. Fibrous connective tissue (black arrow) was found apart from new formed bone marrow and bone in bone tunnel and more osteoclasts (blue arrows) scattered in bone marrow (10×); B3: ROI magnified from the dotted rectangular frame of B2, showing numerous mononuclear cells (black arrows) infiltrated into the bone marrow apart from fibrous connective tissue in bone tunnel and accompanied by active resorptive activities by osteoclasts (blue arrows), thin trabeculae with more active osteoblasts lying at the surface of bone (20×); B4: The same ROI of B3 observed under polarized light, showing less organized collagen fibers (white arrow) (20×). C: Average number of osteoclasts in bone tunnel (*: $p<0.05$); D: Average osteoblast perimeter percentage in bone tunnel (*: $p<0.05$).

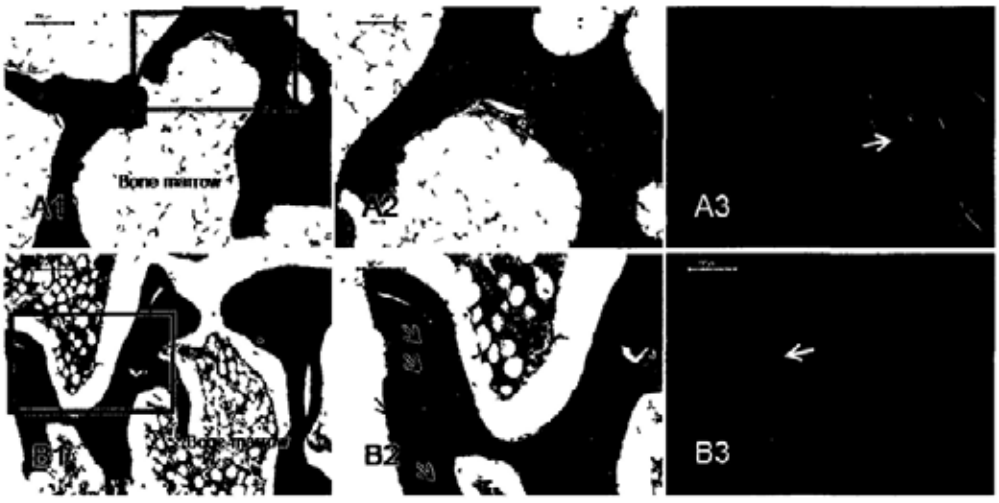

Fig.5.4. Representative histology of trabecular bone next to the bone tunnel (H&E staining: A1-A2 and B1-B2; Polarized microscopy: A3 and B3) of bone around the tunnel in CD-normal group (A) and CD-ON group (B) 12 weeks after core decompression or 14 weeks after ON induction. A1: Mature bony tissue and bone marrow found around the bone tunnel in CD-normal group (10×, magnified from the dotted rectangular frame Fig.5.4 A1); A2: ROI magnified from the frame of A1, showing mature and thick trabeculae with numerous osteocytes within bone matrix but less osteoblasts alone the trabecular surface (20×); A3: The same ROI of A2 observed under polarized light, showing typical lamellar pattern (white arrows) of collagen fibers (20×); B1: Bone tissue and bone marrow around the bone tunnel in CD-ON group (10×, magnified from the dotted rectangular frame Fig.5.4 B1), the bone marrow was infiltrated by many mononuclear cells; B2: Region of interest that is magnified from frame of B1. A number of empty lacunae (black arrows) were found in the bone trabeculae and the reparative osteogenesis(blue arrows) were found around them (20×); B3: Observation under polarized light for B2, the collagen fibers arrange regularly and parallel with the direction of bone (white arrows) (20×).

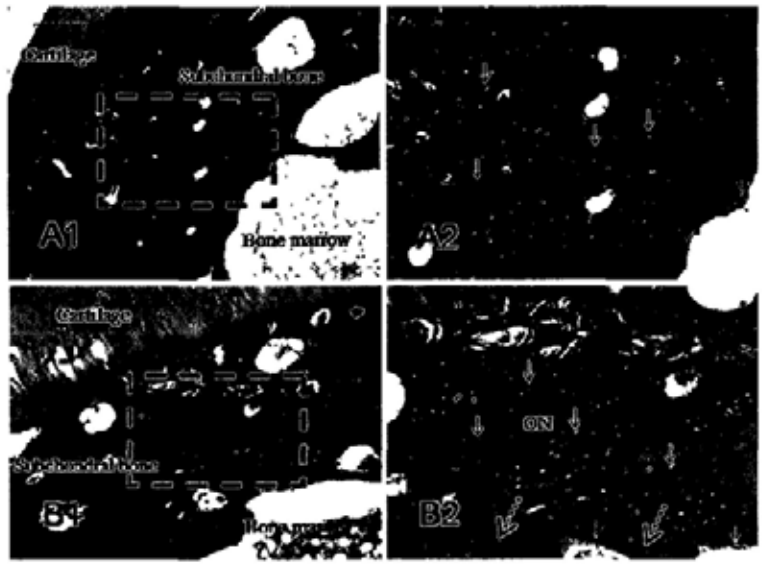

Fig.5.5. Representative histology of subchondral bone around the tunnel in CD-normal group (A) and CD-ON (B) group at 12 weeks after core decompression or 14 weeks after ON induction (H&E staining). A1: Normal subchondral bone shown in the CD-normal group (10×); A2: ROI magnified from the rectangular frame of A1, showing numerous lacunae with normal osteocytes (black arrows) within bone matrix and osteoblasts (yellow arrows) alone the surface of subchondral bone (20×); B1: Necrotic bone tissue under cartilage in CD-ON group (10×); B2: ROI magnified from the frame of B1, showing typical empty lacunae (black arrows) within the necrotic bone (ON) and scattered osteoblasts (yellow arrows) alone the surface of the subchondral bone combined with little reparative osteogenesis(black broken arrows) (20×).

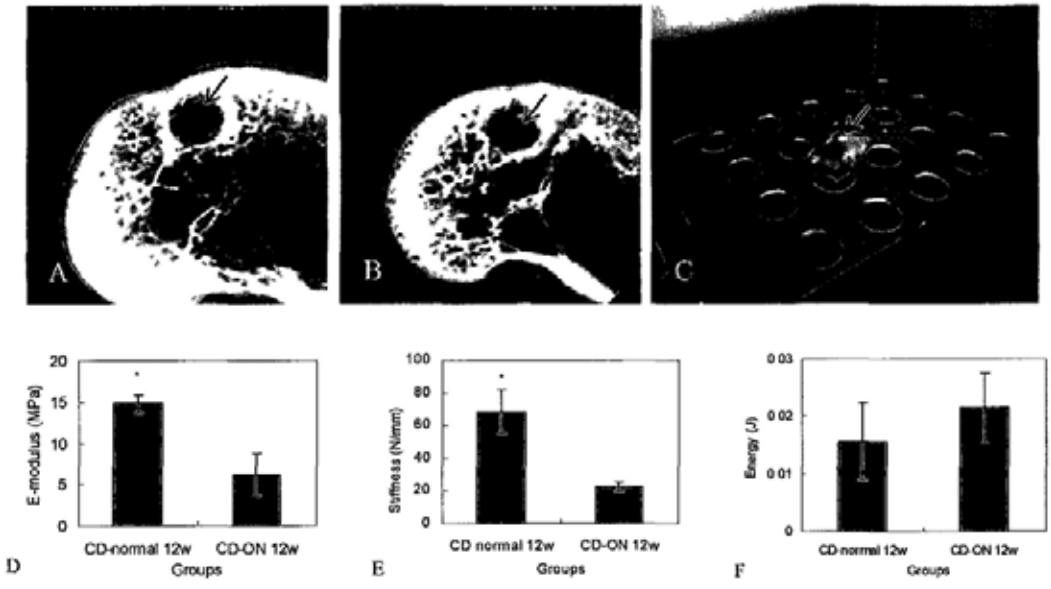

Fig.5.6. Compression test results compared between the CD-normal group (n=10) and CD-ON group (n=10) at 12 weeks after core decompression. A: Position of bone tunnel (arrow) with new formed bone in CD-normal group observed under X-ray; B: Position of bone tunnel (arrow) with newly formed bone in CD-ON group observed under X-ray; C: Compression test of the bone within the bone tunnel (arrow) using an indenter of 2.5mm in diameter; D: E-modulus compared between CD-normal group and CD-ON group (*: $p < 0.05$); E: Compression stiffness compared between CD-normal group and CD-ON group (*: $p < 0.05$); F: Energy compared between CD-normal group and CD-ON group.

Chapter 6

Bone repair in steroid-associated osteonecrosis lesion enhanced by porous PLGA/TCP/Icaritin composite scaffold

6.1. Introduction

As observed in Chapter 5, the bone healing was delayed in a trabecular bone defect after core decompression in rabbits with SAON. In clinic, the SAON is a common orthopaedic problem secondary to several medical conditions using steroid (Assouline-Dayan Y. et al. 2002; Lieberman J. R. et al. 2003; Chan M. H. et al. 2006; Mont M. A. et al. 2006; Law R. K. et al. 2008). It occurs mostly in large joints such as hip that may subsequently develop to joint collapse and end up with joint replacement surgery (Saito S. et al. 1989; Seyler T. M. et al. 2007). But the prognosis of joint replacement in SAON patents are also poor (Devlin V. J. et al. 1988; Assouline-Dayan Y. et al. 2002; Nowicki P. et al. 2007). The current consensus on effective prevention of subchondral collapse in SAON is to perform core decompression, i.e. one of the least invasive surgical procedures in early ON stages when the ON lesion is still small. Biologically, core decompression helps to reduce intraosseous pressure and provide a conduit for angiogenesis to revascularize subchondral bone (Wang G. J. et al. 2000). But subchondral collapse post core decompression often occurs in SAON, which is due to both lack of osteogenic platform after removal of relatively large size necrotic bone and impaired osteogenic potential of stem-cell-pool under influence of a pulsed steroid regime (Gangji V. et al. 2005b; Hernigou P. et al. 2005; Li X. et al. 2005; Yin L. et al. 2006; Sheng H. H. et al. 2007). Based on tissue engineering strategy, both local healing environment and stimulating biological factors should be provided (Griffith L. G. et al. 2002). To promote the bone repair effectively using bone regenerative medicine, it is important

to develop safe and cheap drugs that can potently induce bone formation.

In previous chapters, the studies showed that Icaritin, a small bioactive molecule with osteogenic effect, could be incorporated into the PLGA/TCP using computer-controlled fine biospinning technology under low temperature to form a porous composite scaffold PLGA/TCP/Icaritin. This composite scaffold had a foundation with characteristics of slow release of Icaritin during its degradation, a porous architecture to allow for tissue ingrowth, and mechanical support to the affected area. We have also identified that this composite scaffold was non-toxic and had good compatibility to facilitate the adhesion, proliferation and osteogenic differentiation of BMSCs in vitro.

We hypothesized that this composite scaffold could provide the platform to conduct the new bone ingrowth and the osteogenic factor to promote the osteogenic ability of BMSCs around the necrotic lesion. Thus the purpose of the present experimental study was to examine the osteogenesis inside surgical tunnel in the SAON lesion after implantation of PLGA/TCP/Icaritin scaffold in a rabbit model.

6.2. Materials and methods

6.2.1. Preparation of PLGA/TCP/Icaritin scaffold for in vivo implantation

According to the results from Chapter 3 and 4, the scaffold in PLGA/TCP/Icaritin-H group was selected for in vivo implantation due to its better material and biological findings in terms of biodegradation and facilitating for attachment, proliferation and differentiation of BMSCs. In order to facilitate the in vivo implantation procedure, the PLGA/TCP/Icaritin scaffolds were cut into a

cylinder with 3mm in diameter (Fig.6.1 A) to fit the bone tunnel created in rabbits. From its facilitation for cells attachment, proliferation and differentiation in previous work, the scaffold containing the high concentration of Icaritin was selected in this study. The cylinders of scaffold were sterilized with 75% ethanol and washed with sterilized PBS, and then they were put into a dish and exposed to ultraviolet for 30 minutes before implantation.

6.2.2. Animal model

Ten 28-week-old male New Zealand white rabbits were used in this study and housed in an environmentally controlled animal care laboratory. The experimental protocol was approved by Animal Experiment Ethics Committee of the Chinese University of Hong Kong (09-472 in DH/HA&P/8.2.1 Pt.10). The SAON model was established in rabbits according our published ON-induction protocol (Qin L. et al. 2006) that was also described in details in Chapter 5. One injection of 10μg/kg of LPS was given intravenously. 24 hours later, three injections of 20mg/kg of MPS were given intramuscularly at a time interval of 24 hours. Two weeks after induction, ON would happen at multi-skeletal sites including both distal and proximal femora (Qin L. et al. 2006). Then under general anesthesia with xylazine (20mg/kg body weight) and ketamine (50mg/kg body weight), a 3.0mm trephine was drilled through the distal femora, from the attachment of the medial collateral ligament to the contralateral cortex, parallel to the coronal plane of knee joint. Thus a bone tunnel was created at the coronal plane at bilateral distal femora. The cylinders of PLGA/TCP (P/T group) and PLGA/TCP/Icaritin (P/T/I group) scaffolds were

randomly implanted into left or right distal femora (Fig.6.1). Then the wound was carefully sutured and analgesic was given when needed. The consideration for using distal femora for this study was that this region was surgically easier to approach and to monitor osteogenesis and remodelling within the bone tunnel using micro-CT in vivo over time as specified below. Micro-CT evaluation, histological, histomorphometrical and biomechanical analysis were performed after the sacrifice of animals.

6.2.3. Micro-CT analysis on new bone formation in bone tunnel

After the operation, region of surgery in rabbits were scanned for follow-up using an in vivo micro-CT, i.e. a high-resolution peripheral CT (XtremeCT, Scanco Medical, Brüttisellen, Switzerland) with a spatial resolution of 40μm according to the published protocol at 0, 2, 4, 8 and 12 weeks respectively (Qin L. et al. 2006). The structure of the newly formed bone in VOI (the entire tunnel of 3mm in diameter and the centre of tunnel with 2mm in diameter were defined (Fig.6.2) for evaluation of histomorphometric parameters reported previously (Yeung H. Y. et al. 2005; Ho S. T. et al. 2006). The bone at the centre of the tunnel with 2mm in diameter was also evaluated which indicated the ability of new formed bone penetrating into the centre of the scaffold. Images of the new bone were reconstructed using proper threshold (range from 130-1000). Average volumetric bone mineral density (vBMD, mg/cm^3), bone mineral content (BMC, mg/cm^3), bone tissue volume density (BV/TV, %), connectivity density (Conn.D, $1/mm^3$), trabecular number (Tb.N, 1/mm), trabecular thickness (Tb.Th, mm), trabecula Separation (Tb.Sp, mm) and structure model index

(SMI) in bone tunnel were measured.

6.2.4. Evaluation of neovascularization ex vivo

At 12 weeks post-operation, half of the rabbits were perfused with heparinized saline. The vascular system will be injected with a radiopaque, lead chromate based contrast agent (Flow Tech, USA) though abdominal aorta, which was allowed to polymerize for 24 hours at 4°C. The rabbit was anesthetized by muscular injections of xylazine (20mg/kg body weight) and ketamine (50mg/kg body weight). After opening the abdomen cavity using operational apparatus, the abdomial aorta and cardinal vein were separated carefully. Then the pre-warmed heparinized saline 100ml was injected into ear vein and both of t the abdomial aorta and cardinal vein proximal to heart were ligated using silk. Then a scurf-needle (cut needlepoint) was inserted into abdomial aorta distally to heart and linked to a pump apparatus. After continuously flushing the blood circulation using pre-warmed normal saline 600ml, the pre-warmed formalin 100ml was inject through abdomial aorta. Then liquid compound of MV-Diluent, MV-117 Orange and MV Curing Agent (Microfil, Flow Tech, INC.; Carver, MA, USA) was injected as soon as they were just mixed. After that, the cadaver was stored under 18°C for 4 hours.

For examination of neovascularization in bone tunnel, the distal femora were taken out and prepared for decalcification in the 9% buffered formalin acid in order to differentiate radiodensity-based segmentation of the contrast-filled vessels from the surrounding mineralized tissues using micro-CT-based angiography (vivaCT, μ40, Scanco Medical, Brüttisellen, Switzerland) established by published protocols (Qin L.

et al. 2006; Duvall C. L. et al. 2007; Zhang G. et al. 2007a; Zhang G. et al. 2009a). The specimens were then scanned at a 10μm isotropic voxel size, and 2D tomograms were reconstructed. The VOI in bone tunnel was defined for evaluation of contrast-agent filled vascular network, including vessel number and size, their absolute volume and volume fraction within VOI (Zhang G. et al. 2007a).

6.2.5. Descriptive histology and histomorphometry

After micro-CT scanning, the samples with decalcification were embedded in paraffin and longitudinal sections of specimens (each 7μm thick) were prepared using paraffin slicing machine and stained with Hematoxylin and Eosin (H&E). Sections were examined using a light microscope (Leica DMLS, Germany, a digital camera of 0.63X, Leica, Germany) to evaluate the changes of new bone and scaffold materials within the bone tunnel. For histomorphometry, 6 slices at the intermediate piece of tunnel in each sample were observed under light microscope and the pictures were taken. The area of new formed bone (%, bone area/tunnel area) in tunnel was analyzed by image-pro plus 6.0.

6.2.6. Mechanical test analysis

The lateral half of the specimens without decalcification in each group were prepared with an identical thickness vertical to the axis of bone tunnel (Fig.6.10) for compression test to obtain the surrogate index of ingrowth tissue into the bony tunnel using an indenter of 2.5mm in diameter (Qin L. et al. 2005a; Qin L. et al. 2005b). After positioning the bone tunnel under X-ray (32kv,3s), a material test machine (H25K-S, Hounsfield Test Equipment, UK) was used to compress the bone at the

bone tunnel at a rate of 5mm/min with a 2.5mm diameter indenter to get the F-λ graph and record the E-modulus (MPa), the displacement for maximum load, compression stiffness (N/mm) and energy (J) using our established custom-made testing jag (Siu W. S. et al. 2004; Deng H. W. et al. 2005).

6.2.7. Statistical analysis

All quantitative data were expressed as mean ± standard error (SE). ANOVA was used to compare the temporal change in new bone within the bone tunnel over time that was measured in vivo at 5 time points and Student t-test was used to compare the difference in histomorphometric and mechanical data between two groups using SPSS 10.0 (SPSS, Chicago, IL, USA). The level of significance was set at $p < 0.05$.

6.3. Results

The composite scaffold biomaterials showed good biocompatibility and no inflammation was found at the surgery area. The wound healing was excellent.

6.3.1. Micro-CT quantification of bone repair in entire bone tunnel with 3mm in diameter

2D images in a transverse view and 3D images in a coronal view of distal femora of rabbits at week 4, 8 and 12 after core decompression were showed at Fig.6.3. The results showed that the defect of whole bone tunnel was complete and seldom new bone could be found at week 4 in two groups, but there were some new bone formed in the tunnel at week 8, especially at area close to the cortical bone. The new formed bone was very obvious at week 12, the intermediate piece of tunnel was filled with

new bone in P/T/I group. Fig.6.4 showed the representative 3D structure of the new bone formed within bone tunnel of 3mm in diameters at week 4, 8 and 12 after scaffold implantation and it seemed that the bone volume increased with time in two groups.

Micro-CT-based histomorphometric analysis showed the changes from week 0 to week 12 in bone tunnel in P/T and P/T/I groups (Fig.6.5). At week 0 and 2, the bone tunnel was almost empty and there were seldom residual bone in the tunnel in both groups. At week 4, new formed bone could be observed but the volume of them was very small (about 1.61% for P/T group and 1.87% for P/T/I group). At week 8, the bone volume and bone mineral density in both groups increased obvious when compared with those at different time points before ($p<0.05$). The BMD, BV/TV, Tb.N and Tb.Th in P/T/I group were higher than those in P/T group but the difference was not obvious. Only the Conn.D in P/T/I group were higher than that in P/T group ($p<0.05$). At week 12, the bone volume and bone mineral density in both groups increased more obvious when compared with those at week 8 ($p<0.05$). There were no difference for BMC, Tb.N, and Tb.Th and TB.Sp between two groups but the BMD, BV/TV and Conn.D in P/T/I group were higher than those in P/T group ($p<0.05$). The SMI in P/T/I group was lower than that in P/T group ($p<0.05$).

6.3.2. Micro-CT quantification of bone repair at the centre of scaffolds with 2mm in diameters

Fig.6.6 showed the representative 3D structure of the new bone formed at the centre of scaffold with 2mm in diameters at week 4, 8 and 12 after scaffold

implantation and it also seemed that the bone volume increased with time in two groups. But seldom bone was found at the centre of scaffold at week 4.

With regard to the new formed bone with 2mm in diameters at the centre of scaffold at week 0, 2, 4, 8 and 12 after scaffolds implantation, the micro-CT-based histomorphometric analysis were showed at Fig.6.7. At week 0, 2 and 4, seldom bone was found at the centre of scaffolds in two groups, but the quantity of bone ingrowth increased obviously at week 8 and 12 when compared with time points before ($p<0.05$). At week 8, the BMD, BMC, BV/TV, Conn.D, Tb.N and Tb.Th in both groups increased obvious when compared with those at week 4 ($p<0.05$). The BV/TV, Tb.N and Tb.Th in *P/T/I* group were higher than those in P/T group but the difference was not obvious. No difference was found for BMC and only the Conn.D in P/T/I group were higher than that in P/T group ($p<0.05$). At week 12, the BMD, BV/TV, Conn.D and Tb.Th in both groups increased more obvious when compared with those at week 8 ($p<0.05$). There were no difference for BMC and TB.Sp between two groups but the BV/TV and Conn.D in P/T/I group were higher than those in P/T group ($p<0.05$). The BMD, BMC, Tb.N and Tb.Th in P/T/I group were higher than those in P/T group but the difference was not significant. The SMI in P/T/I group was lower than that in P/T group ($p<0.05$).

6.3.3. Evaluation of neovascularization ex vivo

The Fig.6.8 A and B showed 3D images of the neovascularization in bone tunnel at week 12 after the scaffold implantation. The volume, number and the size of the neovascularization were about 0.17%, 0.62(1/mm), 0.09mm for P/T group and about

0.14%, 0.61(1/mm), 0.09mm for P/T/I group, respectively. There was no significant difference for them between two groups. The size distribution of new formed vessels (Fig.6.8 C) in bone tunnel indicated the similar trend in P/T and P/T/I groups and the thickness of vessel ranged from 0.03mm to 0.18mm.

6.3.4. Descriptive histomorphology of new bone formed within bone tunnel

The histology results showed that the outline of the scaffolds in bone tunnel were clear as a circle which was match to the bone tunnel and no shrink and collapse were observed in both P/T and P/T/I groups at week 12 after scaffold implantation (Fig.6.9 A1 and B1). The scaffolds were surrounded with the normal bone and the bone marrow without any fibrous connective tissues and much new bone was observed within the scaffolds. Fig.6.9 A2 and B2 showed that the macro-pores of the scaffold were filled with bone marrow and much bone grew along the all of the trabecula of the scaffolds in both groups. The outline of trabecula of the scaffolds was kept, but when it was magnified (Fig.6.9 A3 and B3), we found that the trabecula of the scaffold was separated into many regions by some new bone, bone marrow and some fibrous connective tissue. The residue of scaffold was stained as blue under H&E staining. Though new bone was observed within scaffold in both groups, the histomorphometry (Fig.6.9 C) showed that the bone area in P/T/I group ($15.2 \pm 2.9\%$) was higher than that in P/T group ($11.2 \pm 2.9\%$)($p<0.05$).

6.3.5. Mechanical test

Before performance of compression test, the samples were observed under X-ray to assist the positioning the bone tunnel and the new bone could be visualized

in the bone tunnel in both groups (Fig.6.10 A2 and B2). The density of newly formed bone in tunnel in P/T/I group seemed higher than that in P/T group, which indicated more bone formed in P/T/I group. The result was confirmed with the micro-CT analysis. As for the mechanical test (Fig.6.11), the E-modulus (22.0 ± 4.0MPa) and the compression stiffness (92.1 ± 20.5N/mm) in P/T group were higher than those (18.6 ± 3.8MPa for E-modulus and 71.7 ± 17.2N/mm for compression stiffness) in P/T/I group at week 12 after operation ($p<0.05$). Relatively higher energy and smaller displacement for the maximum load were observed in P/T/I group, though there was no significant difference between two groups.

6.4. Discussion

The work designed for this chapter employed iconography, histology and histomorphometry, mechanics to investigate the bone repair effect within bone tunnel using PLGA/TCP/Icaritin scaffold materials after core decompression in rabbits with SAON. The results confirmed the hypothesis that the PLGA/TCP/Icaritin scaffold could promote the osteogenesis at the bone defect region when the necrotic bone was removed in rabbits with SAON.

The pore size and the porosity of scaffold are important morphological properties for bone regeneration. High porosity and large pores could facilitate the bone ingrowth and osseointegration of the implant with the host bone tissue after implantation (Roy T. D. et al. 2003; Karageorgiou V. et al. 2005). In this study, we implanted the PLGA/TCP/Icaritin and PLGA/TCP scaffolds with macro-pore size about 400-500μm and porosity 70-80% into the bon tunnel with 3mm in diameters.

The micro-CT results and the histological results showed that the much bone and the bone marrow could penetrate into the centre of the scaffold though the macro-pores which indicated both porous scaffolds facilitated the bone ingrowth during the bone repair. The results in this were consonant with the reports from others. It was reported early that the minimum recommended pore size for a scaffold was 100μm (Hulbert S. F. et al. 1970) and the followed studies showed that the pores more than 300μm were relatively better for osteogenesis for porous implants (Kuboki Y. et al. 2001; Gotz H. E. et al. 2004). The proper porosity and the pore size would result in the increased cell migration and proliferation because they would facilitate the transport of oxygen and nutrients (Takahashi Y. et al. 2004).

Angiogenesis is a prerequisite processes for tissue engineering. It has been demonstrated that the angiogenesis was affected by altering the porosity of porous implantation and a more open pore structure is more conducive to tissue invasion and growth (Oates M. et al. 2007). Relatively larger pores lead to direct osteogenesis because they allowed vascularization and high oxygenation (Karageorgiou V. et al. 2005). In this study, we found the new vessels grew into the scaffolds from micro-CT analysis at week 12 after operation combined with the new bone and bone marrow formation. Though there was no difference for the neovascularization between PLGA/TCP/Icaritin and PLGA/TCP groups, it also indicated that this porous scaffold could facilitate the vessel ingrowth, thus facilitate the nutrients exchange and the new bone formation. It was reported that the angiogenesis represented an important process during the formation and repair of tissue and was essential for nourishment

and supply of reparative and immunological cells (Barralet J. et al. 2009).

As an exogenous phytomolecule, Icaritin is steady due to its stable phytochemical structure (Shen P. et al. 2009). After being incorporated into PLGA/TCP to form a PLGA/TCP/Icaritin porous scaffold, we demonstrated its osteopromotive efficacy in SAON rabbit model. Our experimental data from micro-CT and histology analysis confirmed that the bone formation in bone tunnel in P/T/I group was higher than that in P/T group at week 12 after implantation, which may due to the released Icaritin because we have proved that Icaritin could be released from scaffold and had osteopromotive effect in vitro (Huang J. et al. 2007; Wang X. L. 2008; Wang X. L. et al. 2008; Zhao J. et al. 2009). The compression test also showed the good mechanical properties of new bone in bone tunnel in P/T/I group. In this study, the PLGA/TCP/Icaritin porous scaffold satisfied two requirements to promote the bone repair in SAON rabbit model: one is the porous structure worked as a platform to conduct the bone in growth; another is the osteogenic factor, Icaritin, to promote the osteogenesis ability.

Degradation is also an important prerequisite for bone substitute. A balance must be reached depending on the repair rate of bone remodeling and rate of degradation of the scaffold material. In this study, we found the trabecula of scaffold was separated into many regions by new bone, bone marrow and fibrous connective tissues from histological observation, which indicated that the scaffold has degraded partly. Only when the materials degraded, could the new tissue penetrate into the inner of the scaffold. No collapse and no shrink of scaffold were found at week 12,

which indicated that the scaffold had proper degradation rate for the new tissue to grow in because the rapid depletion of the biomaterial would compromise the mechanical and structural integrity before substitution by newly formed bone (Karageorgiou V. et al. 2005). At week 4 after operation, just small number of bone exited in the bone tunnel and there was no bone at the centre of the scaffold according to the micro-CT analysis, which indicated that the new formed bone was concentrated on the edge of the scaffold at the early stage. But after that, there was an outbreak of the bone volume could be found not only at the edge of the bone tunnel but also at the centre of the scaffold at week 8 and 12, which might be due to the conduction of the porous structure and the degradation of the materials.

6.5. Conclusion

Based on our findings in this part, it could be concluded that the PLGA/TCP/Icaritin composite scaffold could promote bone repair of necrotic lesion after core decompression in rabbit model with SAON. PLGA/TCP/Icaritin porous composite scaffold might be a promising material for orthopaedic applications.

6.6. Figures and legends

Fig.6.1. The implantation procedure of scaffold cylinder in distal femora in rabbits with SAON. A: the cylinder of scaffold with 3mm in diameter; B; A 3.0mm trephine (arrow) was drilled through the distal femora; C: A bone tunnel (arrow) was created at the coronal plane at distal femora; D: The cylinder of scaffold (arrow) was implanted into the bone tunnel.

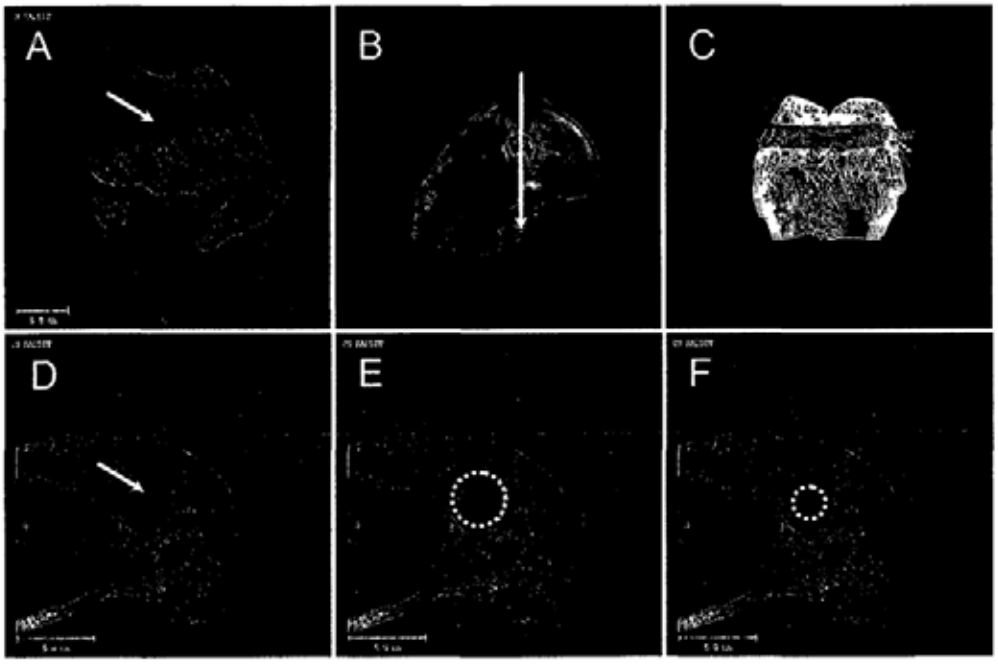

Fig.6.2. Procedures for evaluating the bone tunnel using micro-CT after core decompression. A: 2D images of coronal view for bone tunnel (arrow) after scanning of micro-CT; B: 3D images of distal femur with section line along the axis of bone tunnel; C: Sectional images of bone tunnel along the axis, 3 red points around the tunnel were positioned and used to transfer the image into 2D images of sagittal view. D: 2D images of sagittal view for bone tunnel (arrow); E: ROI with 3mm in diameters in bone tunnel (dotted circulation); F: ROI with 2mm in diameters at the centre of bone tunnel (dotted circulation).

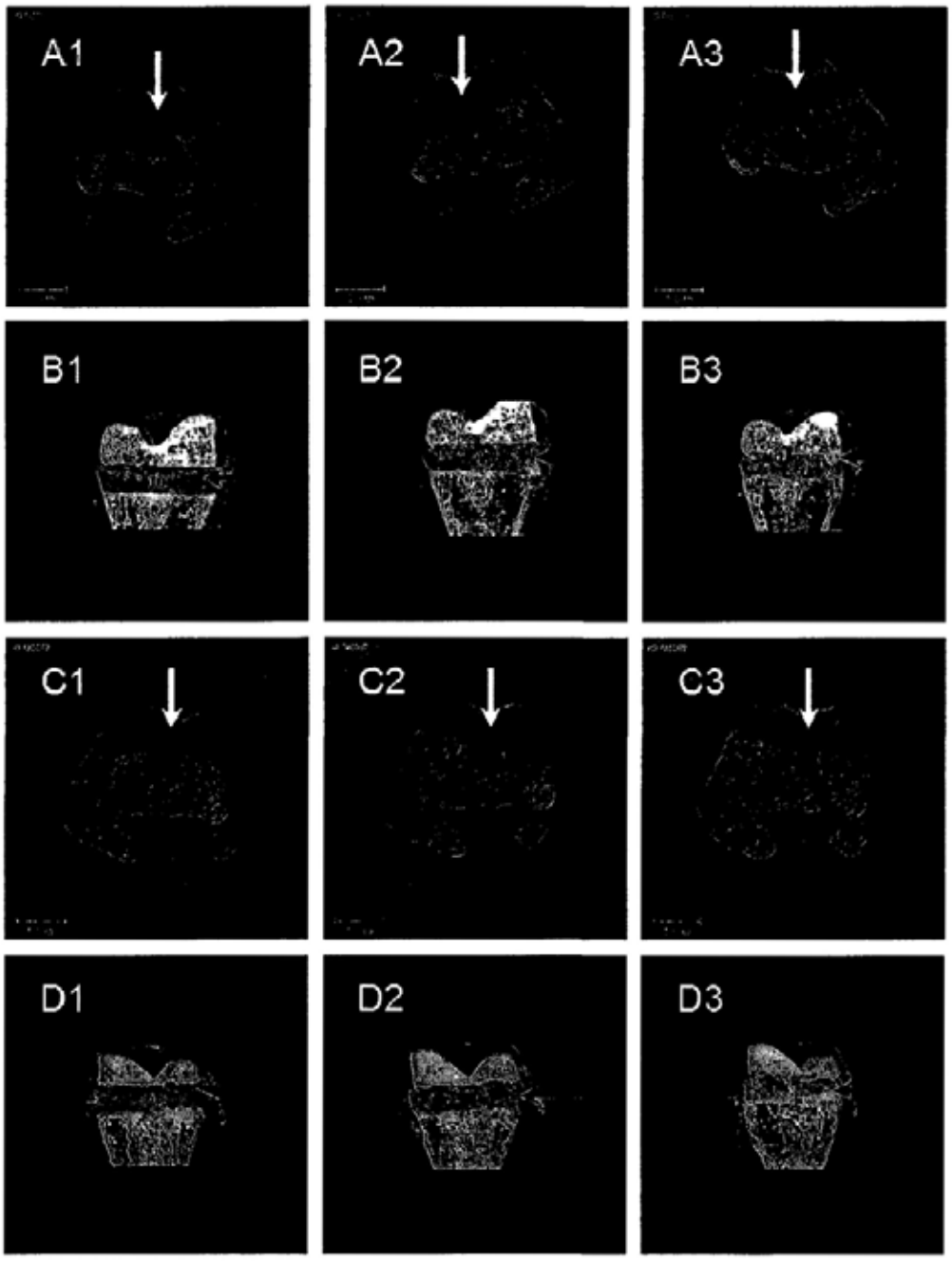

Fig.6.3. Bone tunnel images (arrows) from micro-CT. 2D images in a transverse view (A, C) and 3D images (B, D) in a coronal view of distal femora of rabbits at week 4, 8 and 12 after core decompression. A and B: P/T group; C and D: P/T/I group; (1: 4 weeks; 2: 8 weeks; 3: 12 weeks).

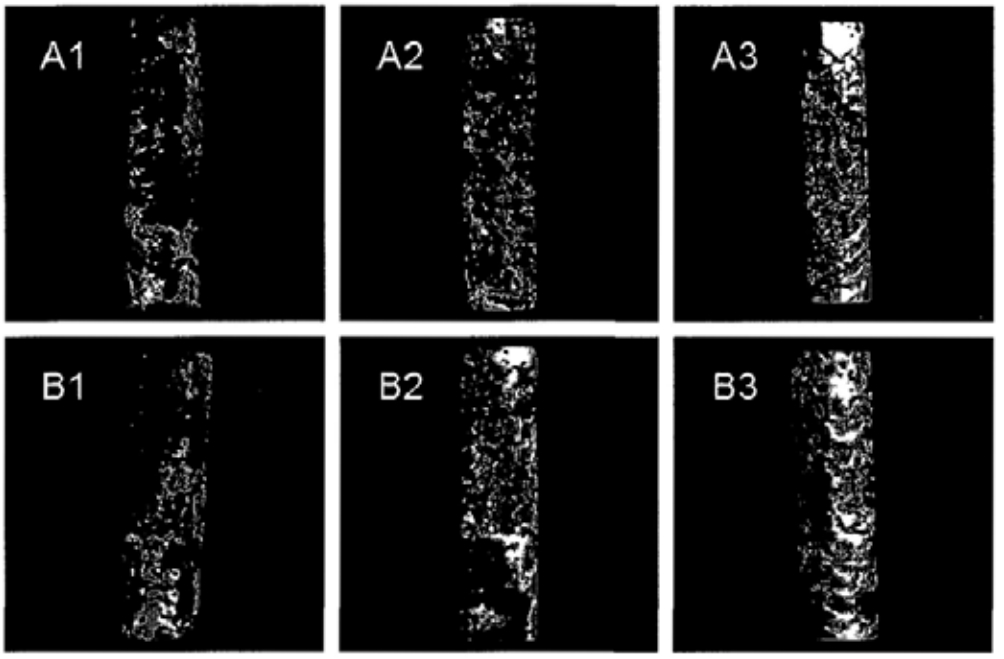

Fig.6.4. Representative micro-CT 3D images of the new bone formed within bone tunnel of 3mm in diameters at week 4, 8 and 12 after scaffold implantation. A: P/T group (A1: 4 weeks; A2: 8 weeks; A3: 12 weeks); B: P/T/I group (B1: 4 weeks; B2: 8 weeks; B3: 12 weeks).

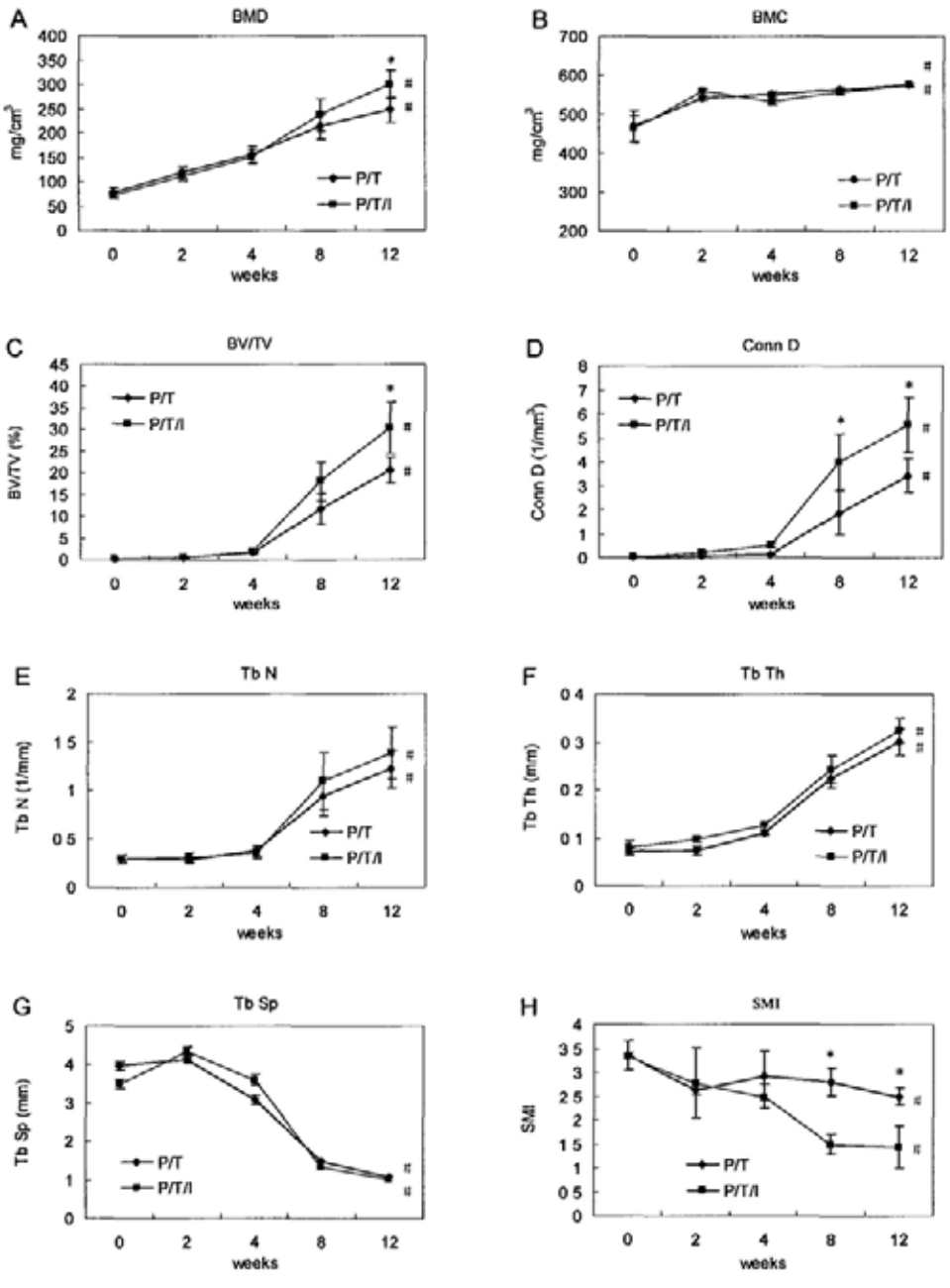

Fig.6.5. Micro-CT quantitative analysis. Bone mineral and structural data of the newly formed bone tissue within bone tunnel of 3mm in diameter in the P/T group (n=10) and P/T/I group (n=10) at week 0, 2, 4, 8 and 12 after core decompression (A-H). *: $p<0.05$ when compared between P/T group and P/T/I group; #: $p<0.05$ when compared at week 0, 2, 4, 8 and 12 in each group.

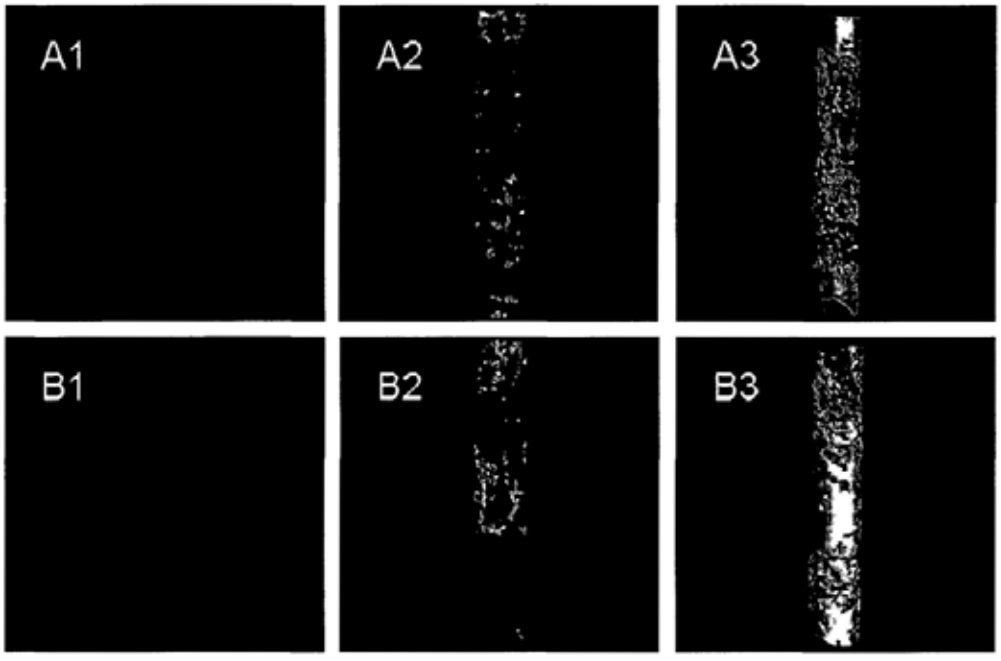

Fig.6.6. Representative micro-CT 3D images of new bone formed within 2mm in diameters reconstructed from the centre of scaffold at week 4, 8 and 12 after scaffold implantation. A: P/T group (A1: 4 weeks; A2: 8 weeks; A3: 12 weeks); B: P/T/I group (B1: 4 weeks; B2: 8 weeks; B3: 12 weeks).

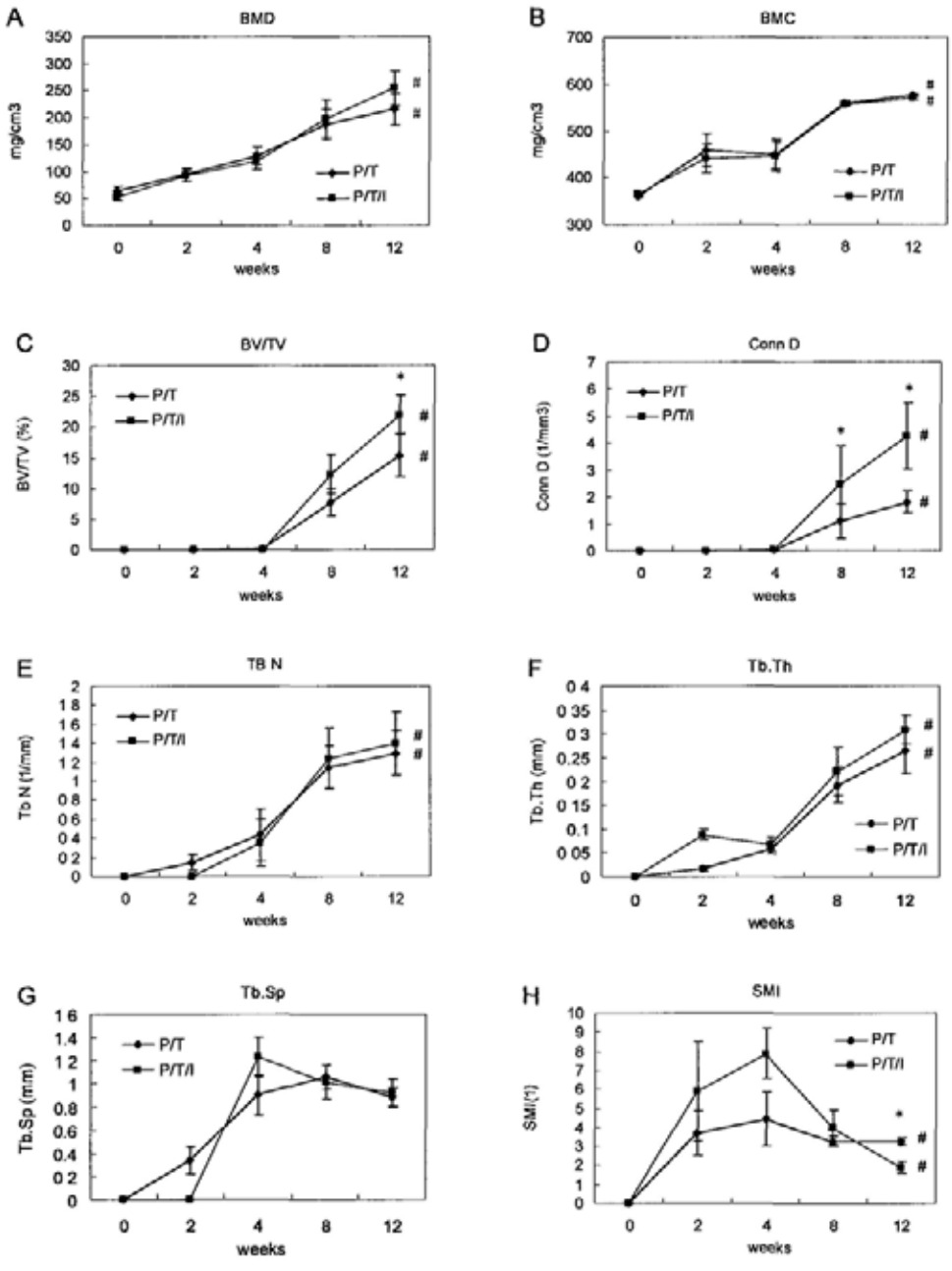

Fig.6.7. Micro-CT quantitative analysis. Bone mineral and structural data of the newly formed bone tissue at the centre of bone tunnel with 2mm in diameter in the P/T group (n=10) and P/T/I group (n=10) at week 0, 2, 4, 8 and 12 after core decompression (A-H). *: $p<0.05$ when compared between P/T group and P/T/I group; #: $p<0.05$ when compared at week 0, 2, 4, 8 and 12 in each group.

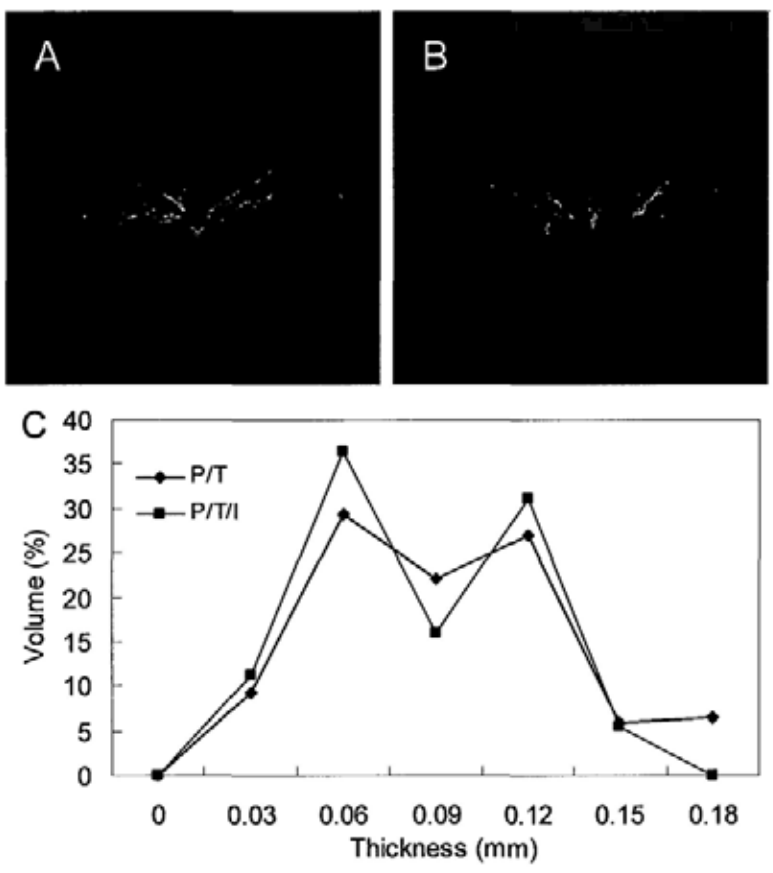

Fig.6.8. Representative micro-CT 3D images of neovascularization formed in bon tunnel at 12 after scaffold implantation (A: P/T group; B: P/T/I group). C: Distribution of mean vessel thickness for neovascularization in bone tunnel.

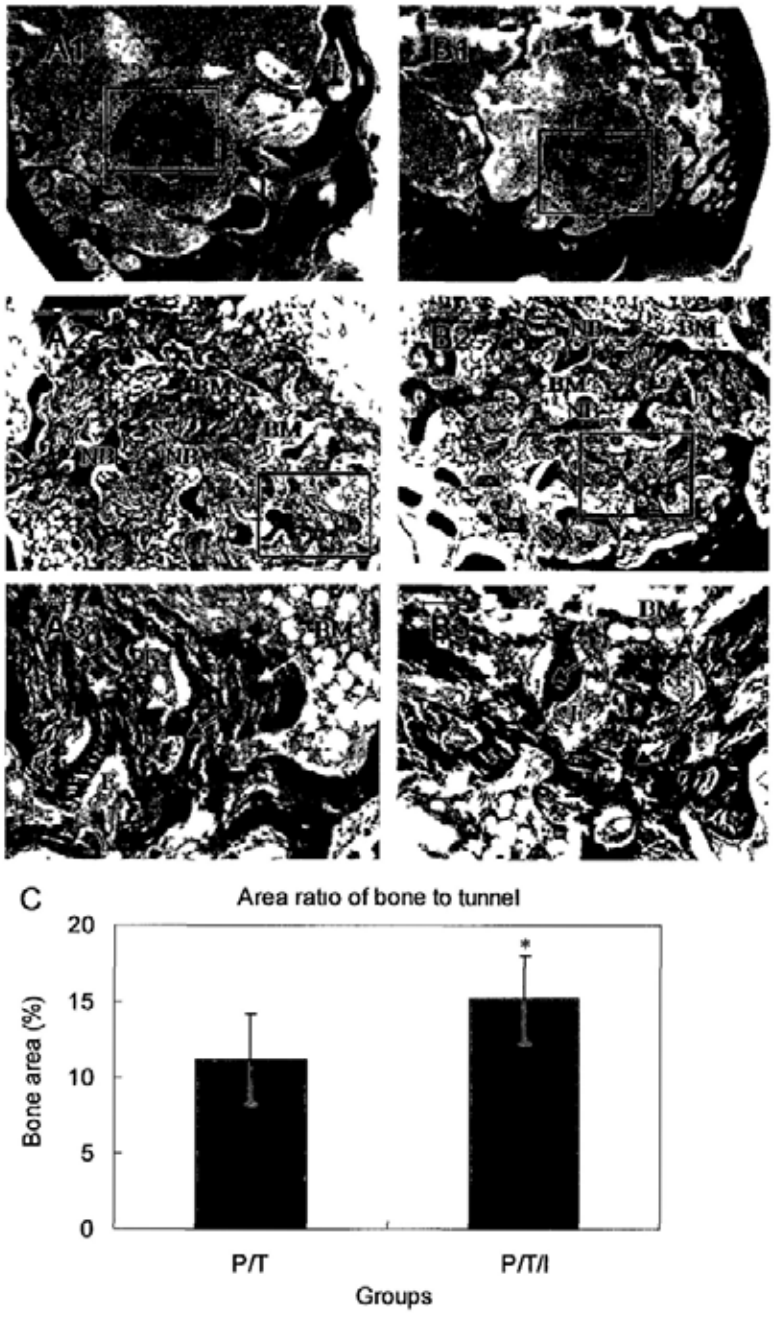

Fig.6.9. Representative histology at the intermediate piece of bone tunnel in P/T group (A) and P/T/I group (B) at week 12 after scaffold implantation (H&E staining). A1: New bone (included in black dotted circle) formed within bone tunnel in P/T group (1.6×), the rectangular frame was magnified to A2; A2: ROI magnified from the rectangular frame of A1, showing new formed bone marrow(BM) and new bone (NB) with normal structure at the macro-pores of the scaffold (S) (5×); A3: ROI

magnified from the rectangular frame of A2, showing new bone formation(black arrows), residue scaffold materials (white arrows) and some fibrous tissues (F) at the trabecula of the scaffold (20×); B1: New bone (included in black dotted circle) formed within bone tunnel in P/T/I group (1.6×), the rectangular frame was magnified to B2; B2: ROI magnified from the rectangular frame of B1, showing new formed bone marrow(BM) and new bone (NB) with normal structure at the macro-pores of the scaffold (S) (5×); B3: ROI magnified from the rectangular frame of B2, showing new bone formation(black arrows), residue scaffold materials (white arrows) and some fibrous tissues (F) at the trabecula of the scaffold (20×); C: The new bone area ratio (%, bone area/tunnel area) at the intermediate piece of bone tunnel in both groups at week 12 after scaffold implantation ($p<0.05$).

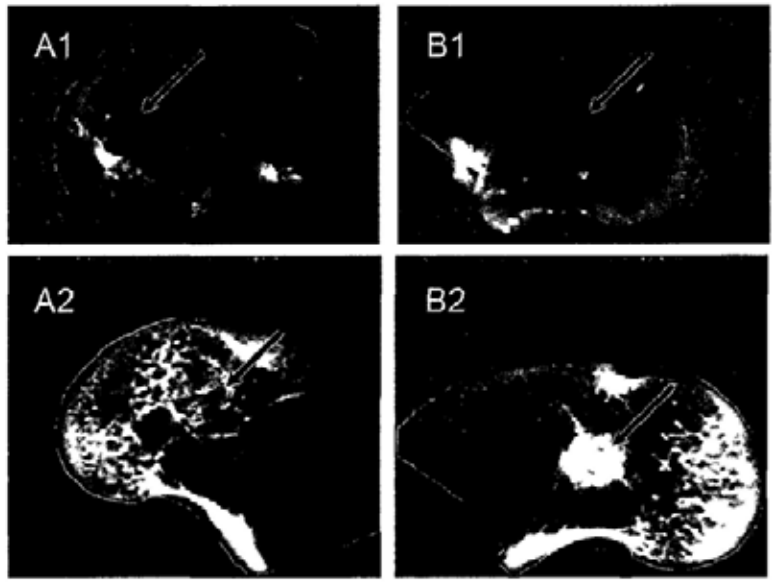

Fig.6.10. The preparation process of samples for compression test (A: P/T group; B: P/T/I group). The specimens without decalcification vertical to the axis of bone tunnel (arrow) were prepared with an identical thickness (A1, B1). Position of bone tunnel (arrow) with new formed bone could be observed under X-ray (A2, B2).

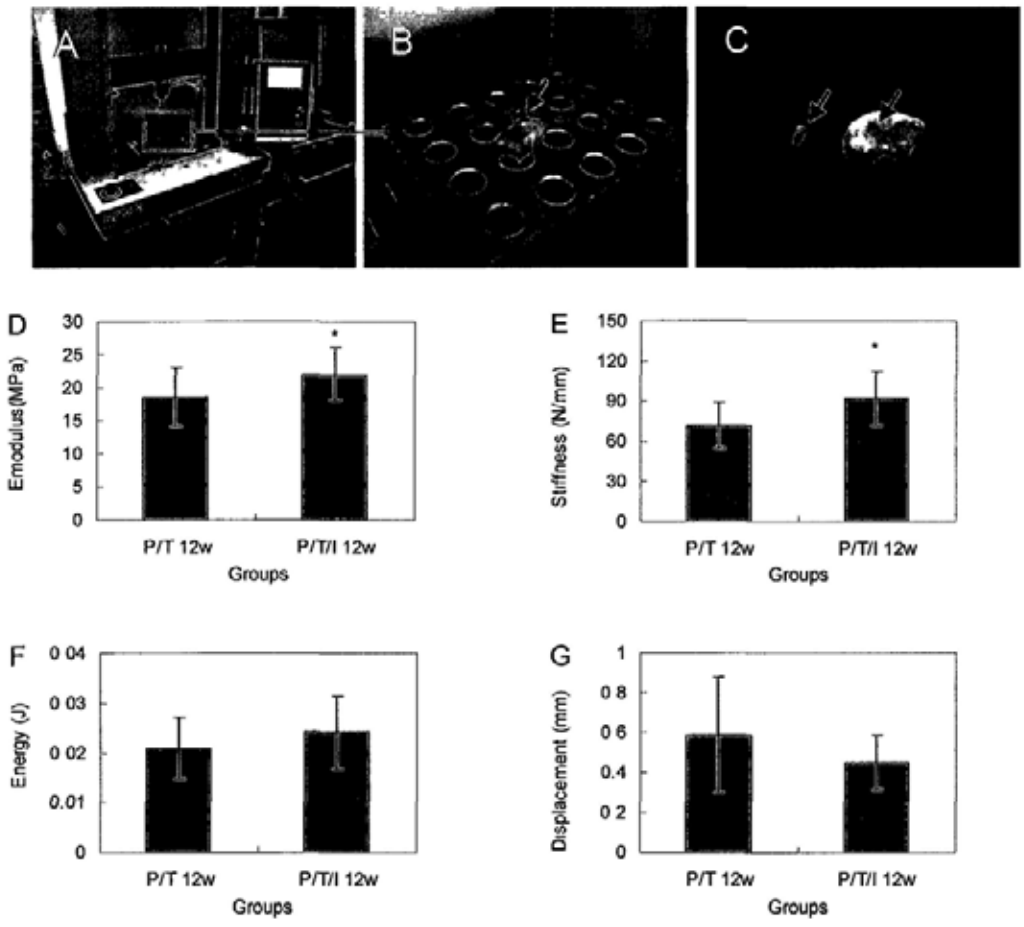

Fig.6.11. Compression test results compared between the P/T group (n=10) and P/T/I group (n=10) at 12 weeks after core decompression. A: A material test machine for compression test; B: Compression test for the bone within the bone tunnel using an indenter of 2.5mm in diameter(arrow); C: The tissue pushed out from the bone tunnel (arrow); D: E-modulus compared between P/T group and P/T/I group (* $p < 0.05$); E: Compression stiffness compared between P/T group and P/T/I group (* $p < 0.05$); F: Energy compared between P/T group and P/T/I group; G: The displacement for maximum load compared with P/T group and P/T/I group.

CHAPTER 7

Summary of the study and future research

7.1. Summary of the study

According to overall findings of thesis study, it was successfully designed an innovative composite scaffold porous material by incorporating the bioactive molecular Icaritin into the PLGA/TCP scaffold using a computer-controlled fine bio-spinning technology. Its fine biodegradation (Icaritin released with the degradation of the scaffold), biocompatibility, non-cytotoxicity and osteopromotion effects determined in vitro indicated its potential application for in vivo testing. Because of the impaired bone regeneration capability in a trabecular defect area attributed to decreased activity of BMSCs in rabbits with SAON, the PLGA/TCP/Icaritin porous composite scaffold was demonstrated its effects on enhancement of the bone repair at necrotic defect lesion by providing the structure reinforcement and osteopromotive factors. The findings implied that the porous composite PLGA/TCP/Icaritin scaffold would be an appropriate osteopromotive scaffold implant or bone graft substitute biomaterial for potential application in skeletal tissue engineering. It was first time that we successfully incorporated or homogenized an osteopromotive herbal molecule into PLGA/TCP composite scaffold biomaterials for medical testing. It might provide a new ideal or new treatment strategy for treatment of early stage of SAON, which will help to delay potential joint replacement.

7.2. Limitations of the study

Several limitations shall be pointed out for further research or improvement for future studies:

1). Though the Icaritin release could be tested in vitro, if the in vivo Icaritin release pattern from PLGA/TCP/Icaritin composite scaffold was the same or similar to that demonstrated in vitro remained unexplained and remained for further characterization.

2). In order to observe the bone repair effect, the acellular PLGA/TCP/Icaritin scaffold was designed and evaluated in this study. However, it would also be of interests to test potential synergistic effects of BMSCs to be seeded onto the pores of the porous composite scaffold in vivo because the supplement of cells is also another way to increase the cells activity at the necrotic region and then promote the effect of bone repair potentially in a synergistic way.

3). Though the osteopromotive effect of PLGA/TCP/Icaritin in vitro and in vivo was determined statistically, the exactly underlying molecular mechanisms involved in repair enhancement was not systemically evaluated, such as osteogenic or/and angiogenic signal pathway(s) which play the major role during bone repair.

4). Though the rabbit model of SAON mimics the pathology of SAON in human, it could not be used to mimic the mechanical loading in human as lest in aspect of loading conditions, e.g. loading difference in hip joint found between quadrupedal animal models vs. bipedal humans.

7.3. Future research

1). To understand the effect of Icaritin at the local skeletal site, the release property of Icaritin from scaffold in vivo might be examined in spite of local biological complicity involving new bone regeneration and its remodeling. The adjustment of

Icaritin to PLGA/TCP scaffold should be performed, for example, change the concentration of Icaritin or the composition ratios of the three elements, in order to make the composite is reabsorbed or dissolved fairly naturally as bone growth occurs, yielding newly remodeled bone, the bone portion will ideally start to degrade during the bone in growth process.

2). According to the principle of tissue engineering, the scaffold combined with the autologous bone marrow or stem cells will be used to promote the bone repair effect in SAON or other type of bone defect. The bone marrow will be obtained from area beside the femora and stem cells will be obtained from bone marrow or other tissues such as adipose.

3). To examine the molecular mechanism of osteopromotion effect of Icaritin and early biological response when the composite was implanted in vivo.

4). To mimic the mechanical loading in human completely, the bipedal animal such as emu will be used to built up the SAON model and evaluated the treatment effect of this scaffold.

5). Novel exogenous molecule with more potential on osteogenesis will also be developed.

6). Potential dosing effects of Icaritin incorporated into the composite scaffold on osteogenesis will be evaluated both in vitro and in vivo.

7). The innovative composite scaffold developed for the thesis study was tested in short time (two months) after production. How long this composite scaffold material can be stored will be examined based on their release property and bioactivity.

APPENDIX

Animal license: 09-472 in DH/HA&P/8.2.1 Pt.10

Form 2

License to Conduct Experiments

Name : [illegible] (09-472) in DH/HA&P/8.2.1 Pt.10]

Address : Department of Orthopaedics and Traumatology, The Chinese University of Hong Kong

By virtue of section 7 of the Animals (Control of Experiments) Ordinance, Chapter 340, the above named is hereby licensed to conduct the type of experiments at the places and upon the conditions, hereinafter mentioned

Type of experiment(s)

Rabbits will be used in the experiment. An osteonecrosis model will be established by giving the animals an intravenous injection of lipopolysaccharide followed by three intramuscular injections of methylprednisolone. Two weeks later, core decompression will be performed and bone tunnels will be created at the femur under anaesthesia. Poly(L-lactide-co-glycolide), tricalcium phosphate and fibrin (PLGA/TCP/fibrin) bone grafts will then be implanted into the tunnel. Conditions of the animals will be monitored. Analgesic will be given when needed. Animals that show signs of distress will be sacrificed with an overdose of anesthetic. At the end of the experiment, the animals will be sacrificed with an overdose of anesthetic.

Place(s) where experiment(s) may be conducted

1. 10/F, Room 1009, Animal Surgery Room, Li Ka Shing Medical Sciences Building, Prince of Wales Hospital, Shatin
2. 11/F, Room 1201, Musculoskeletal Research Laboratory, Li Ka Shing Medical Sciences Building, Prince of Wales Hospital, Shatin
3. Animal House Laboratory, Animal Services Centre, G/F, Prince of Wales Hospital, Shatin

Conditions

1 Such experiment(s) may only be conducted for the following purposes

To investigate the effect of PLGA/TCP/fibrin composite scaffold on repair of bone defect in steroid associated osteonecrosis using animal models

2 This licence is valid from 14 December 2009 to 13 December 2011

Dated 14 December 2009

DEPARTMENT OF HEALTH

Licensing Authority

REFERENCES

Aaron R. (1998). Osteonecrosis: etiology, pathophysiology and diagnosis. The adult hip. J. Callaghan, A. Rosenberg and H. Rubash. Philadelphia: 457.

Ajmal M., Matas A. J., Kuskowski M. and Cheng E. Y. (2009). "Does statin usage reduce the risk of corticosteroid-related osteonecrosis in renal transplant population?" Orthop Clin North Am 40(2): 235-9.

Akgun I. and Unlu M. C. (2007). "[Osteonecrosis of the knee]." Acta Orthop Traumatol Turc 41 Suppl 2: 123-37.

Alemdaroglu K. B., Tiftikci U., Iltar S., Aydogan N. H., Kara T., Atlihan D. and Atesalp A. S. (2009). "Factors affecting the fracture healing in treatment of tibial shaft fractures with circular external fixator." Injury 40(11): 1151-6.

Ara M., Watanabe M. and Imai Y. (2002). "Effect of blending calcium compounds on hydrolytic degradation of poly(DL-lactic acid-co-glycolic acid)." Biomaterials 23(12): 2479-83.

Arlet J. and Ficat P. (1964). "Forage-biopsie de la tête fémorale dans l'ostéonécrose primitive. Observations histopathologiques portant sur huit forages." Rev Rheum Mal Osteoartic 31: 257.

Asada T., Kushida T., Umeda M., Oe K., Matsuya H., Wada T., Sasai K., Ikehara S. and Iida H. (2008). "Prevention of corticosteroid-induced osteonecrosis in rabbits by intra-bone marrow injection of autologous bone marrow cells." Rheumatology (Oxford) 47(5): 591-6.

Aslan M., Simsek G. and Yildirim U. (2005). "Effects of short-term treatment with systemic prednisone on bone healing: an experimental study in rats." Dent Traumatol 21(4): 222-5.

Assouline-Dayan Y., Chang C., Greenspan A., Shoenfeld Y. and Gershwin M. E. (2002). "Pathogenesis and natural history of osteonecrosis." Semin Arthritis Rheum 32(2): 94-124.

Babhulkar S. (2009). "Osteonecrosis of femoral head: Treatment by core

decompression and vascular pedicle grafting." Indian J Orthop 43(1): 27-35.

Barralet J., Gbureck U., Habibovic P., Vorndran E., Gerard C. and Doillon C. J. (2009). "Angiogenesis in calcium phosphate scaffolds by inorganic copper ion release." Tissue Eng Part A 15(7): 1601-9.

Behling C. A. and Spector M. (1986). "Quantitative characterization of cells at the interface of long-term implants of selected polymers." J Biomed Mater Res 20(5): 653-66.

Berend K. R., Gunneson E. E. and Urbaniak J. R. (2003). "Free vascularized fibular grafting for the treatment of postcollapse osteonecrosis of the femoral head." J Bone Joint Surg Am 85-A(6): 987-93.

Biondi M., Ungaro F., Quaglia F. and Netti P. A. (2008). "Controlled drug delivery in tissue engineering." Adv Drug Deliv Rev 60(2): 229-42.

Bitto A., Polito F., Burnett B., Levy R., Di Stefano V., Armbruster M. A., Marini H., Minutoli L., Altavilla D. and Squadrito F. (2009). "Protective effect of genistein aglycone on the development of osteonecrosis of the femoral head and secondary osteoporosis induced by methylprednisolone in rats." J Endocrinol 201(3): 321-8.

Bodde E. W., de Visser E., Duysens J. E. and Hartman E. H. (2003). "Donor-site morbidity after free vascularized autogenous fibular transfer: subjective and quantitative analyses." Plast Reconstr Surg 111(7): 2237-42.

Bostman O., Paivarinta U., Partio E., Vasenius J., Manninen M. and Rokkanen P. (1992). "Degradation and tissue replacement of an absorbable polyglycolide screw in the fixation of rabbit femoral osteotomies." J Bone Joint Surg Am 74(7): 1021-31.

Bourne B. C. and van der Meulen M. C. (2004). "Finite element models predict cancellous apparent modulus when tissue modulus is scaled from specimen CT-attenuation." J Biomech 37(5): 613-21.

Bromage T. G., Goldman H. M., McFarlin S. C., Warshaw J., Boyde A. and Riggs C. M. (2003). "Circularly polarized light standards for investigations of collagen fiber orientation in bone." Anat Rec B New Anat 274(1): 157-68.

Butler M. J. and Sefton M. V. (2007). "Poly(butyl methacrylate-co-methacrylic acid) tissue engineering scaffold with pro-angiogenic potential in vivo." J Biomed Mater Res A 82(2): 265-73.

Cancedda R., Giannoni P. and Mastrogiacomo M. (2007). "A tissue engineering approach to bone repair in large animal models and in clinical practice." Biomaterials 28(29): 4240-50.

Castro F. P., Jr. and Barrack R. L. (2000). "Core decompression and conservative treatment for avascular necrosis of the femoral head: a meta-analysis." Am J Orthop (Belle Mead NJ) 29(3): 187-94.

Chan M. H., Chan P. K., Griffith J. F., Chan I. H., Lit L. C., Wong C. K., Antonio G. E., Liu E. Y., Hui D. S., Suen M. W., Ahuja A. T., Sung J. J. and Lam C. W. (2006). "Steroid-induced osteonecrosis in severe acute respiratory syndrome: a retrospective analysis of biochemical markers of bone metabolism and corticosteroid therapy." Pathology 38(3): 229-35.

Chan T. W., Dalinka M. K., Steinberg M. E. and Kressel H. Y. (1991). "MRI appearance of femoral head osteonecrosis following core decompression and bone grafting." Skeletal Radiol 20(2): 103-7.

Chen K. M., Ge B. F., Ma H. P. and Zheng R. L. (2004). "The serum of rats administered flavonoid extract from Epimedium sagittatum but not the extract itself enhances the development of rat calvarial osteoblast-like cells in vitro." Pharmazie,Die 59(1).

Chen K. M., Ma H. P., Ge B. F., Liu X. Y., Ma L. P., Bai M. H. and Wang Y. (2007). "Icariin enhances the osteogenic differentiation of bone marrow stromal cells but has no effects on the differentiation of newborn calvarial osteoblasts of rats." Pharmazie 62(10): 785-9.

Chen V. J. and Ma P. X. (2006). "The effect of surface area on the degradation rate of nano-fibrous poly(L-lactic acid) foams." Biomaterials 27(20): 3708-15.

Cheng X. G., Qu H., Liu W., Liu X., Cheng K. B., Zhao T., Li X. S., Liang W. and Guo J. (2006). "The prevalence of osteonecrosis in 448 SARS patients: a screening study with MRI." Clinical Imaging 30(2): 150-50.

Chiodo C. P. and Herbst S. A. (2004). "Osteonecrosis of the talus." Foot Ankle Clin 9(4): 745-55, vi.

Coimbra M. E., Salles M. B., Yoshimoto M., Allegrini S., Fancio E., Higa O., Suzuki M. and Coelho P. G. (2009). "Physico/Chemical characterization, in vitro, and in vivo evaluation of ReOss and SynthoGraft particulate grafting materials." Titanium 1(1): 16-28.

Cui Q., Wang G. J. and Balian G. (2000). "Pluripotential marrow cells produce adipocytes when transplanted into steroid-treated mice." Connect Tissue Res 41(1): 45-56.

D'Aubigne R. M. and Frain P. G. (1972). "[Theory of osteotomies]." Rev Chir Orthop Reparatrice Appar Mot 58(3): 159-67.

Davis E. T., McKee M. D., Waddell J. P., Hupel T. and Schemitsch E. H. (2006). "Total hip arthroplasty following failure of free vascularized fibular graft." J Bone Joint Surg Am 88 Suppl 3: 110-5.

De Ugarte D. A., Morizono K., Elbarbary A., Alfonso Z., Zuk P. A., Zhu M., Dragoo J. L., Ashjian P., Thomas B., Benhaim P., Chen I., Fraser J. and Hedrick M. H. (2003). "Comparison of multi-lineage cells from human adipose tissue and bone marrow." Cells Tissues Organs 174(3): 101-9.

Demirors H., Kaya A., Akpinar S., Tuncay C. and Tandogan R. N. (2002). "Effect of long-term steroid use on prognosis for patients with surgically treated avascular necrosis of the hip." Transplant Proc 34(6): 2114-8.

Deng H. W. and Liu Y. Z., Eds. (2005). Current Topics of Bone Biology. Mechanical testing for bone specimens. Singapore, World Scientific.

Devlin V. J., Einhorn T. A., Gordon S. L., Alvarez E. V. and Butt K. M. (1988). "Total hip arthroplasty after renal transplantation. Long-term follow-up study and assessment of metabolic bone status." J Arthroplasty 3(3): 205-13.

Donahue T. L., Hull M. L., Rashid M. M. and Jacobs C. R. (2002). "A finite element model of the human knee joint for the study of tibio-femoral contact." J Biomech Eng 124(3): 273-80.

Drescher W., Schneider T., Becker C., Hobolth J., Ruther W., Hansen E. S. and

Bunger C. (2001). "Selective reduction of bone blood flow by short-term treatment with high-dose methylprednisolone. An experimental study in pigs." J Bone Joint Surg Br 83(2): 274-7.

Drescher W., Varoga D., Liebs T. R., Lohse J., Herdegen T., Hassenpflug J. and Pufe T. (2006). "Femoral artery constriction by norepinephrine is enhanced by methylprednisolone in a rat model." J Bone Joint Surg Am 88 Suppl 3: 162-6.

Drescher W., Weigert K. P., Bunger M. H., Ingerslev J., Bunger C. and Hansen E. S. (2004). "Femoral head blood flow reduction and hypercoagulability under 24 h megadose steroid treatment in pigs." J Orthop Res 22(3): 501-8.

Drosse I., Volkmer E., Capanna R., De Biase P., Mutschler W. and Schieker M. (2008). "Tissue engineering for bone defect healing: an update on a multi-component approach." Injury 39 Suppl 2: S9-20.

Dudkiewicz I., Covo A., Salai M., Israeli A., Amit Y. and Chechik A. (2004). "Total hip arthroplasty after avascular necrosis of the femoral head: does etiology affect the results?" Arch Orthop Trauma Surg 124(2): 82-5.

Dunn A. S., Campbell P. G. and Marra K. G. (2001). "The influence of polymer blend composition on the degradation of polymer/hydroxyapatite biomaterials." J Mater Sci Mater Med 12(8): 673-7.

Duvall C. L., Taylor W. R., Weiss D., Wojtowicz A. M. and Guldberg R. E. (2007). "Impaired angiogenesis, early callus formation, and late stage remodeling in fracture healing of osteopontin-deficient mice." J Bone Miner Res 22(2): 286-97.

Eberhardt A. W., Yeager-Jones A. and Blair H. C. (2001). "Regional trabecular bone matrix degeneration and osteocyte death in femora of glucocorticoid- treated rabbits." Endocrinology 142(3): 1333-40.

Ehrenfried L. M., Patel M. H. and Cameron R. E. (2008). "The effect of tri-calcium phosphate (TCP) addition on the degradation of polylactide-co-glycolide (PLGA)." J Mater Sci Mater Med 19(1): 459-66.

El-Ghannam A., Amin H., Nasr T. and Shama A. (2004). "Enhancement of bone regeneration and graft material resorption using surface-modified bioactive

glass in cortical and human maxillary cystic bone defects." Int J Oral Maxillofac Implants 19(2): 184-91.

Eppley B. L. and Reilly M. (1997). "Degradation characteristics of PLLA-PGA bone fixation devices." J Craniofac Surg 8(2): 116-20.

Fan H., Hu Y., Li X., Wu H., Lv R., Bai J., Wang J. and Qin L. (2006a). "Ectopic cartilage formation induced by mesenchymal stem cells on porous gelatin-chondroitin-hyaluronate scaffold containing microspheres loaded with TGF-beta1." Int J Artif Organs 29(6): 602-11.

Fan H., Hu Y., Qin L., Li X., Wu H. and Lv R. (2006b). "Porous gelatin-chondroitin-hyaluronate tri-copolymer scaffold containing microspheres loaded with TGF-beta1 induces differentiation of mesenchymal stem cells in vivo for enhancing cartilage repair." J Biomed Mater Res A 77(4): 785-94.

Fan H., Hu Y., Zhang C., Li X., Lv R., Qin L. and Zhu R. (2006c). "Cartilage regeneration using mesenchymal stem cells and a PLGA-gelatin/chondroitin/hyaluronate hybrid scaffold." Biomaterials 27(26): 4573-80.

Fan H., Zhang C., Li J., Bi L., Qin L., Wu H. and Hu Y. (2008). "Gelatin microspheres containing TGF-beta3 enhance the chondrogenesis of mesenchymal stem cells in modified pellet culture." Biomacromolecules 9(3): 927-34.

Fang B., Wan Y. Z., Tang T. T., Gao C. and Dai K. R. (2009). "Proliferation and osteoblastic differentiation of human bone marrow stromal cells on hydroxyapatite/bacterial cellulose nanocomposite scaffolds." Tissue Eng Part A 15(5): 1091-8.

Ficat R. P. (1985). "Idiopathic bone necrosis of the femoral head. Early diagnosis and treatment." J Bone Joint Surg Br 67(1): 3-9.

Gangji V. and Hauzeur J. P. (2005a). "Treatment of osteonecrosis of the femoral head with implantation of autologous bone-marrow cells. Surgical technique." J Bone Joint Surg Am 87 Suppl 1(Pt 1): 106-12.

Gangji V., Hauzeur J. P., Matos C., De Maertelaer V., Toungouz M. and Lambermont M. (2004). "Treatment of osteonecrosis of the femoral head with implantation of autologous bone-marrow cells. A pilot study." J Bone Joint Surg Am 86-A(6): 1153-60.

Gangji V., Toungouz M. and Hauzeur J. P. (2005b). "Stem cell therapy for osteonecrosis of the femoral head." Expert Opin Biol Ther 5(4): 437-42.

Gao Y. S. and Zhang C. Q. (2010). "Cytotherapy of osteonecrosis of the femoral head: a mini review." Int Orthop.

Gardeniers J. W. M. (1993). ARCO Committee on Terminology and Staging.The ARCO perspective for reaching one uniform staging system of osteonecrosis. Bone circulation and vascularization in normal and pathological conditions. A. Schoutens, J. Arlet, J. W. M. Gardeniers and S. P. F. Hughes. New York, Plenum Press: 375-80.

Gaston M. S. and Simpson A. H. (2007). "Inhibition of fracture healing." J Bone Joint Surg Br 89(12): 1553-60.

Giesen E. B., Ding M., Dalstra M. and van Eijden T. M. (2001). "Mechanical properties of cancellous bone in the human mandibular condyle are anisotropic." J Biomech 34(6): 799-803.

Glueck C. J., Freiberg R. A., Sieve L. and Wang P. (2005). "Enoxaparin prevents progression of stages I and II osteonecrosis of the hip." Clin Orthop Relat Res(435): 164-70.

Gonzalez Della Valle A., Bates J., Di Carlo E. and Salvati E. A. (2005). "Failure of free vascularized fibular graft for osteonecrosis of the femoral head: a histopathologic study of 6 cases." J Arthroplasty 20(3): 331-6.

Gotz H. E., Muller M., Emmel A., Holzwarth U., Erben R. G. and Stangl R. (2004). "Effect of surface finish on the osseointegration of laser-treated titanium alloy implants." Biomaterials 25(18): 4057-64.

Griffith J. F., Antonio G. E., Kumta S. M., Hui D. S., Wong J. K., Joynt G. M., Wu A. K., Cheung A. Y., Chiu K. H., Chan K. M., Leung P. C. and Ahuja A. T. (2005). "Osteonecrosis of hip and knee in patients with severe acute respiratory

syndrome treated with steroids." Radiology 235(1): 168-75.

Griffith L. G. (2002). "Emerging design principles in biomaterials and scaffolds for tissue engineering." Ann N Y Acad Sci 961: 83-95.

Griffith L. G. and Naughton G. (2002). "Tissue engineering--current challenges and expanding opportunities." Science 295(5557): 1009-14.

Gruson K. I. and Kwon Y. W. (2009). "Atraumatic osteonecrosis of the humeral head." Bull NYU Hosp Jt Dis 67(1): 6-14.

Guan L. and Davies J. E. (2004). "Preparation and characterization of a highly macroporous biodegradable composite tissue engineering scaffold." J Biomed Mater Res A 71(3): 480-7.

Gugala Z. and Gogolewski S. (2005). "The in vitro growth and activity of sheep osteoblasts on three-dimensional scaffolds from poly(L/DL-lactide) 80/20%." J Biomed Mater Res A 75(3): 702-9.

Hao W., Hu Y. Y., Wei Y. Y., Pang L., Lv R., Bai J. P., Xiong Z. and Jiang M. (2008). "Collagen I gel can facilitate homogenous bone formation of adipose-derived stem cells in PLGA-beta-TCP scaffold." Cells Tissues Organs 187(2): 89-102.

He K., Wang X. L., Kumta S. M., Qin L., Yan Y. N., Zhang R. J. and Wang X. H. (2009). "Fabrication of a two-level tumor bone repair biomaterial based on a rapid prototyping technique." Biofabrication 1 No 2 (June 2009) 025003 (7pp)

He Q., Wan C. and Li G. (2007). "Concise review: multipotent mesenchymal stromal cells in blood." Stem Cells 25(1): 69-77.

Hedberg E. L., Kroese-Deutman H. C., Shih C. K., Crowther R. S., Carney D. H., Mikos A. G. and Jansen J. A. (2005). "In vivo degradation of porous poly(propylene fumarate)/poly(DL-lactic-co-glycolic acid) composite scaffolds." Biomaterials 26(22): 4616-23.

Hench L. L. and Polak J. M. (2002). "Third-generation biomedical materials." Science 295(5557): 1014-7.

Henry J. A., Burugapalli K., Neuenschwander P. and Pandit A. (2009). "Structural variants of biodegradable polyesterurethane in vivo evoke a cellular and angiogenic response that is dictated by architecture." Acta Biomater 5(1):

29-42.

Heo S. J., Kim S. E., Wei J., Kim D. H., Hyun Y. T., Yun H. S., Kim H. K., Yoon T. R., Kim S. H., Park S. A., Shin J. W. and Shin J. W. (2009). "In vitro and animal study of novel nano-hydroxyapatite/poly(epsilon-caprolactone) composite scaffolds fabricated by layer manufacturing process." Tissue Eng Part A 15(5): 977-89.

Hernigou P. and Beaujean F. (1997). "Abnormalities in the bone marrow of the iliac crest in patients who have osteonecrosis secondary to corticosteroid therapy or alcohol abuse." J Bone Joint Surg Am 79(7): 1047-53.

Hernigou P. and Beaujean F. (2002). "Treatment of osteonecrosis with autologous bone marrow grafting." Clin Orthop Relat Res(405): 14-23.

Hernigou P., Beaujean F. and Lambotte J. C. (1999). "Decrease in the mesenchymal stem-cell pool in the proximal femur in corticosteroid-induced osteonecrosis." J Bone Joint Surg Br 81(2): 349-55.

Hernigou P., Manicom O., Poignard A., Nogier A., Filippini P. and De Abreu L. (2004). "Core decompression with marrow stem cells." Operative Techniques in Orthopaedics 14(2): 68-74.

Hernigou P., Poignard A., Manicom O., Mathieu G. and Rouard H. (2005). "The use of percutaneous autologous bone marrow transplantation in nonunion and avascular necrosis of bone." J Bone Joint Surg Br 87(7): 896-902.

Hernigou P., Poignard A., Zilber S. and Rouard H. (2009). "Cell therapy of hip osteonecrosis with autologous bone marrow grafting." Indian J Orthop 43(1): 40-5.

Ho S. T. and Hutmacher D. W. (2006). "A comparison of micro CT with other techniques used in the characterization of scaffolds." Biomaterials 27(8): 1362-76.

Hogevold H. E., Grogaard B. and Reikeras O. (1992). "Effects of short-term treatment with corticosteroids and indomethacin on bone healing. A mechanical study of osteotomies in rats." Acta Orthop Scand 63(6): 607-11.

Hollinger J. O. and Battistone G. C. (1986). "Biodegradable bone repair materials.

Synthetic polymers and ceramics." Clin Orthop Relat Res(207): 290-305.

Hollister S. J. (2005). "Porous scaffold design for tissue engineering." Nat Mater 4(7): 518-24.

Holtorf H. L., Jansen J. A. and Mikos A. G. (2005). "Flow perfusion culture induces the osteoblastic differentiation of marrow stroma cell-scaffold constructs in the absence of dexamethasone." J Biomed Mater Res A 72(3): 326-34.

Huang J., Yuan L., Wang X., Zhang T. L. and Wang K. (2007). "Icaritin and its glycosides enhance osteoblastic, but suppress osteoclastic, differentiation and activity in vitro." Life Sci 81(10): 832-40.

Hulbert S. F., Young F. A., Mathews R. S., Klawitter J. J., Talbert C. D. and Stelling F. H. (1970). "Potential of ceramic materials as permanently implantable skeletal prostheses." J Biomed Mater Res 4(3): 433-56.

Hungerford D. S. (1990). "[Role of core decompression as treatment method for ischemic femur head necrosis]." Orthopade 19(4): 219-23.

Hungerford D. S. (2007). "Treatment of osteonecrosis of the femoral head: everything's new." J Arthroplasty 22(4 Suppl 1): 91-4.

Hutmacher D. W. (2000). "Scaffolds in tissue engineering bone and cartilage." Biomaterials 21(24): 2529-43.

Ignatius A. A. and Claes L. E. (1996). "In vitro biocompatibility of bioresorbable polymers: poly(L, DL-lactide) and poly(L-lactide-co-glycolide)." Biomaterials 17(8): 831-9.

Ignjatovic N., Ninkov P., Kojic V., Bokurov M., Srdic V., Krnojelac D., Selakovic S. and Uskokovic D. (2006). "Cytotoxicity and fibroblast properties during in vitro test of biphasic calcium phosphate/poly-dl-lactide-co-glycolide biocomposites and different phosphate materials." Microsc Res Tech 69(12): 976-82.

Irisa T., Yamamoto T., Miyanishi K., Yamashita A., Iwamoto Y., Sugioka Y. and Sueishi K. (2001). "Osteonecrosis induced by a single administration of low-dose lipopolysaccharide in rabbits." Bone 28(6): 641-9.

Ishida M., Fujioka M., Takahashi K. A., Arai Y. and Kubo T. (2008).

"Electromagnetic fields: a novel prophylaxis for steroid-induced osteonecrosis." Clin Orthop Relat Res 466(5): 1068-73.

ISO (1992). 10993-5:1992(E). Biological evaluation of medical devices - Part 5: Tests for cytotoxicity: in vitro methods.

Ivirico J. L., Salmeron-Sanchez M., Ribelles J. L., Pradas M. M., Soria J. M., Gomes M. E., Reis R. L. and Mano J. F. (2009). "Proliferation and differentiation of goat bone marrow stromal cells in 3D scaffolds with tunable hydrophilicity." J Biomed Mater Res B Appl Biomater 91(1): 277-86.

Jiang H. J., Huang X. J., Tan Y. C., Liu D. Z. and Wang L. (2009). "Core decompression and implantation of calcium phosphate cement/Danshen drug delivery system for treating ischemic necrosis of femoral head at Stages I, II and III of antigen reactive cell opsonization." Chin J Traumatol 12(5): 285-90.

Jilek S., Walter E., Merkle H. P. and Corthesy B. (2004). "Modulation of allergic responses in mice by using biodegradable poly(lactide-co-glycolide) microspheres." J Allergy Clin Immunol 114(4): 943-50.

Jones J. R., Tsigkou O., Coates E. E., Stevens M. M., Polak J. M. and Hench L. L. (2007). "Extracellular matrix formation and mineralization on a phosphate-free porous bioactive glass scaffold using primary human osteoblast (HOB) cells." Biomaterials 28(9): 1653-63.

Kacey G. M. (2005). Biodegradable polymers and microspheres in tissue engineering. Bone Tissue Engineering

J. O. Hollinger, T. A. Einhorn, B. Doll and C. Sfeir: 149-65.

Kang P., Gao H., Pei F., Shen B., Yang J. and Zhou Z. (2010). "Effects of an anticoagulant and a lipid-lowering agent on the prevention of steroid-induced osteonecrosis in rabbits." Int J Exp Pathol.

Kang Y., Wu J., Yin G., Huang Z., Yao Y., Liao X., Chen A., Pu X. and Liao L. (2008). "Preparation, characterization and in vitro cytotoxicity of indomethacin-loaded PLLA/PLGA microparticles using supercritical CO2 technique." European Journal of Pharmaceutics and Biopharmaceutics 70(1): 85-97.

Karageorgiou V. and Kaplan D. (2005). "Porosity of 3D biomaterial scaffolds and osteogenesis." Biomaterials 26(27): 5474-91.

Kawate K., Yajima H., Ohgushi H., Kotobuki N., Sugimoto K., Ohmura T., Kobata Y., Shigematsu K., Kawamura K., Tamai K. and Takakura Y. (2006). "Tissue-engineered approach for the treatment of steroid-induced osteonecrosis of the femoral head: transplantation of autologous mesenchymal stem cells cultured with beta-tricalcium phosphate ceramics and free vascularized fibula." Artif Organs 30(12): 960-2.

Keizer S. B., Kock N. B., Dijkstra P. D., Taminiau A. H. and Nelissen R. G. (2006). "Treatment of avascular necrosis of the hip by a non-vascularised cortical graft." J Bone Joint Surg Br 88(4): 460-6.

Kerachian M. A., Seguin C. and Harvey E. J. (2009). "Glucocorticoids in osteonecrosis of the femoral head: a new understanding of the mechanisms of action." J Steroid Biochem Mol Biol 114(3-5): 121-8.

Kim M. S., Ahn H. H., Shin Y. N., Cho M. H., Khang G. and Lee H. B. (2007). "An in vivo study of the host tissue response to subcutaneous implantation of PLGA- and/or porcine small intestinal submucosa-based scaffolds." Biomaterials 28(34): 5137-43.

Komatsubara S., Mori S., Mashiba T., Nonaka K., Seki A., Akiyama T., Miyamoto K., Cao Y., Manabe T. and Norimatsu H. (2005). "Human parathyroid hormone (1-34) accelerates the fracture healing process of woven to lamellar bone replacement and new cortical shell formation in rat femora." Bone 36(4): 678-87.

Kruyt M. C., de Bruijn J. D., Wilson C. E., Oner F. C., van Blitterswijk C. A., Verbout A. J. and Dhert W. J. (2003). "Viable osteogenic cells are obligatory for tissue-engineered ectopic bone formation in goats." Tissue Eng 9(2): 327-36.

Kuboki Y., Jin Q. and Takita H. (2001). "Geometry of carriers controlling phenotypic expression in BMP-induced osteogenesis and chondrogenesis." J Bone Joint Surg Am 83-A Suppl 1(Pt 2): S105-15.

Kuribayashi M., Fujioka M., Takahashi K. A., Arai Y., Ishida M., Goto T. and Kubo T. "Vitamin E prevents steroid-induced osteonecrosis in rabbits." Acta Orthop.

Ladd A. L. and Pliam N. B. (1999). "Use of bone-graft substitutes in distal radius fractures." J Am Acad Orthop Surg 7(5): 279-90.

Lai K. A., Shen W. J., Yang C. Y., Shao C. J., Hsu J. T. and Lin R. M. (2005). "The use of alendronate to prevent early collapse of the femoral head in patients with nontraumatic osteonecrosis. A randomized clinical study." J Bone Joint Surg Am 87(10): 2155-9.

Lai Y. M., Qin L., Yeung H. Y., Lee K. K. and Chan K. M. (2005). "Regional differences in trabecular BMD and micro-architecture of weight-bearing bone under habitual gait loading--a pQCT and microCT study in human cadavers." Bone 37(2): 274-82.

Lalik E., Mirek R., Rakoczy J. and Groszek A. (2006). "Microcalorimetric study of sorption of water and ethanol in zeolites 3A and 5A." Catalysis Today 114(2-3): 242-47

Lane N. E. (2006). "Therapy Insight: osteoporosis and osteonecrosis in systemic lupus erythematosus." Nat Clin Pract Rheumatol 2(10): 562-9.

Langer R. and Vacanti J. P. (1993). "Tissue engineering." Science 260(5110): 920-6.

Laurie S. W., Kaban L. B., Mulliken J. B. and Murray J. E. (1984). "Donor-site morbidity after harvesting rib and iliac bone." Plast Reconstr Surg 73(6): 933-8.

Lavernia C. J., Sierra R. J. and Grieco F. R. (1999). "Osteonecrosis of the femoral head." J Am Acad Orthop Surg 7(4): 250-61.

Law R. K., Lee E. W., Poon P. Y., Lau T. C., Kwok K. M. and Chan A. C. (2008). "The functional capacity of healthcare workers with history of severe acute respiratory distress syndrome (SARS) complicated with avascular necrosis--case report." Work 30(1): 17-26.

Lawrence W. H., Ed. (1999.263-73). In: von Recum AF, editor. Handbook of biomaterials evaluation Scientific, technical and clinical testing of implant materials. Philadelphia: Taylor and Francis. .

Lee H. S., Huang G. T., Chiang H., Chiou L. L., Chen M. H., Hsieh C. H. and Jiang C. C. (2003). "Multipotential mesenchymal stem cells from femoral bone marrow near the site of osteonecrosis." Stem Cells 21(2): 190-9.

Leng Y., Chen J. and Qu S. (2003). "TEM study of calcium phosphate precipitation on HA/TCP ceramics." Biomaterials 24(13): 2125-31.

Leung K. S., Siu W. S., Li S. F., Qin L., Cheung W. H., Tam K. F. and Lui P. P. (2006). "An in vitro optimized injectable calcium phosphate cement for augmenting screw fixation in osteopenic goats." J Biomed Mater Res B Appl Biomater 78(1): 153-60.

Levin L. S. (2006). "Vascularized fibula graft for the traumatically induced long-bone defect." J Am Acad Orthop Surg 14(10 Spec No.): S175-6.

Li E. K., Zhu T. Y., Tam L. S., Hung V. W., Griffith J. F., Li T. K., Li M., Wong K. C., Leung P. C., Kwok A. K. and Qin L. (2010). "Bone microarchitecture assessment by high-resolution peripheral quantitative CT in patients with systemic lupus erythematosus on corticosteroids." J of Ruematology (in print).

Li X., Jin L., Cui Q., Wang G. J. and Balian G. (2005). "Steroid effects on osteogenesis through mesenchymal cell gene expression." Osteoporos Int 16(1): 101-8.

Li Y., Han R., Geng C., Wang Y. and Wei L. (2009). "A new osteonecrosis animal model of the femoral head induced by microwave heating and repaired with tissue engineered bone." Int Orthop 33(2): 573-80.

Lieberman J. R., Berry D. J., Mont M. A., Aaron R. K., Callaghan J. J., Rajadhyaksha A. D. and Urbaniak J. R. (2003). "Osteonecrosis of the hip: management in the 21st century." Instr Course Lect 52: 337-55.

Lieberman J. R., Conduah A. and Urist M. R. (2004). "Treatment of osteonecrosis of the femoral head with core decompression and human bone morphogenetic protein." Clin Orthop Relat Res(429): 139-45.

Lin C. Y., Schek R. M., Mistry A. S., Shi X., Mikos A. G., Krebsbach P. H. and Hollister S. J. (2005). "Functional bone engineering using ex vivo gene therapy

and topology-optimized, biodegradable polymer composite scaffolds." Tissue Eng 11(9-10): 1589-98.

Liu H., Granch E. P. and Thomas J. W. (2008). Biocomposites. Encyclopedia of biomaterials and biomedical engineering. E. W. Gary and L. B. Gary: 179-94.

Loher S., Reboul V., Brunner T., Simonet M., Dora C. and Neuenschwander P. (2006). "Improved degradation and bioactivity of amorphous aerosol derived tricalcium phosphate nanoparticles in poly(lactide-co-glycolide)." Nanotechnology 17: 2054-61.

Lord C. F., Gebhardt M. C., Tomford W. W. and Mankin H. J. (1988). "Infection in bone allografts. Incidence, nature, and treatment." J Bone Joint Surg Am 70(3): 369-76.

Lu H. H., El-Amin S. F., Scott K. D. and Laurencin C. T. (2003). "Three-dimensional, bioactive, biodegradable, polymer-bioactive glass composite scaffolds with improved mechanical properties support collagen synthesis and mineralization of human osteoblast-like cells in vitro." J Biomed Mater Res A 64(3): 465-74.

Lu L., Peter S. J., Lyman M. D., Lai H. L., Leite S. M., Tamada J. A., Uyama S., Vacanti J. P., Langer R. and Mikos A. G. (2000). "In vitro and in vivo degradation of porous poly(DL-lactic-co-glycolic acid) foams." Biomaterials 21(18): 1837-45.

Lu X., Leng Y., Zhang X., Xu J., Qin L. and Chan C. W. (2005). "Comparative study of osteoconduction on micromachined and alkali-treated titanium alloy surfaces in vitro and in vivo." Biomaterials 26(14): 1793-801.

Malizos K. N., Karantanas A. H., Varitimidis S. E., Dailiana Z. H., Bargiotas K. and Maris T. (2007). "Osteonecrosis of the femoral head: etiology, imaging and treatment." Eur J Radiol 63(1): 16-28.

Malizos K. N. and Papatheodorou L. K. (2005). "The healing potential of the periosteum molecular aspects." Injury 36 Suppl 3: S13-9.

Manigrasso M. B. and O'Connor J. P. (2004). "Characterization of a closed femur fracture model in mice." J Orthop Trauma 18(10): 687-95.

Maniwa S., Nishikori T., Furukawa S., Kajitani K., Iwata A., Nishikawa U. and Ochi

M. (2000). "Evaluation of core decompression for early osteonecrosis of the femoral head." Arch Orthop Trauma Surg 120(5-6): 241-4.

Marchant R. E. (1989). "The cage implant system for determining in vivo biocompatibility of medical device materials." Fundam Appl Toxicol 13(2): 217-27.

Marker D. R., Seyler T. M., Ulrich S. D., Srivastava S. and Mont M. A. (2008). "Do modern techniques improve core decompression outcomes for hip osteonecrosis?" Clin Orthop Relat Res 466(5): 1093-103.

Marston S. B., Gillingham K., Bailey R. F. and Cheng E. Y. (2002). "Osteonecrosis of the femoral head after solid organ transplantation: a prospective study." J Bone Joint Surg Am 84-A(12): 2145-51.

Meland N. B., Maki S., Chao E. Y. and Rademaker B. (1992). "The radial forearm flap: a biomechanical study of donor-site morbidity utilizing sheep tibia." Plast Reconstr Surg 90(5): 763-73.

Miao X., Tan D. M., Li J., Xiao Y. and Crawford R. (2008). "Mechanical and biological properties of hydroxyapatite/tricalcium phosphate scaffolds coated with poly(lactic-co-glycolic acid)." Acta Biomater 4(3): 638-45.

Minamiguchi S., Takechi M., Yuasa T., Momota Y., Tatehara S., Takano H., Miyamoto Y., Satomura K. and Nagayama M. (2008). "Basic research on aw-AC/PLGA composite scaffolds for bone tissue engineering." J Mater Sci Mater Med 19(3): 1165-72.

Miyanishi K., Yamamoto T., Irisa T., Motomura G., Jingushi S., Sueishi K. and Iwamoto Y. (2005). "Effects of different corticosteroids on the development of osteonecrosis in rabbits." Rheumatology (Oxford) 44(3): 332-6.

Mok C. C. and Lau C. S. (2003). "Lupus in Hong Kong Chinese." Lupus 12(9): 717-22.

Mok C. C., Lau C. S. and Wong R. W. (1998). "Risk factors for avascular bone necrosis in systemic lupus erythematosus." Br J Rheumatol 37(8): 895-900.

Mont M. A., Carbone J. J. and Fairbank A. C. (1996). "Core decompression versus nonoperative management for osteonecrosis of the hip." Clin Orthop Relat

Res(324): 169-78.

Mont M. A., Jones L. C., Einhorn T. A., Hungerford D. S. and Reddi A. H. (1998). "Osteonecrosis of the femoral head. Potential treatment with growth and differentiation factors." Clin Orthop Relat Res(355 Suppl): S314-35.

Mont M. A., Jones L. C. and Hungerford D. S. (2006). "Nontraumatic osteonecrosis of the femoral head: ten years later." J Bone Joint Surg Am 88(5): 1117-32.

Mont M. A., Jones L. C. and LaPorte D. M. (1999). "Symptomatic multifocal osteonecrosis. A multicenter study." Clin Orthop Relat Res(369): 312-26.

Morgan S. M., Tilley S., Perera S., Ellis M. J., Kanczler J., Chaudhuri J. B. and Oreffo R. O. (2007). "Expansion of human bone marrow stromal cells on poly-(DL-lactide-co-glycolide) (PDL LGA) hollow fibres designed for use in skeletal tissue engineering." Biomaterials 28(35): 5332-43.

Naganathan V., Jones G., Nash P., Nicholson G., Eisman J. and Sambrook P. N. (2000). "Vertebral fracture risk with long-term corticosteroid therapy: prevalence and relation to age, bone density, and corticosteroid use." Arch Intern Med 160(19): 2917-22.

Ninin E., Milpied N., Moreau P., Andre-Richet B., Morineau N., Mahe B., Vigier M., Imbert B. M., Morin O., Harousseau J. L. and Richet H. (2001). "Longitudinal study of bacterial, viral, and fungal infections in adult recipients of bone marrow transplants." Clin Infect Dis 33(1): 41-7.

Nishida J. and Shimamura T. (2008). "Methods of reconstruction for bone defect after tumor excision: a review of alternatives." Med Sci Monit 14(8): RA107-13.

Nishida K., Yamamoto T., Motomura G., Jingushi S. and Iwamoto Y. (2008). "Pitavastatin may reduce risk of steroid-induced osteonecrosis in rabbits: a preliminary histological study." Clin Orthop Relat Res 466(5): 1054-8.

Nogler M. (2004). "Navigated minimal invasive total hip arthroplasty." Surg Technol Int 12: 259-62.

Nowicki P. and Chaudhary H. (2007). "Total hip replacement in renal transplant patients." J Bone Joint Surg Br 89(12): 1561-6.

Oates M., Chen R., Duncan M. and Hunt J. A. (2007). "The angiogenic potential of three-dimensional open porous synthetic matrix materials." Biomaterials 28(25): 3679-86.

Okazaki S., Nishitani Y., Nagoya S., Kaya M., Yamashita T. and Matsumoto H. (2009). "Femoral head osteonecrosis can be caused by disruption of the systemic immune response via the toll-like receptor 4 signalling pathway." Rheumatology (Oxford) 48(3): 227-32.

Ortiguera C. J., Pulliam I. T. and Cabanela M. E. (1999). "Total hip arthroplasty for osteonecrosis: matched-pair analysis of 188 hips with long-term follow-up." J Arthroplasty 14(1): 21-8.

Patschan D., Loddenkemper K. and Buttgereit F. (2001). "Molecular mechanisms of glucocorticoid-induced osteoporosis." Bone 29(6): 498-505.

Petrigliano F. A. and Lieberman J. R. (2007). "Osteonecrosis of the hip: novel approaches to evaluation and treatment." Clin Orthop Relat Res 465: 53-62.

Place E. S., Evans N. D. and Stevens M. M. (2009). "Complexity in biomaterials for tissue engineering." Nat Mater 8(6): 457-70.

Plancher K. D. and Razi A. (1997). "Management of osteonecrosis of the femoral head." Orthop Clin North Am 28(3): 461-77.

Plenk H., Jr., Gstettner M., Grossschmidt K., Breitenseher M., Urban M. and Hofmann S. (2001). "Magnetic resonance imaging and histology of repair in femoral head osteonecrosis." Clin Orthop Relat Res(386): 42-53.

Porter J. R., Ruckh T. T. and Popat K. C. (2009). "Bone tissue engineering: a review in bone biomimetics and drug delivery strategies." Biotechnol Prog 25(6): 1539-60.

Pritchett J. W. (2001). "Statin therapy decreases the risk of osteonecrosis in patients receiving steroids." Clin Orthop Relat Res(386): 173-8.

Qin L., Chan K., B R. and Guo X. (1997). "Bone Mineral Content Measurement Using QCT for Predicting the Cortical and Trabecular Bone Mechanical Properties." Chinese Journal of Orthopaedics 17(12): 66-70.

Qin L., Zhang G., Hung W. Y., Shi Y., Leung K., Yeung H. Y. and Leung P. (2005a).

"Phytoestrogen-rich herb formula "XLGB" prevents OVX-induced deterioration of musculoskeletal tissues at the hip in old rats." J Bone Miner Metab 23 Suppl: 55-61.

Qin L., Zhang G., Sheng H., Wang X. L., Wang Y. X., Yeung K. W., Griffith J. F., Li Z. R., Leung K. S. and Yao X. S. (2008). "Phytoestrogenic compounds for prevention of steroid-associated osteonecrosis." J Musculoskelet Neuronal Interact 8(1): 18-21.

Qin L., Zhang G., Sheng H., Yeung K. W., Yeung H. Y., Chan C. W., Cheung W. H., Griffith J., Chiu K. H. and Leung K. S. (2006). "Multiple bioimaging modalities in evaluation of an experimental osteonecrosis induced by a combination of lipopolysaccharide and methylprednisolone." Bone 39(4): 863-71.

Qin L. and Zhang M. (2005b). Mechanical testing for bone specimens. Current Topics of Bone Biology. H. W. Deng and Y. Z. Liu. Singapore, World Scientific: 177-212.

Rüegsegger P. and Qin L. (2007). In-Vivo Bone Mineral Density and Structures in Humans:From Isotom Over Densiscan to Xtreme-CT. Advanced Bioimaging Technologies in Assessment of the Quality of Bone and Scaffold Materials. L. Qin, H. K. Genant, J. Griffith and K. S. Leung: 65-78.

Raddatz D., Middel P., Bockemuhl M., Benohr P., Wissmann C., Schworer H. and Ramadori G. (2004). "Glucocorticoid receptor expression in inflammatory bowel disease: evidence for a mucosal down-regulation in steroid-unresponsive ulcerative colitis." Aliment Pharmacol Ther 19(1): 47-61.

Rezwan K., Chen Q. Z., Blaker J. J. and Boccaccini A. R. (2006). "Biodegradable and bioactive porous polymer/inorganic composite scaffolds for bone tissue engineering." Biomaterials 27(18): 3413-31.

Richardson T. P., Peters M. C., Ennett A. B. and Mooney D. J. (2001). "Polymeric system for dual growth factor delivery." Nat Biotechnol 19(11): 1029-34.

Rico H., Gomez-Castresana F., Cabranes J. A., Almoguera I., Lopez Duran L. and Matute J. A. (1985). "Increased blood cortisol in alcoholic patients with aseptic

necrosis of the femoral head." Calcif Tissue Int 37(6): 585-7.

Roy T. D., Simon J. L., Ricci J. L., Rekow E. D., Thompson V. P. and Parsons J. R. (2003). "Performance of degradable composite bone repair products made via three-dimensional fabrication techniques." J Biomed Mater Res A 66(2): 283-91.

Sahajpal D. T. and Zuckerman J. D. (2008). "Core decompression for nontraumatic osteonecrosis of the humeral head: a technique article." Bull NYU Hosp Jt Dis 66(2): 118-9.

Saito S., Saito M., Nishina T., Ohzono K. and Ono K. (1989). "Long-term results of total hip arthroplasty for osteonecrosis of the femoral head. A comparison with osteoarthritis." Clin Orthop Relat Res(244): 198-207.

Sakamoto M., Shimizu K., Iida S., Akita T., Moriya H. and Nawata Y. (1997). "Osteonecrosis of the femoral head: a prospective study with MRI." J Bone Joint Surg Br 79(2): 213-9.

Sanjeev K. and A.Einhorn T. (2005). Tisue engineering of bone. Bone Tissue Engineering

J. O. Hollinger, T. A. Einhorn, B. Doll and C. Sfeir: 277-302.

Sarris I., Weiser R. and Sotereanos D. G. (2004). "Pathogenesis and treatment of osteonecrosis of the shoulder." Orthop Clin North Am 35(3): 397-404, xi.

Satturwar P. M., Fulzele S. V. and Dorle A. K. (2003). "Biodegradation and in vivo biocompatibility of rosin: a natural film-forming polymer." AAPS PharmSciTech 4(4): E55.

Schneider E., Goldhahn J. and Burckhardt P. (2005). "The challenge: fracture treatment in osteoporotic bone." Osteoporos Int 16 Suppl 2: S1-2.

Schneider O. D., Weber F., Brunner T. J., Loher S., Ehrbar M., Schmidlin P. R. and Stark W. J. (2009). "In vivo and in vitro evaluation of flexible, cottonwool-like nanocomposites as bone substitute material for complex defects." Acta Biomater 5(5): 1775-84.

Scully S. P., Aaron R. K. and Urbaniak J. R. (1998). "Survival analysis of hips treated with core decompression or vascularized fibular grafting because of

avascular necrosis." J Bone Joint Surg Am 80(9): 1270-5.

Seyler T. M., Cui Q., Mihalko W. M., Mont M. A. and Saleh K. J. (2007). "Advances in hip arthroplasty in the treatment of osteonecrosis." Instr Course Lect 56: 221-33.

Shen P., Wong S. P., Li J. and Yong E. L. (2009). "Simple and sensitive liquid chromatography-tandem mass spectrometry assay for simultaneous measurement of five Epimedium prenylflavonoids in rat sera." Journal of Chromatography B-Analytical Technologies in the Biomedical and Life Sciences 877(1-2): 71-78.

Shen P., Wong S. P. and Yong E. L. (2007). "Sensitive and rapid method to quantify icaritin and desmethylicaritin in human serum using gas chromatography-mass spectrometry." J Chromatogr B Analyt Technol Biomed Life Sci 857(1): 47-52.

Sheng H., Zhang G., Wang X., Lee K., Yao X., Leung K., Li G. and Qin L. (2008). "Phytochemical molecule icariin stimulates osteogenic but inhibits adipogenic differentiation of mesenchymal stem cells." Bone 43(Supplement 1): S42-S43.

Sheng H., Zhang G., Wang Y. X., Yeung D. K., Griffith J. F., Leung K. S. and Qin L. (2009). "Functional perfusion MRI predicts later occurrence of steroid-associated osteonecrosis: an experimental study in rabbits." J Orthop Res 27(6): 742-7.

Sheng H. H., Zhang G. G., Cheung W. H., Chan C. W., Wang Y. X., Lee K. M., Wang H. F., Leung K. S. and Qin L. L. (2007). "Elevated adipogenesis of marrow mesenchymal stem cells during early steroid-associated osteonecrosis development." J Orthop Surg 2: 15.

Sherwood J. K., Riley S. L., Palazzolo R., Brown S. C., Monkhouse D. C., Coates M., Griffith L. G., Landeen L. K. and Ratcliffe A. (2002). "A three-dimensional osteochondral composite scaffold for articular cartilage repair." Biomaterials 23(24): 4739-51.

Shimizu E., Matsuda-Honjyo Y., Samoto H., Saito R., Nakajima Y., Nakayama Y., Kato N., Yamazaki M. and Ogata Y. (2004). "Static magnetic fields-induced bone sialoprotein (BSP) expression is mediated through FGF2 response

element and pituitary-specific transcription factor-1 motif." J Cell Biochem 91(6): 1183-96.

Siu W. S., Qin L., Cheung W. H. and Leung K. S. (2004). "A study of trabecular bones in ovariectomized goats with micro-computed tomography and peripheral quantitative computed tomography." Bone 35(1): 21-6.

Skouteris C. A. and Sotereanos G. C. (1989). "Donor site morbidity following harvesting of autogenous rib grafts." J Oral Maxillofac Surg 47(8): 808-12.

Songlin P., Ge Z., Yixin H., Xinluan W., Pingchung L., Kwoksui L. and Ling Q. (2009). "Epimedium-derived flavonoids promote osteoblastogenesis and suppress adipogenesis in bone marrow stromal cells while exerting an anabolic effect on osteoporotic bone." Bone 45(3): 534-44.

Steinberg M. E., Brighton C. T., Hayken G. D., Tooze S. E. and Steinberg D. R. (1984a). "Early results in the treatment of avascular necrosis of the femoral head with electrical stimulation." Orthop Clin North Am 15(1): 163-75.

Steinberg M. E., Hayken G. D. and Steinberg D. R. (1984b). A new method for evaluation and staging of avascular necrosis of the femoral head. Bone Circulation. J. Arlet, P. Ficat and Hungerford. Baltimore, Md: Williams and Wilkins: 398-403.

Stevenson S. (1987). "The immune response to osteochondral allografts in dogs." J Bone Joint Surg Am 69(4): 573-82.

Stevenson S., Shaffer J. W. and Goldberg V. M. (1996). "The humoral response to vascular and nonvascular allografts of bone." Clin Orthop Relat Res(326): 86-95.

Stiehl J. B., Ulrich S. D., Seyler T. M., Bonutti P. M., Marker D. R. and Mont M. A. (2008). "Bone morphogenetic proteins in total hip arthroplasty, osteonecrosis and trauma surgery." Expert Rev Med Devices 5(2): 231-8.

Stronach B. M., Duke J. N., Rozensweig S. D. and Stewart R. L. (2009). "Subtrochanteric Femur Fracture After Core Decompression and Placement of a Tantalum Strut for Osteonecrosis of the Femoral Head." J Arthroplasty.

Stulberg B. N., Davis A. W., Bauer T. W., Levine M. and Easley K. (1991).

"Osteonecrosis of the femoral head. A prospective randomized treatment protocol." Clin Orthop Relat Res(268): 140-51.

Sumitomo N., Noritake K., Hattori T., Morikawa K., Niwa S., Sato K. and Niinomi M. (2008). "Experiment study on fracture fixation with low rigidity titanium alloy: plate fixation of tibia fracture model in rabbit." J Mater Sci Mater Med 19(4): 1581-6.

Sun W., Wang B. L., Liu B. L., Zhao F. C., Shi Z. C., Guo W. S., Liu Z. H. and Li Z. R. "Osteonecrosis in patients after severe acute respiratory syndrome (SARS): possible role of anticardiolipin antibodies." J Clin Rheumatol 16(2): 61-3.

Sun Y., Feng Y. and Zhang C. (2009a). "The effect of bone marrow mononuclear cells on vascularization and bone regeneration in steroid-induced osteonecrosis of the femoral head." Joint Bone Spine 76(6): 685-90.

Sun Y., Zhang C. Q., Chen S. B., Sheng J. G., Jin D. X. and Zeng B. F. (2009b). "Treatment of femoral head osteonecrosis in patients with systemic lupus erythematosus by free vascularised fibular grafting." Lupus 18(12): 1061-5.

Tabata Y. (2009). "Biomaterial technology for tissue engineering applications." J R Soc Interface 6 Suppl 3: S311-24.

Takahashi Y. and Tabata Y. (2004). "Effect of the fiber diameter and porosity of non-woven PET fabrics on the osteogenic differentiation of mesenchymal stem cells." J Biomater Sci Polym Ed 15(1): 41-57.

Takano-Murakami R., Tokunaga K., Kondo N., Ito T., Kitahara H., Ito M. and Endo N. (2009). "Glucocorticoid inhibits bone regeneration after osteonecrosis of the femoral head in aged female rats." Tohoku J Exp Med 217(1): 51-8.

Tang T. T., Lu B., Yue B., Xie X. H., Xie Y. Z., Dai K. R., Lu J. X. and Lou J. R. (2007). "Treatment of osteonecrosis of the femoral head with hBMP-2-gene-modified tissue-engineered bone in goats." J Bone Joint Surg Br 89(1): 127-9.

Tian L., Xin Z. C., Liu W. J., Yang Y. M., Liu G., Chen L., Fu J. and Wang L. L. (2004). "[Effects of icariin on the erectile function and expression of nitrogen oxide synthase isoforms in corpus cavernosum of arterigenic erectile

dysfunction rat model]." Zhonghua Yi Xue Za Zhi 84(11): 954-7.

Tsugeno H., Tsugeno H., Fujita T., Goto B., Sugishita T., Hosaki Y., Ashida K., Mitsunobu F., Tanizaki Y. and Shiratori Y. (2002). "Vertebral fracture and cortical bone changes in corticosteroid-induced osteoporosis." Osteoporos Int 13(8): 650-6.

Turner J. E., Lawrence W. H. and Autian J. (1973). "Subacute toxicity testing of biomaterials using histopathologic evaluation of rabbit muscle tissue." J Biomed Mater Res 7(1): 39-58.

Tzaribachev N., Vaegler M., Schaefer J., Reize P., Rudert M., Handgretinger R. and Muller I. (2008). "Mesenchymal stromal cells: a novel treatment option for steroid-induced avascular osteonecrosis." Isr Med Assoc J 10(3): 232-4.

Vail T. P. and Urbaniak J. R. (1996). "Donor-site morbidity with use of vascularized autogenous fibular grafts." J Bone Joint Surg Am 78(2): 204-11.

VandeVord P. J., Matthew H. W., DeSilva S. P., Mayton L., Wu B. and Wooley P. H. (2002). "Evaluation of the biocompatibility of a chitosan scaffold in mice." J Biomed Mater Res 59(3): 585-90.

Velayudhan S., Anilkumar T. V., Kumary T. V., Mohanan P. V., Fernandez A. C., Varma H. K. and Ramesh P. (2005). "Biological evaluation of pliable hydroxyapatite-ethylene vinyl acetate co-polymer composites intended for cranioplasty." Acta Biomater 1(2): 201-9.

Vestergaard P., Olsen M. L., Paaske Johnsen S., Rejnmark L., Sorensen H. T. and Mosekilde L. (2003). "Corticosteroid use and risk of hip fracture: a population-based case-control study in Denmark." J Intern Med 254(5): 486-93.

Viereck V., Grundker C., Friess S. C., Frosch K. H., Raddatz D., Schoppet M., Nisslein T., Emons G. and Hofbauer L. C. (2005). "Isopropanolic extract of black cohosh stimulates osteoprotegerin production by human osteoblasts." J Bone Miner Res 20(11): 2036-43.

Visscher G. E., Robison R. L., Maulding H. V., Fong J. W., Pearson J. E. and Argentieri G. J. (1985). "Biodegradation of and tissue reaction to 50:50

poly(DL-lactide-co-glycolide) microcapsules." J Biomed Mater Res 19(3): 349-65.

Wan C., He Q. and Li G. (2006). "Allogenic peripheral blood derived mesenchymal stem cells (MSCs) enhance bone regeneration in rabbit ulna critical-sized bone defect model." J Orthop Res 24(4): 610-8.

Wang B. L., Sun W., Shi Z. C., Zhang N. F., Yue D. B., Guo W. S., Xu S. Q., Lou J. N. and Li Z. R. (2009). "Treatment of nontraumatic osteonecrosis of the femoral head with the implantation of core decompression and concentrated autologous bone marrow containing mononuclear cells." Arch Orthop Trauma Surg.

Wang C. J., Wang F. S., Ko J. Y., Huang H. Y., Chen C. J., Sun Y. C. and Yang Y. J. (2008). "Extracorporeal shockwave therapy shows regeneration in hip necrosis." Rheumatology (Oxford) 47(4): 542-6.

Wang G. J., Cui Q. and Balian G. (2000). "The Nicolas Andry award. The pathogenesis and prevention of steroid-induced osteonecrosis." Clin Orthop Relat Res(370): 295-310.

Wang X., Ma J., Wang Y. and He B. (2001). "Structural characterization of phosphorylated chitosan and their applications as effective additives of calcium phosphate cements." Biomaterials 22(16): 2247-55.

Wang X., Yan Y., Pan Y., Xiong Z., Liu H., Cheng J., Liu F., Lin F., Wu R., Zhang R. and Lu Q. (2006). "Generation of three-dimensional hepatocyte/gelatin structures with rapid prototyping system." Tissue Eng 12(1): 83-90.

Wang X., Yan Y. and Zhang R. (2007). "Rapid prototyping as a tool for manufacturing bioartificial livers." Trends Biotechnol 25(11): 505-13.

Wang X. L. (2008). Anti-osteoporotic constituents in Drynaria fortunei and anti-osteoporotic mechanism of Epimedium brevicornum. Shenyang, Shenyang Pharmaceutical University. Ph.D.

Wang X. L., Zhang G., Wang N. L., Qin L. and Yao X. S. (2007). Phytoestrogenic Molecule Icaritin: A Novel Selective-Estrogen-Receptor-Modulator developed

for treatment of osteoporosis. International Osteoporosis Conference. Beijing , China.

Wang X. L., Zhang G., Xie X. H., Lee K. M., Li G., Wang X. O., Yao X. S., Leng Y., Leung K. S. and Qin L. (2009). "In vitro release of osteoinductive molecule Icaritin from porous PLGA/TCP/Icaritin scaffolds for repairing steroid-associated osteonecrosis lesion." Bone 45(Supplement 2): S105-S05.

Wang X. L., Zhang G., Xie X. H., Yao X. S. and Qin L. (2008). "Antagonistic Estrogen Receptor Beta Signaling Required in Promoting Periosteum Bone Formation and Inhibiting Osteoclastic Bone Resorption by Icaritin - a Novel Synthetic Small Molecule." Bone 43 (Supplement1): S115.

Wang Y. K. and Huang Z. Q. (2005). "Protective effects of icariin on human umbilical vein endothelial cell injury induced by H2O2 in vitro." Pharmacol Res 52(2): 174-82.

Waters R. V., Gamradt S. C., Asnis P., Vickery B. H., Avnur Z., Hill E. and Bostrom M. (2000). "Systemic corticosteroids inhibit bone healing in a rabbit ulnar osteotomy model." Acta Orthop Scand 71(3): 316-21.

Weinstein R. S., Jilka R. L., Parfitt A. M. and Manolagas S. C. (1998). "Inhibition of osteoblastogenesis and promotion of apoptosis of osteoblasts and osteocytes by glucocorticoids. Potential mechanisms of their deleterious effects on bone." J Clin Invest 102(2): 274-82.

Weinstein R. S., Nicholas R. W. and Manolagas S. C. (2000). "Apoptosis of osteocytes in glucocorticoid-induced osteonecrosis of the hip." J Clin Endocrinol Metab 85(8): 2907-12.

Wen Q., Ma L., Chen Y. P., Yang L., Luo W. and Wang X. N. (2008). "Treatment of avascular necrosis of the femoral head by hepatocyte growth factor-transgenic bone marrow stromal stem cells." Gene Ther 15(23): 1523-35.

Xia Z., Huang Y., Adamopoulos I. E., Walpole A., Triffitt J. T. and Cui Z. (2006). "Macrophage-mediated biodegradation of poly(DL-lactide-co-glycolide) in vitro." J Biomed Mater Res A 79(3): 582-90.

Xie X. H., Zhang G., Wang X. L., He Y. X., Sheng H., Li G., Leung K. and Qin L. (2008). Icaritin promotes osteogenic potential of marrow mesenchymal stem cells from rabbit with steroid-associated osteonecrosis. The Third International Congress of Chinese Orthopaedic Association. Suzhou.

Yamamoto T., Hirano K., Tsutsui H., Sugioka Y. and Sueishi K. (1995). "Corticosteroid enhances the experimental induction of osteonecrosis in rabbits with Shwartzman reaction." Clin Orthop Relat Res(316): 235-43.

Yamamoto T., Irisa T., Sugioka Y. and Sueishi K. (1997). "Effects of pulse methylprednisolone on bone and marrow tissues: corticosteroid-induced osteonecrosis in rabbits." Arthritis Rheum 40(11): 2055-64.

Yamamoto T., Miyanishi K., Motomura G., Nishida K., Iwamoto Y. and Sueishi K. (2007). "[Animal models for steroid-induced osteonecrosis]." Clin Calcium 17(6): 879-86.

Yamamoto T., Schneider R., Iwamoto Y. and Bullough P. G. (2006). "Rapid destruction of the femoral head after a single intraarticular injection of corticosteroid into the hip joint." J Rheumatol 33(8): 1701-4.

Yang F., Cui W. J., Xiong Z., Liu L., Bei J. and Wang S. (2006). "Poly(L, L-lactide-co-glycolide)/tricalcium phosphate composite scaffold and its various changes during degradation in vitro." Polymer degradation and stability[Polym. Degrad. Stab.] 91: 3065-73.

Yang J., Cao C., Wang W., Tong X., Shi D., Wu F., Zheng Q., Guo C., Pan Z., Gao C. and Wang J. (2009). "Proliferation and osteogenesis of immortalized bone marrow-derived mesenchymal stem cells in porous polylactic glycolic acid scaffolds under perfusion culture." J Biomed Mater Res A.

Yang L., Boyd K., Kaste S. C., Kamdem Kamdem L., Rahija R. J. and Relling M. V. (2009). "A mouse model for glucocorticoid-induced osteonecrosis: effect of a steroid holiday." J Orthop Res 27(2): 169-75.

Yang Y., Zhao Y., Tang G., Li H., Yuan X. and Fan Y. (2008). "In vitro degradation of porous poly(l-lactide-co-glycolide)/β-tricalcium phosphate (PLGA/β-TCP) scaffolds under dynamic and static conditions." Polymer Degradation and

Stability[Polym. Degrad. Stab.] 93(10): 1838-45.

Ye L., Zeng X., Li H. and Ai Y. (2009). "Fabrication and biocompatibility of nano non-stoichiometric apatite and poly(epsilon-caprolactone) composite scaffold by using prototyping controlled process." J Mater Sci Mater Med.

Yeap S. S. and Hosking D. J. (2002). "Management of corticosteroid-induced osteoporosis." Rheumatology (Oxford) 41(10): 1088-94.

Yeh C. H., Chang J. K., Ho M. L., Chen C. H. and Wang G. J. (2009). "Different differentiation of stroma cells from patients with osteonecrosis: a pilot study." Clin Orthop Relat Res 467(8): 2159-67.

Yeung H. Y., Qin L., Lee K. M., Zhang M., Leung K. S. and Cheng C. Y. (2005). "Novel approach for quantification of porosity for biomaterial implants using microcomputed tomography (microCT)." J Biomed Mater Res B Appl Biomater 75(2): 234-42.

Yildiz N., Ardic F. and Deniz S. (2008). "Very early onset steroid-induced avascular necrosis of the hip and knee in a patient with idiopathic thrombocytopenic purpura." Intern Med 47(22): 1989-92.

Yin L., Li Y. B. and Wang Y. S. (2006). "Dexamethasone-induced adipogenesis in primary marrow stromal cell cultures: mechanism of steroid-induced osteonecrosis." Chin Med J (Engl) 119(7): 581-8.

Yoon S. J., Kim S. H., Ha H. J., Ko Y. K., So J. W., Kim M. S., Yang Y. I., Khang G., Rhee J. M. and Lee H. B. (2008). "Reduction of inflammatory reaction of poly(d,l-lactic-co-glycolic Acid) using demineralized bone particles." Tissue Eng Part A 14(4): 539-47.

Young W. F., Brown D., Kendler A. and Clements D. (2002). "Delayed post-traumatic osteonecrosis of a vertebral body (Kummell's disease)." Acta Orthop Belg 68(1): 13-9.

Yu D., Li Q., Mu X., Chang T. and Xiong Z. (2008). "Bone regeneration of critical calvarial defect in goat model by PLGA/TCP/rhBMP-2 scaffolds prepared by low-temperature rapid-prototyping technology." Int J Oral Maxillofac Surg 37(10): 929-34.

Yuan B. and Liu Z. (2007). "Treatment of osteonecrosis of the femoral head: combination of operation and multiple cellular mediators." Med Hypotheses 68(3): 502-5.

Yuan B., Taunton M. J. and Trousdale R. T. (2009). "Total hip arthroplasty for alcoholic osteonecrosis of the femoral head." Orthopedics 32(6): 400.

Zein I., Hutmacher D. W., Tan K. C. and Teoh S. H. (2002). "Fused deposition modeling of novel scaffold architectures for tissue engineering applications." Biomaterials 23(4): 1169-85.

Zhang G., Pan X. H., Xie X. H., He Y. X., Li G., Leung K. S. and Qin L. (2008). "Icaritin, a potential estrogen receptor beta antagonist molecule Icaritin, promote osteoporotic fracture repair in ovariectomized mice: Preliminary finding at 3 Weeks post fracture." Bone 43 (Supplement1) s76-7.

Zhang G., Qin L., Cheung W. H., Griffith J. and Leung K. S. (2006). Insufficient Repair Associated with reparative Neo-vasculature Characterized as Abnormalities in both Function-Structure and VEGF-VEGFR expression: A Steroid-associated Osteonecrosis Rabbit Model. International Osteoporosis Foundation (IOF) & 3rd Asia-Pacific Regional Conference on Osteoporosis & Australian and New Zealand Bone and Mineral Society (ANZBMS). Sheraton Mirage, Port Douglas, Australia.

Zhang G., Qin L., Sheng H., Wang X. L., Wang Y. X., Yeung D. K., Griffith J. F., Yao X. S., Xie X. H., Li Z. R., Lee K. M. and Leung K. S. (2009a). "A novel semisynthesized small molecule icaritin reduces incidence of steroid-associated osteonecrosis with inhibition of both thrombosis and lipid-deposition in a dose-dependent manner." Bone 44(2): 345-56.

Zhang G., Qin L., Sheng H., Yeung K. W., Yeung H. Y., Cheung W. H., Griffith J., Chan C. W., Lee K. M. and Leung K. S. (2007a). "Epimedium-derived phytoestrogen exert beneficial effect on preventing steroid-associated osteonecrosis in rabbits with inhibition of both thrombosis and lipid-deposition." Bone 40(3): 685-92.

Zhang G., Qin L. and Shi Y. Y. (2007b). "Epimedium-Derived Phytoestrogen

Flavonoids Exert Beneficial Effect on Preventing Bone Loss in Late Postmenopausal Women: A 24-Month Randomized, Double-Blind and Placebo-Controlled Trial." Journal of Bone and Mineral Research 22: 1072-79

Zhang G., Sheng H., He Y. X., Xie X. H., Wang Y. X., Lee K. M., Yeung K. W., Li Z. R., He W., Griffith J. F., Leung K. S. and Qin L. (2009b). "Continuous occurrence of both insufficient neovascularization and elevated vascular permeability in rabbit proximal femur during inadequate repair of steroid-associated osteonecrotic lesions." Arthritis Rheum 60(10): 2966-77.

Zhang G., Wang X. L., Pan X. H., Lee K. M., Leung K. S. and Qin L. (2008). Promotion effect of Icaritin on bone formation of human periosteal cells requires antagonistic estrogen receptor beta pathway. The Hong Kong Orthopaedic Association Annual Congress. Hong Kong.

Zhang G., Wang X. L., Sheng H., Xie X. H., He Y. X., Yao X. S., Li Z. R., Lee K. M., He W., Leung K. S. and Qin L. (2009c). "Constitutional flavonoids derived from Epimedium dose-dependently reduce incidence of steroid-associated osteonecrosis not via direct action by themselves on potential cellular targets." PLoS One 4(7): e6419.

Zhang R., An Y., Toth C. A., Draughn R. A., Dimaano N. M. and Hawkins M. V. (2004). "Osteogenic protein-1 enhances osseointegration of titanium implants coated with peri-apatite in rabbit femoral defect." J Biomed Mater Res B Appl Biomater 71(2): 408-13.

Zhang R. and Ma P. X. (1999). "Poly(alpha-hydroxyl acids)/hydroxyapatite porous composites for bone-tissue engineering. I. Preparation and morphology." J Biomed Mater Res 44(4): 446-55.

Zhang Y. S., Li H. Z., Zhang R. Q. and Wang P. (2005). "[Preliminary research on preparation of porcine bladder acellular matrix graft for tissue engineering applications]." Zhonghua Yi Xue Za Zhi 85(38): 2724-7.

Zhao J., Ohba S., Komiyama Y., Shinkai M., Chung U. I. and Nagamune T. (2009). "Icariin: A Potential Osteoinductive Compound for Bone Tissue Engineering." Tissue Eng Part A.

Zhao J., Ohba S., Shinkai M., Chung U. I. and Nagamune T. (2008). "Icariin induces osteogenic differentiation in vitro in a BMP- and Runx2-dependent manner." Biochem Biophys Res Commun 369(2): 444-8.

Zhao X., Jain S., Benjamin Larman H., Gonzalez S. and Irvine D. J. (2005). "Directed cell migration via chemoattractants released from degradable microspheres." Biomaterials 26(24): 5048-63.

Zibis A. H., Karantanas A. H., Roidis N. T., Hantes M. E., Argiri P., Moraitis T. and Malizos K. N. (2007). "The role of MR imaging in staging femoral head osteonecrosis." Eur J Radiol 63(1): 3-9.

Zolnik B. S., Leary P. E. and Burgess D. J. (2006). "Elevated temperature accelerated release testing of PLGA microspheres." J Control Release 112(3): 293-300.